GEOCHEMICAL ANALYSES OF ORE FLUIDS FROM THE ST. CLOUD - U.S. TREASURY VEIN SYSTEM, CHLORIDE MINING DISTRICT, NEW MEXICO

by

Christina Behr

Submitted in Partial fulfillment
of the Requirements for the Degree of
Master of Science in Geochemistry

New Mexico Institute of Mining and Technology
Socorro, New Mexico

July, 1988

This thesis is accepted on behalf of the faculty of the Institute by the following committee:

David A. Norman
Advisor

Andrew R Campbell

Carl H Papp

July 12, 1988
Date

ACKNOWLEDGEMENTS

This work benefitted from the technical advice and guidance of my academic advisors: Drs. Dave Norman, Andrew Campbell, and Carl Popp. Their expertise and interest in this project improved the quality of the research and are greatly appreciated. The analyses preformed by Drs. K. Brower, A. Campbell, D. Johnson, and D. Norman were significant contributions to this study.

Financial support for the project was provided by a grant from the National Science Foundation (EAR8410481). This research was also funded, in part, by grants from the New Mexico Geological Society and New Mexico Institute of Mining and Technology Alumni Association, as well as the Barkley Wykoff Memorial Scholarship.

The St. Cloud Mining Company generously allowed access to their property, geologic maps, drill core samples, and driller's logs. I am very grateful to the company and their staff for this help. Discussions with Jeff Gerwe and Rich Harrison improved my understanding of Chloride District geology and are greatly appreciated.

I am grateful for the financial and moral support of my family. They instilled values in me and an understanding of what is worth pursuing in life. The support and companionship of Bob Andres aided in the completion of this project.

Finally, and most importantly, I must thank He who originally created the material upon which this thesis is based.

ABSTRACT

Vein mineralization in the St. Cloud-U.S. Treasury epithermal system is fault-hosted within Tertiary volcanic rocks and Pennsylvanian limestone. Ore deposition occurred in two stages. The first stage consists of galena, sphalerite, and chalcopyrite. The second stage bears precious metals within an assemblage of bornite, digenite, chalcocite, and covellite. Analyses of fluid inclusions within vein quartz indicate that the two mineralization stages were deposited by fluids with an average temperature of 260°C. Salinity measurements average 0.8 equivalent weight percent NaCl. Solute analyses indicate the dissolved solids are principally sodium and calcium chloride. Analyses of volatile contents indicate the gaseous species average 0.2 mole percent; major gaseous species are carbon dioxide, nitrogen, C_nH_{2n} compounds, hydrogen sulfide, methane, and hydrogen. Calculated pH-values in the system average 5.8, log oxygen fugacity values average -37.9, and log sulfur fugacity values average -12.4. The fluid of the first stage was slightly more saline and deposited a base-metal-rich ore, while the fluid of the second stage had higher sulfur fugacity values (or lower oxygen fugacity values) and deposited a more precious-metal-rich ore.

Ore controls of the mineralization stages are primarily structural with deposition resulting from boiling of metal-bearing hydrothermal fluids and mixing of these fluids with surface-derived meteoric waters. Boiling in the system is evidenced by observations of high vapor to liquid ratios in some fluid inclusions and measurements of high concentrations of gasses in some samples within ore zones. Mixing of ore-fluids with meteoric waters is evidenced by fluid inclusion microanalyses that show cooling, dilution, and oxidation of solutions with increasing elevation. Stable isotope data suggest two fluids; increasing d D with increasing elevation indicates an increased meteoric water component in ore solutions with elevation. Computer modeling of metal solubilities suggest that boiling and mixing are viable depositional mechanisms for deposition of ore metals in the St. Cloud-U.S. Treasury system.

The physical and chemical characteristics of the St. Cloud-U.S. Treasury system indicate that it is an eroded paleo-geothermal system. The fluid chemistry, sulfide mineral assemblage, propylitic alteration, and geologic environment of this system are consistent with the adularia-sericite classification of epithermal deposits (Heald et al., 1987).

TABLE OF CONTENTS

List of Tables

List of Figures

INTRODUCTION

Purpose of Study

The St. Cloud-U.S. Treasury epithermal vein system is located in the Chloride Mining District, Sierra County, New Mexico (Figure 1). This area is a complexly faulted region of the Datil-Mogollon volcanic field. Mineralization in the district occurs irregularly within fissure veins formed by high-angle, normal faults.

Despite the proximity of the St. Cloud and U.S. Treasury mines (Figure 2), the two ore bodies differ in many respects. The St. Cloud deposit is hosted by Tertiary volcanic rocks which contain allochthonous limestone blocks; these blocks define favorable zones of mineralization. The U.S. Treasury deposit is hosted only by Tertiary volcanic rocks. The ore-body geometry differs between the two deposits (Figure 2). Ore from the U.S. Treasury mine has significant gold values, whereas silver and copper are the primary ore metals at the St. Cloud mine.

While ore controls are primarily structural (Freeman and Harrison, 1984), structure does not account for the irregularity of the mineralization and the differences in metal content between the two mines. Physicochemical parameters are also known to be significant ore-controls and can be determined by fluid inclusion analyses. These analyses provide insight into the metal-transporting capabilities of the fluids and the depositional mechanisms that operated during mineralization (Roedder, 1979, 1984; Roedder and Bodnar, 1980).

Figure 1. Location Map of the Chloride Mining District (after Harrison, 1986):

a. Physiographic map with the district, major cauldrons, and boundary of the Mogollon Plateau indicated;

b. Structural map with the St. Cloud-U.S. Treasury vein system and the Moccasin-John flow dome complex indicated.

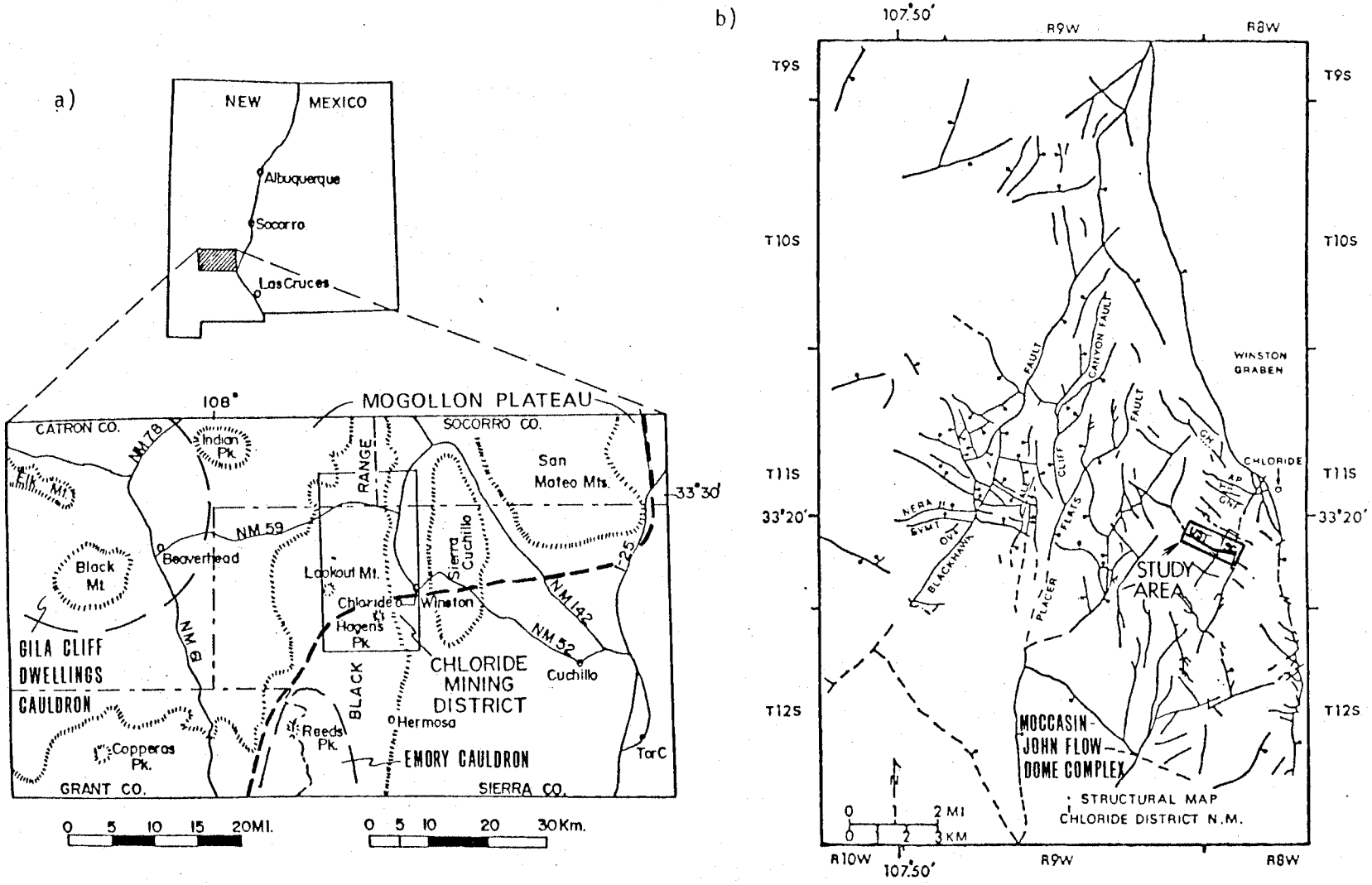
a)
NEW MEXICO
Albuquerque
Socorro
Las Cruces
108°
MOGOLLON PLATEAU
CATRON CO.
SOCORRO CO.
NM 78
Indian Pk.
Elk Mt.
RANGE
San Mateo Mts.
33°30'
NM 59
Beaverhead
Black Mt.
Lookout Mt.
Sierra Cuchillo
Chloride
Winston
Hagens Pk.
I-25
NM 142
NM 52
Cuchillo
GILA CLIFF DWELLINGS
CAULDRON
CHLORIDE MINING DISTRICT
NM 61
BLACK
Hermosa
Reeds Pk.
Copperas Pk.
EMORY CAULDRON
TorC
GRANT CO.
SIERRA CO.
0 5 10 15 20MI.
0 5 10 20 30Km.
b)
107°50'
R9W
R8W
T9S
T10S
T11S
33°20'
T12S
FAULT
CANYON FAULT
WINSTON GRABEN
CLIFF
FLATS
CHLORIDE
STUDY AREA
PLACER
BLACKHAWK
MOCCASIN-JOHN FLOW-DOME COMPLEX
STRUCTURAL MAP
CHLORIDE DISTRICT N.M.
0 1 2 MI
0 2 3 KM
R10W
107.50'

Figure 2. Long-section Diagram of the St. Cloud-U.S. Treasury Vein; the St. Cloud Ore Body lies South-east of the Major Cross-structure and the U.S. Treasury Ore Body lies North-west of it (courtesy of the St. Cloud Mining Company).

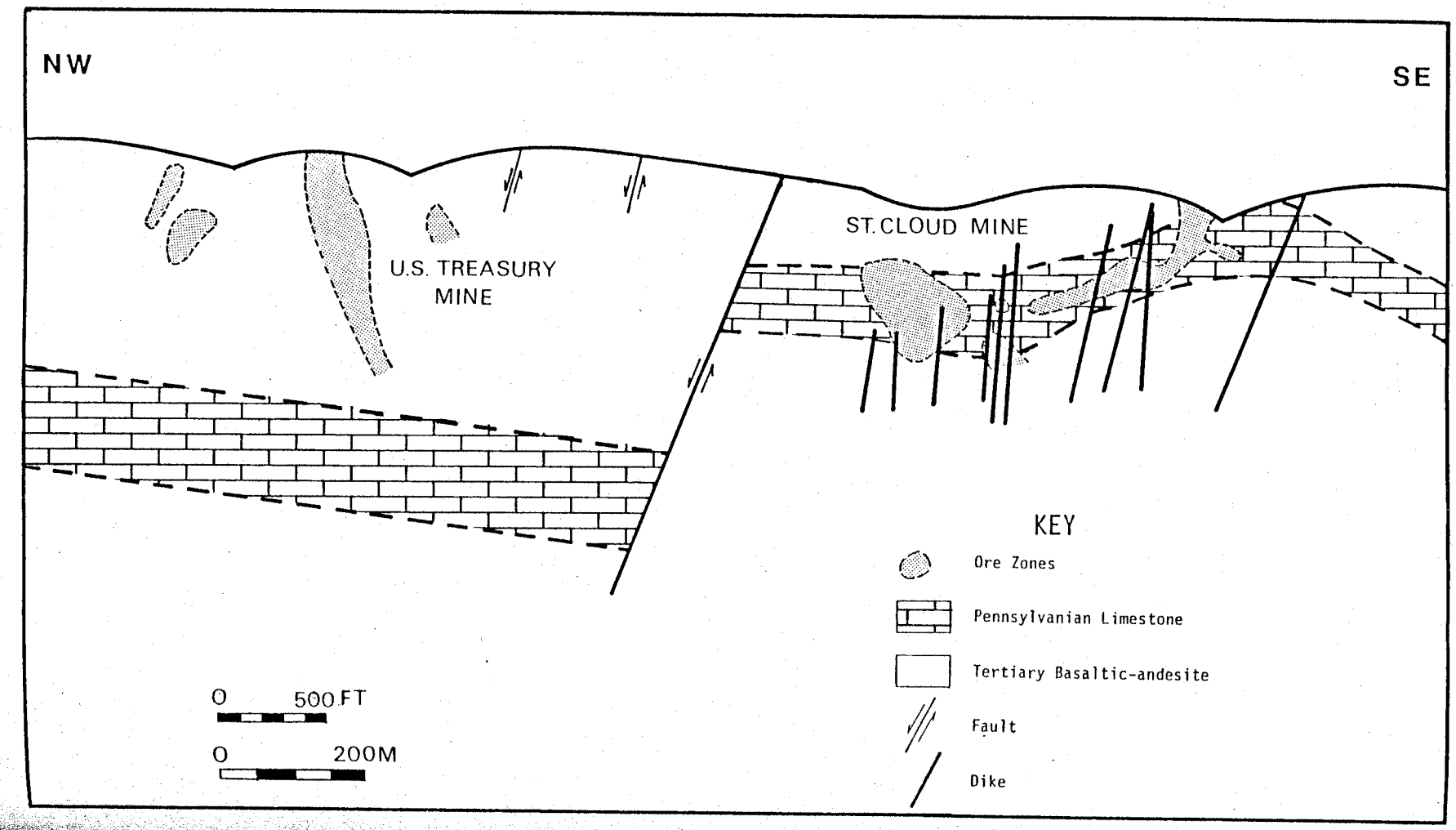
NW
SE
U.S. TREASURY MINE
ST. CLOUD MINE
KEY
Ore Zones
Pennsylvanian Limestone
Tertiary Basaltic-andesite
Fault
Dike
0 500 FT
0 200M

The purpose of this investigation was to characterize the physicochemical environment unique to each of the two mines within the St. Cloud-U.S. Treasury vein system. Of particular interest to this study was the variations in chemical parameters between zones of ore-grade and non-ore-grade mineralization and the depositional mechanisms which formed the metal sulfides observed. The techniques used to determine the chemical nature of the ore solutions were based on fluid inclusion microanalyses. The results of these analyses were evaluated by comparisons to data from presently active geothermal systems.

Previous Work

The St. Cloud and U.S. Treasury mines and other deposits in the Chloride Mining District have been described by Lindgren (1910), Harley (1934), Anderson (1957), and Elston et al. (1976). The district was originally mapped by Maxwell and Heyl (1976). Recent mining activity and geology is reported by Maxwell and Heyl (1980), Freeman and Harrison (1984), and Harrison (1985, 1986, in prep.). Other, formal, geochemical investigations of this system have been done by Norman (1985) and Loucks (1984). The study by Norman (1985) involves gas analyses of surface, channel samples collected along strike of the vein. These analyses reveal anomalously high gas contents in fluid inclusions within quartz deposited over some areas of known sulfide mineralization.

Geology

The Chloride District lies on the eastern slope of the Black Range, which forms part of the eastern edge of the Mogollon plateau. Situated to the east is the Winston graben, a major, north-south structure that parallels the Rio Grande Rift (see Figure 1). Regional features that may have influenced mineralization in the District include the Gila Cliff Dwellings cauldron lying to the west, and the rhyolitic, Moccasin-John flow-dome complex and Emory cauldron to the south.

Within the Chloride Mining District, Proterozoic granite and metasedimentary rocks underlie approximately 1500 meters of Paleozoic sediments (Kottlowski, 1963) and up to 1900 meters of Tertiary volcanic rocks (Harrison, 1986). Outcropping Paleozoic sedimentary units include the Pennsylvanian Madera Formation and the Permian Abo Formation. The Madera Formation is a variably carbonaceous and cherty limestone interbedded with carbonaceous, pyritic shale. The Abo Formation is a sandy, silty, shaly red bed sequence with minor stratabound copper and uranium mineralization (Hatchell et al., 1982). The Tertiary stratigraphy is composed of the Rubio Peak Formation, Kneeling Nun Tuff, and a series of volcaniclastic, basaltic-andesitic and rhyolitic units (Harrison, 1986). This section is dominated by the 37 m.y. old Rubio Peak Formation which is part of the Mogollon-Datil volcanic field. Its 800 to 900 meter thickness is divided into two sequences (Harrison, 1986). The lower sequence consists mainly of volcaniclastic rocks and debris-flow breccias. The upper sequence is bimodal with compositions of quartz-latite to rhyolite ash flow tuffs

and basaltic-andesitic lava flows with intercalated volcaniclastic sediments. Within the Chloride District, the Rubio Peak Formation unconformably overlies the Abo Formation and exposures of the Madera Formation occur as allochthonous blocks within the lower Rubio Peak Formation. These blocks range in size from boulders to slabs up to 150 meters thick and 5 to 10 square kilometers in outcrop; they are interpreted to be gravity-slide blocks (Maxwell and Heyl, 1976). The 35.2 m.y. old Kneeling Nun Tuff is a 170 to 200 meter thick ash-flow tuff unit that unconformably overlies the Rubio Peak Formation. It is unconformably overlain by a series of volcaniclastic units: Caballo Blanco Tuff, Sandstone of Monument Park, and Tuff of Koko Well. These are overlain by a basaltic-andesite flow, more tuff units, and a rhyolite flow (Harrison, 1986).

Faulting in the district is dominated by high-angle, normal faults occurring along north, north-east, and north-west trends (Figure 1). These faults are pre-, syn-, and post-mineralization in origin. The fault in which the St. Cloud-U.S. Treasury vein occurs, trends from N45W to N70W and dips from 65 to 85 degrees to the south-west; it is approximately 2350 meters in strike length and the normal displacement is about 100 meters. The cross-structure that offsets the limestone block between the two deposits is a pre-vein fault (Harrison, personal communication).

The St. Cloud-U.S. Treasury vein system is one of many epithermal deposits in the Chloride Mining District. Other vein deposits located within six kilometers of the St. Cloud-U.S. Treasury vein include the Apache, Hoosier, Colossal, Midnite, Pye Lode, and Bald Eagle deposits. Production from these and other vein systems in the Chloride Mining

District began in the 1880's but ceased after a short-term, boom period. This early activity is estimated to have produced $1,000,000 worth of metals (Harley, 1934). In 1968, exploration drilling by the Goldfield Corporation intersected the main ore zone of the St. Cloud mine and production began anew in 1982. From 1982 to 1986 approximately 235,000 ounces of silver and 4,000 ounces of gold from about 60,000 tons of ore were produced from the U.S. Treasury mine (Harrison, in prep.).

Mineralization dates exist for a few of the systems in the District and were obtained by K-Ar dating on vein adularia (M. Bauman, FRM minerals, unpublished data, 1984). The Apache, Bald Eagle, and St. Cloud ore bodies are dated as 26.9 $\pm$ 2.0, 25.2 $\pm$ 1.1, and 26.5 $\pm$ 1.1 m.y., respectively.

Copper and silver are the dominant metals recovered from the St. Cloud-U.S. Treasury deposit and the other deposits nearby. A regional zonation of increasing gold-values and decreasing base-metals-values to the north is observed in the District (Harrison, 1985).

In the St. Cloud-U.S. Treasury deposit, the mineralization is divided into three stages (Harrison, 1986). The early stage of mineralization consists of medium to coarse-grained galena, sphalerite, and chalcopyrite, with minor amounts of polybasite, pyrargyrite, and pyrite. The second stage of mineralization is responsible for most of the precious-metal mineralization in the mine. Mineralization textures vary from fine-grained gray streaks within quartz to more coarse-grained crystals. The mineral assemblage consists of bornite, digenite, chalcocite, covellite, and betehkenite, with lesser sphalerite, galena, and chalcopyrite. Sulfide mineralization-stages in

this system have little pyrite, hematite, or magnetite. The third mineralization stage is non-ore-bearing and consists of massive quartz and calcite with minor barite and rhodochrosite. The gangue mineralogy of stages 1 and 2 includes quartz, calcite, and minor adularia. The massive silica associated with both stages of mineralization is similar in its milky to clear color and vuggy and cryptocrystalline texture. This type of quartz mineralization is typical in epithermal deposits (Berger, 1983).

Regional alteration is propylitic with a mineralogy comprised of adularia, sericite, kaolinite, chlorite, and epidote; wall-rock silicification adjacent to the epithermal veins is also common (Harrison, 1985, 1986).

In the St. Cloud-U.S. Treasury system, repeated movement along the fault during mineralization is indicated by the brecciated nature of the veins. Fragments of early-formed mineralization are rotated and cemented with later mineralization. Motion along the fault apparently separated the hangingwall from each mineralization-stage so that in general, stage 1 mineralization occurs on the footwall, overlain by stage 2, and stage 3 contacts the hangingwall (Harrison, personal communication).

Systematics of Metal Complexation and Deposition

In order to understand the localization of ore zones within the St. Cloud-U.S. Treasury vein system, mechanisms of metal transport and deposition are examined. Based on the ore-mineral assemblage, the metals of interest are copper, lead, zinc, silver, and gold. The

capacity of a fluid to transport these metals depends upon its concentrations of complex-forming ligands. The ligands complexing metals under hydrothermal conditions include chloride, bisulfide, hydrogen sulfide, hydroxide, and possibly ammonia and fluoride (Barnes, 1979; Helgeson, 1964). The thermodynamic data for the metal-complexing reactions are limited, but for a hydrothermal environment, the data indicate that chloride and bisulfide complexes are the most important (Helgeson, 1964, 1969, 1970; Seward, 1973; Drummond and Ohmoto, 1985). The general forms of the reactions for mono- and divalent metals of both ligand-types are: (M represents metal in the reactions)

Chloride-complexed metals:

monovalent $\longrightarrow 2\ MCl + H_2S \longleftrightarrow M_2S + 2\ H^+ + 2\ Cl^-$

divalent $\longrightarrow MCl_2 + H_2S \longleftrightarrow MS + 2\ H^+ + 2\ Cl^-$

Bisulfide-complexed metals:

monovalent $\longrightarrow 2\ M(HS)_2^- + H_2 \longleftrightarrow 2\ M + 2\ HS^- + 2\ H_2S$

divalent $\longrightarrow M(HS)_2 \longleftrightarrow MS + H_2S$

The stabilities of the chloride and bisulfide-complexed metals depend on six factors: temperature, pressure, chloride and sulfide concentrations, pH, and redox conditions. A decrease in either temperature or pressure will dissociate either complex-type, with metals depositing more efficiently through a decrease in temperature (Helgeson, 1964; Barnes, 1979; Norton and Cathles, 1979).

Dilution of chloride and bisulfide concentrations in an ore fluid will also deposit metals. A decrease in the chloride concentration will deposit chloride-complexed metals and a decrease in the bisulfide and hydrogen sulfide concentrations will deposit bisulfide-complexed metals. However, an increase in hydrogen sulfide will stabilize

bisulfide complexes and counteract deposition of metals from these complexes. It will also act very effectively to deposit chloride-complexed metals. The number of moles of hydrogen sulfide added to a fluid results in an almost equal number of moles of metal sulfide deposited from chloride complexes (Barnes, 1979).

Changes in ore-fluid pH are a very effective mineralization process, but have inverse effects on the deposition of metals from the two complexes. Increasing pH deposits chloride-complexed metals and decreasing pH deposits bisulfide-complexed metals. The efficiency of ore-fluid pH-changes to deposit metals differs between the two ligands. Deposition of 99 percent of chloride-complexed metals occurs through an increase in pH by 1 unit, while only 90 percent of the bisulfide-complexed metal is deposited by a decrease in pH by 2 units (Barnes, 1979).

Changing the redox conditions within an ore fluid has opposing effects to the stabilities of the two ligands due to the oxidation of hydrogen sulfide. As sulfate ions are produced by ore-fluid oxidation, hydrogen sulfide is depleted. The stability of chloride-complexed metals is maintained, but bisulfide-complexed metals become saturated and deposit from the ore fluid. If conditions become reducing, the inverse is true and chloride-complexed metals are deposited.

There are three general processes occurring in a hydrothermal environment that may effect the chemical conditions of an ore fluid and result in mineralization: ore fluid interactions with wall rock, ore fluid mixing with meteoric water, and ore-fluid boiling (or effervescence) (Barton and Toulmin, 1961).

Cooling ore-fluids through heat exchange with wall rock requires a large thermal gradient between the fluid and rock. However, wall rock is a very poor heat-insulator and thermal equilibria is more probable, thus this cooling mechanism is unlikely. Depending on the mineralogy of the host rocks, they may react with ore fluids to change pH. For example, an acidic fluid would be buffered by interactions with carbonate rocks which could initiate deposition of chloride-complexed metals and result in limestone dissolution. If this mechanism operated to mineralize a system, calcite gangue would not precipitate. However, initial quartz deposition in epithermal systems covers wall rocks and thus prevents continued interactions between ore fluids and wall rocks. The efficiency of mineral deposition from ore fluid interactions with wall rocks is considered to be minimal, and does not play a major role in the formation of ore deposits (Ewers and Keays, 1977).

The importance of meteoric waters in hydrothermal systems has been noted by O'Neil and Silberman (1974), Taylor (1974) and White (1981) and mixing of ore fluids with meteoric water has been recognized as an effective means of metal deposition (Barton and Toulmin, 1961; Helgeson, 1964; Henley et al., 1984). Meteoric water is usually cooler than the ore fluid, carries minimal concentrations of dissolved species with respect to the ore fluid, and is oxygenated from previous interactions with the atmosphere. Typical molal concentrations of oxygen in ground water are approximately $10^{-3.6}$. These characteristics of meteoric water can effectively initiate ore deposition through the mechanisms of cooling, dilution, and oxygenation. Cooling and dilution can destabilize both chloride and bisulfide-complexes; oxygenation can breakdown bisulfide-complexes. Cooling of 100°C can result in the

deposition of approximately 90 percent of the chloride-complexed metal and 75 percent of the bisulfide-complexed metal; dilution of an ore fluid by an equal amount of chloride and bisulfide-free water can result in the deposition of approximately 85 percent of the chloride-complexed metals and 75 percent of the bisulfide-complexed metals (Barnes, 1979). Oxygenation effects on deposition have not been similarly quantified.

The process of boiling has been invoked to account for zones of high-grade mineralization. Boiling is considered to be the most effective depositional process due to contributions of cooling and changes in pH and ore fluid chemistry produced by the exsolution of gaseous species from an ore fluid (Ewers and Keays, 1977; Buchanan, 1981; Berger, 1983; Henley et al., 1984; Drummond and Ohmoto, 1985; Fournier, 1985a,b). Boiling in a hydrothermal fluid initiates by decreasing pressure which occurs as fluid rises in a system (Reed and Spycher, 1985). However, large pressure decreases may also occur if a fluid enters a large open space; this process of throttling is an effective mechanism of inciting boiling (Barton and Toulmin, 1961).

By definition, boiling implies that the vapor and liquid phases have the same compositions; however, in hydrothermal systems, boiling is actually effervescence. Hydrothermal fluids may initially contain high concentrations of gaseous species which preferentially partition into the vapor phase upon fluid boiling (Giggenbach, 1980). As boiling starts, the first vapor formed contains mostly volatile species. As boiling continues, the volatiles are depleted from the hydrothermal liquid and the vapor phase is dominated by water. At 300°C, the relation of partition coefficients of the major gaseous species is:

$$N_2 >> H_2 > CH_4 >> CO_2 > H_2S.$$

The volatile with the greatest partition coefficient has the greatest affinity for the vapor phase. Although carbon dioxide has a relatively low partition coefficient, its relatively high initial solubility results in carbon dioxide occurring in the greatest concentrations in the vapor phase. As carbon dioxide exsolves from the aqueous phase, the pH increases in the residual fluids because of the reaction:

$$HCO_3^- + H^+ \rightarrow H_2O + CO_2.$$

Hydrogen sulfide exsolution also results in increased pH and decreased bisulfide and hydrogen sulfide concentrations in the residual fluid because of the reaction:

$$HS^- + H^+ \rightarrow H_2S.$$

Other effects of the boiling process are increased salinity in the residual fluids; loss of heat from the aqueous to the vapor phase, thereby cooling the residual liquid; and oxidation from loss of reducing gasses (i.e. H_2 and CH_4).

Evidence for the boiling process in a hydrothermal system can be seen in the alteration of host rocks. The buoyant segregation of gasses from the aqueous phase produces a decrease in pH in near-surface fluids over boiling zones as volatiles condense and hydrogen sulfide oxidizes to sulfate. These acid waters leach the overlying strata and produce distinctive, intense kaolinization. Within the vein mineralization, boiling is revealed by higher and more variable vapor to liquid ratios in fluid inclusions and vertically-localized ore-zone geometries; because boiling is such an efficient depositional process, metal deposition occurs over short vertical ranges.

All of the depositional mechanisms previously discussed, with the exception of changing redox conditions, can act to deposit silica, the major gangue mineral observed in epithermal systems (Fournier, 1983, 1985a,b). The concentrations of silica in hydrothermal fluids, between 250 and 300°C, can be up to 1000 ppm and deposition as amorphous silica is indicative of high degrees of supersaturation brought on by rapid changes in the physical or chemical nature of the system.

Silica supersaturation is evidenced in geothermal systems by silica minerals precipitating in well casings. Precipitation occurs when fluids rise in the wells and fluid temperature and pressure decrease. Silica deposition in epithermal systems during vein mineralization may have acted to decrease permeability around a heat source (or source of heated fluids). Resulting pressure increases from self-sealing allow concentrations of silica and metal complexes to increase. The system may rupture upon tectonic movement, or pressures exceeding lithostatic, causing decompressional boiling. This process results in the deposition of amorphous silica and sulfide minerals. This mineralization could reestablish an impermeable seal and cause the cycle to repeat (Fournier, 1983). Episodic sealing and refracturing is noted by Buchanan (1981) in many of the deposits in his study of over 60 epithermal vein systems.

PROCEDURES

Sample Selection

Sample areas were chosen to include the major ore zones of the two mines. Samples over a vertical interval of 1200 feet (366 meters) were obtained from surface outcrops, underground exposures, and drill core. The samples represent the best distribution possible given the sampling conditions---the vein is not exposed along its entire strike length, much of the mine is unaccessible, and most of the drill core was utilized for assay purposes or is no longer available. The sample locations are shown in Figure 3.

The multiple periods of mineralization and the similarity of quartz from ore-bearing mineralization stages in the St. Cloud-U.S. Treasury ore bodies made determinations of which stage a particular sample was from difficult. Metal ratios (Figure 4) were used to determine which stage was sampled. The ratios associated with stages one and two were determined for the U.S. Treasury mine where the mineralization stages are not mixed, and easily identified by sulfide mineral assemblages. The line, log ((Ag+Au)/(Pb+Zn))=1.0, separates the two mineralization stages in the U.S. Treasury mine and was used to identify mineralization stages in samples from the St. Cloud mine. Samples not classified as being formed from a unique mineralization stage, based on metal ratios or sulfide mineral assemblage, were not used for further analyses.

Figure 3. Long-section Diagrams with Sample Locations for each Mine.

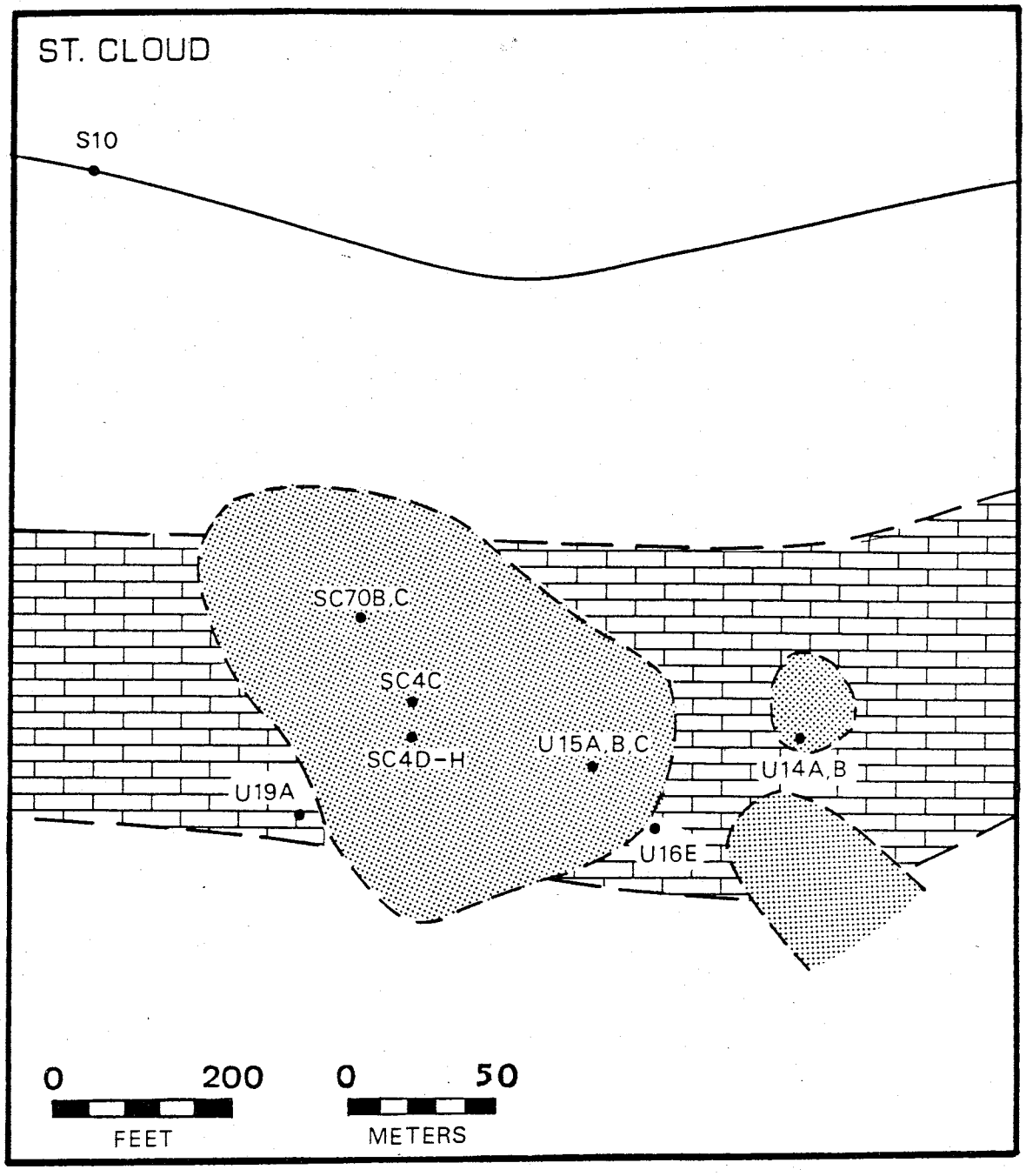
ST. CLOUD
S10
SC70B,C
SC4C
SC4D-H
U15A,B,C
U14A,B
U19A
U16E
0
200
FEET
0
50
METERS

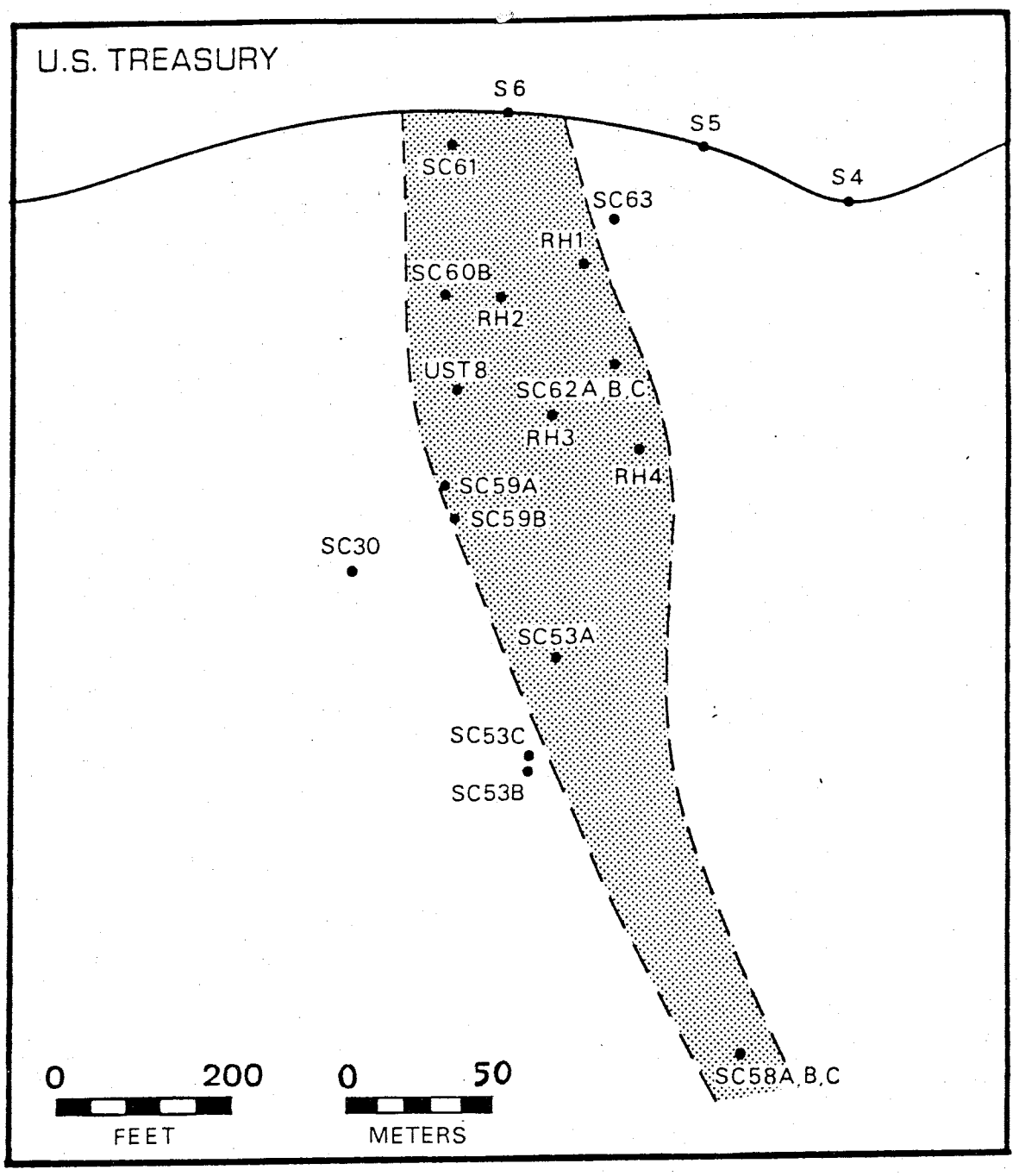
U.S. TREASURY
S6
S5
S4
SC61
SC63
RH1
SC60B
RH2
UST8
SC62A,B,C
RH3
RH4
SC59A
SC59B
SC30
SC53A
SC53C
SC53B
SC58A,B,C
0
200
FEET
0
50
METERS

Figure 4. Plot of Elevation versus log ((Ag+Au)/(Pb+Zn)) for the St. Cloud and U.S. Treasury Mines.

■ = stage 1 ore-mineralization

● = stage 2 ore-mineralization

× = mixed ore-mineralization stages 1 and 2

◆ = non-ore-grade mineralization

St. Cloud

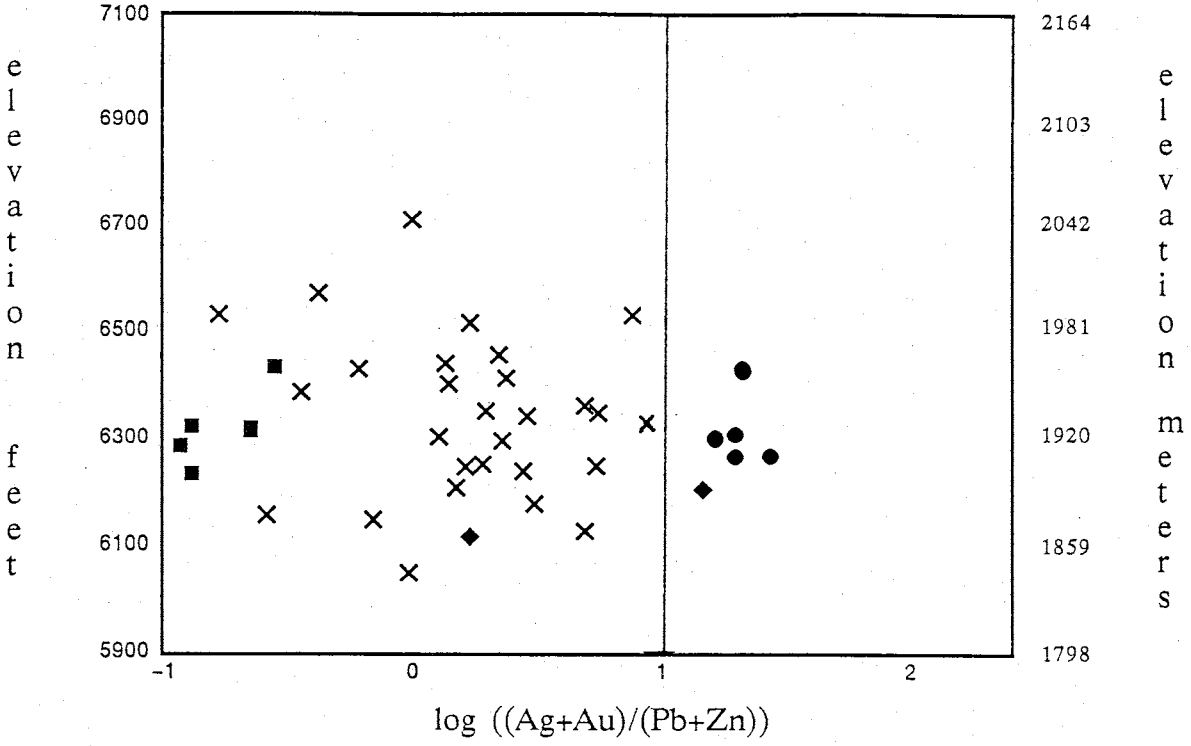

U.S. Treasury

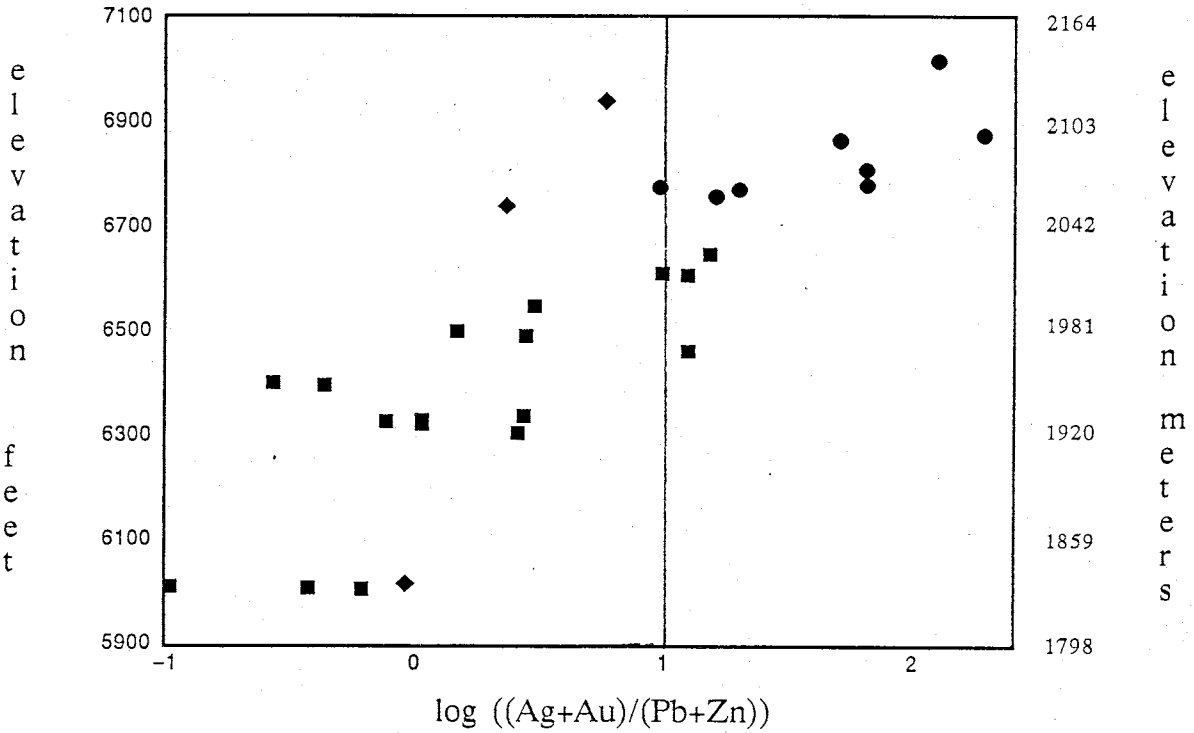

Methods

Doubly-polished sections of quartz were prepared for fluid-inclusion analyses. Thermometric measurements were made on a Linkam TH 600 stage that was calibrated every two to three months using the standards in Table 1. The calibration was checked each day before use by measuring the freezing point of distilled, deionized water.

Table 1. Standards for Calibration of the Linkam TH 600 Stage and their Melting Temperatures.

standard	melting temperature (^{o}C)
chlorobenzene	-45.6
water	0.0
vanilla	81-82
acetanilid	114-116
acetophenetidin	134-136
sulfanilamide	164.5-166.5
sulfapyridine	190-193
caffeine	235-237.5
sodium nitrate	307
potassium dichromate	398
silver chloride	455

Samples for gas analysis were first ground by mortar and pestle to -10, +40 mesh and hand-picked. Quartz was cleaned by boiling each sample for twelve hours each in dilute hydrochloric-acid solution; distilled double-deionized water; dilute sodium-hydroxide solution; and finally, distilled double-deionized water. The sample was then dried in an oven at approximately 100^{o}C.

For the gas analyses, approximately 5 grams of cleaned quartz was placed in a fused-quartz furnace connected to a vacuum-extraction-line mass spectrometer system (Figure 5). The sample was heated to 100^{o}C

and evacuated to a pressure of less than 3×10^{-6} torr before analyses began. The extraction line was then isolated from the mass spectrometer and the sample was heated to 500°C for 30 minutes to decrepitate the fluid inclusions. Volatiles were separated by liquid nitrogen and dry ice-alcohol traps into noncondensible gasses (those gasses not condensed by liquid nitrogen: nitrogen, methane, hydrogen, carbon monoxide, helium, and argon) and condensible gasses (those gasses condensed by liquid nitrogen, but not by a dry ice-alcohol mixture: carbon dioxide, organic species, and hydrogen sulfide). The two fractions were analyzed separately by the mass spectrometer. Water was trapped into a capillary tube with liquid nitrogen, sealed, removed and weighed; condensible gasses remaining after analysis were trapped in a capillary tube in a similar fashion. The organic species contained in this gas fraction were analyzed by gas chromatography/mass spectrometry (GC/MS) at New Mexico Institute of Mining and Technology by Dr. K. Brower.

The decrepitated quartz and the trapped water were used for a number of additional analyses. Six samples of decrepitated quartz and the water extracted from them were analyzed for oxygen and hydrogen isotopes at Yale University by Dr. A. Campbell. Twenty-two samples of decrepitated quartz were also used for measurement of solute concentrations. The quartz grains were rinsed with distilled, double-deionized water to dissolve the solutes dried on the grain surfaces (when inclusions are thermally decrepitated in a vacuum, inclusion fluids deposit solute residue onto grain surfaces (Putnam, 1980)). Cations were measured by inductively-coupled plasma, atomic-emission spectrometry (ICP) using a Perkin-Elmer 5500

Figure 5. Schematic Diagram of the Mass Spectrometer Analytical System for Gas Analyses (Norman and Sawkins, 1987).

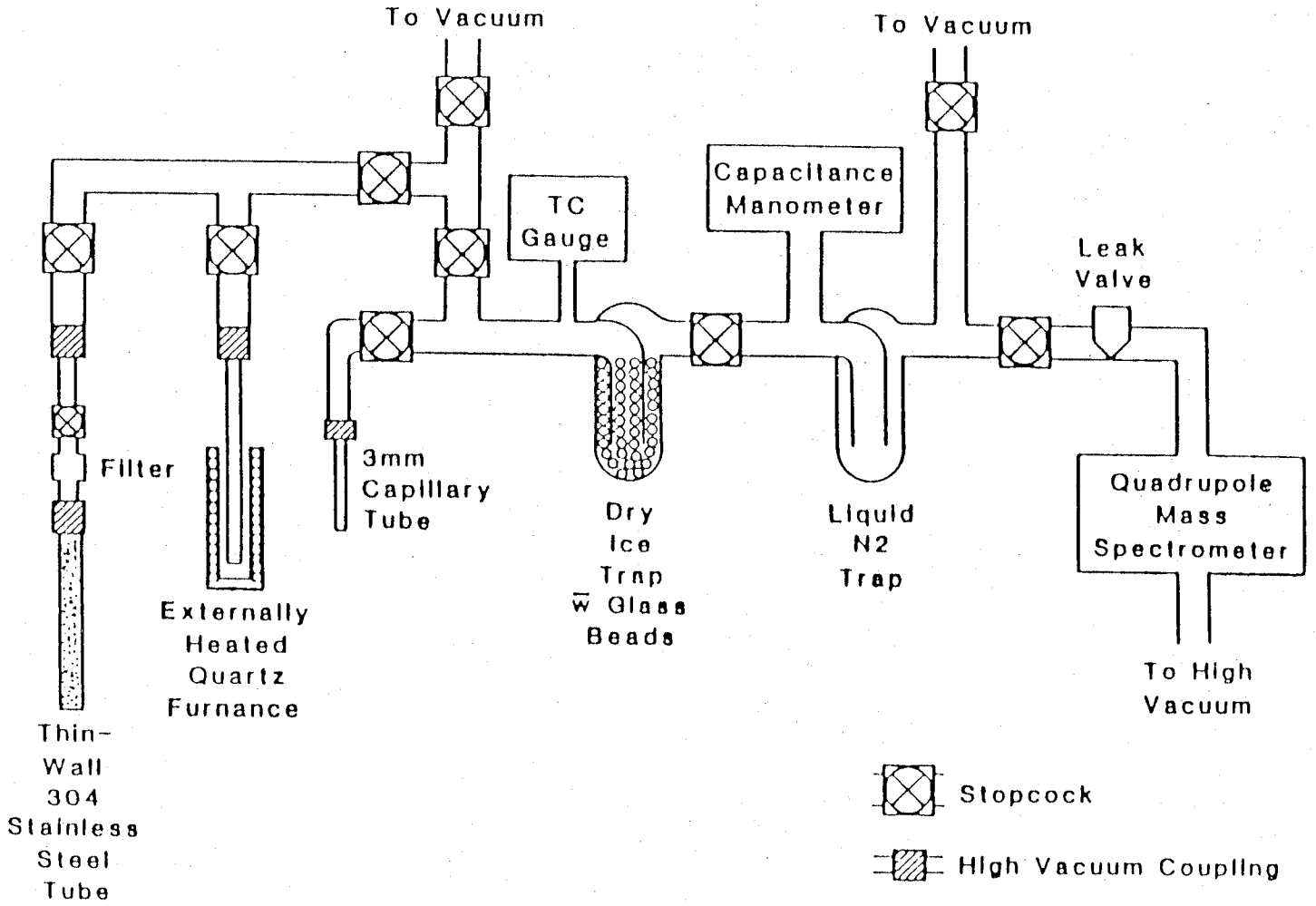
To Vacuum
To Vacuum
TC Gauge
Capacitance Manometer
Leak Valve
Filter
3mm Capillary Tube
Dry Ice Trap w Glass Beads
Liquid N2 Trap
Quadrupole Mass Spectrometer
Externally Heated Quartz Furnance
Thin-Wall 304 Stainless Steel Tube
To High Vacuum
Stopcock
High Vacuum Coupling

spectrometer; a schematic diagram of the ICP system is shown in Figure 6. Standard solutions of 10, 1, and 0.1 ppm were prepared for the following cations and emission lines at the indicated wavelengths (in nanometers) were observed for each:

Na	589.59	Cu	327.40
K	769.90	Pb	220.35
Ca	422.67	Zn	213.86
Mg	279.08	Ag	328.07
Mn	259.37	Au	242.80
Sb	206.83	As	193.70

Anions were measured by high-performance, liquid chromatography (HPLC) using a Beckman chromatograph. Standard solutions of 10, 5, and 1 ppm were prepared for chloride, sulfate, and nitrate. From the amounts of leachate and the measured volume of water extracted from the inclusions, the dilution was determined and a quantitative analysis of the inclusion fluid was calculated.

Two samples of quartz from both ore-bearing mineralization stages were analyzed for helium isotope compositions at the University of Minnesota by Dr. D. Norman.

Four samples of fossiliferous limestone were collected progressively away from the mineralized vein to examine color alteration in the conodonts resulting from heating by hydrothermal fluids. These were analyzed at New Mexico Institute of Mining and Technology by Dr. D. Johnson.

Figure 6. Schematic Diagram of the Inductively-coupled Plasma Spectrometer Analytical System for Cation Analyses (Thompson and Walsh, 1986).

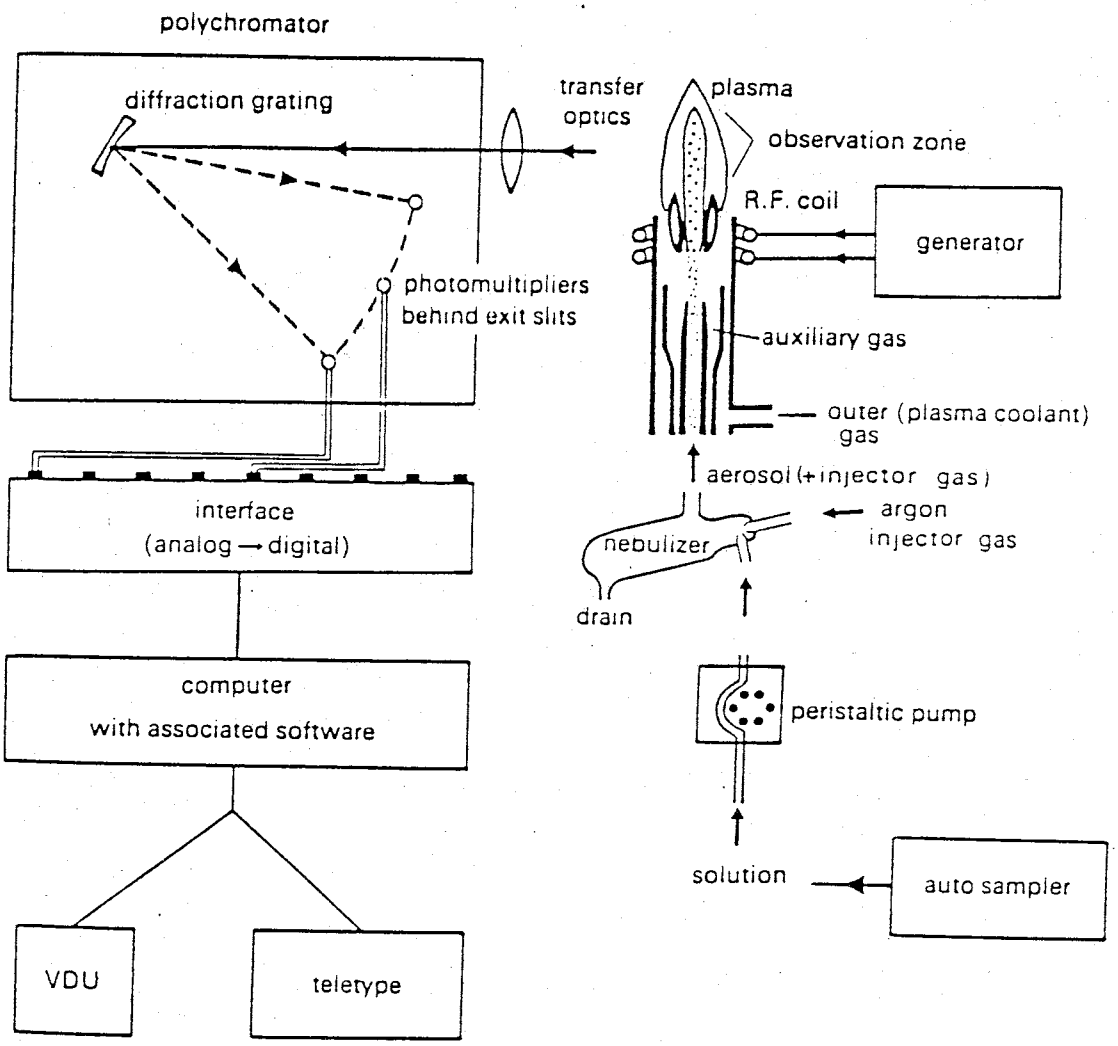
polychromator
diffraction grating
transfer optics
plasma
observation zone
R.F. coil
generator
photomultipliers behind exit slits
auxiliary gas
outer (plasma coolant) gas
aerosol (+injector gas)
argon injector gas
nebulizer
drain
interface (analog → digital)
computer with associated software
peristaltic pump
solution
auto sampler
VDU
teletype

RESULTS

Fluid Inclusion Analyses

Twelve hundred and twenty thermometric measurements were made on six hundred and fifty-six primary inclusions within vein quartz from both stages of ore mineralization and their respective non-ore-grade zones. Fluid inclusion homogenization temperatures and freezing point depression temperatures were measured. The freezing point depression measurements were used to calculate inclusion fluid salinities. These data and corresponding sample elevations are in Appendix A.

The sizes and morphologies of the measured inclusions were highly variable. Inclusion sizes ranged from less than 1 micron to as large as 75 microns; the minimum size of the measured inclusions was approximately 10 microns. The inclusions had high surface-areas that were usually irregular, but were sometimes negative-crystal-shaped. The inclusions contained liquid and vapor phases with low vapor-to-liquid ratios that were fairly consistent in most samples. Some inclusions with high vapor-to-liquid ratios were observed in samples SC4E, F, H, and U14B within the St. Cloud mine and RH1, SC63, and SC59A within the U.S. Treasury mine. These samples were obtained from middle and upper levels of mineralized zones and the occurrence of these inclusions was sporadic within a polished section. In most instances, inclusions with high vapor-to-liquid ratios had morphologies that indicated they had necked-down and no measurements of homogenization were made. If a necked-down inclusion was undetected and measured, the salinity measurement would still be valid; however,

the temperature measurement would be in error either greater or less than the actual temperature depending on whether vapor or liquid was added or removed from the inclusion (Roedder, 1984). Some of the extreme homogenization temperatures reported may be the result of measurements of undetected, necked-down fluid inclusions; for this reason, averages within the 95 percent confidence interval of the bulk mean were calculated. These values and other statistical data are in Appendix B. Errors in measurement of homogenization temperatures are $\pm 2^{\circ}C$ and salinities are ± 0.18 equivalent weight percent NaCl.

An attempt was made to find inclusions with high vapor-to-liquid ratios that had not necked down. Within sample SC4E, an homogenization measurement was made on such an inclusion that homogenized to a vapor at $259^{\circ}C$; another inclusion with an average vapor-to-liquid ratio, in the same field of view, homogenized to a liquid at $253^{\circ}C$. These measurements are evidence of volatile exsolution from the mineralizing fluids and it is assumed that the mineralizing fluids were at, or near, the boiling temperature. This assumption allows for the approximation that homogenization-temperature (Th) equals trapping-temperature and no pressure correction of Th is required (Roedder, 1984).

Averages of the results from measurements of Th and salinities for each mineralization-stage in both mines are in Table 2. Relationships of Th and salinity for each stage of mineralization in both mines are in Figures 7 and 8. Variations in Th and salinity with elevation are in Figure 9.

Figure 7. Th and Salinity Histograms for each Mineralization Stage of Both Mines.

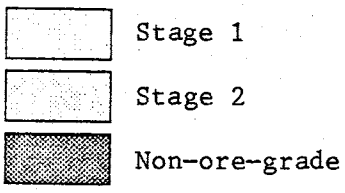

St. Cloud

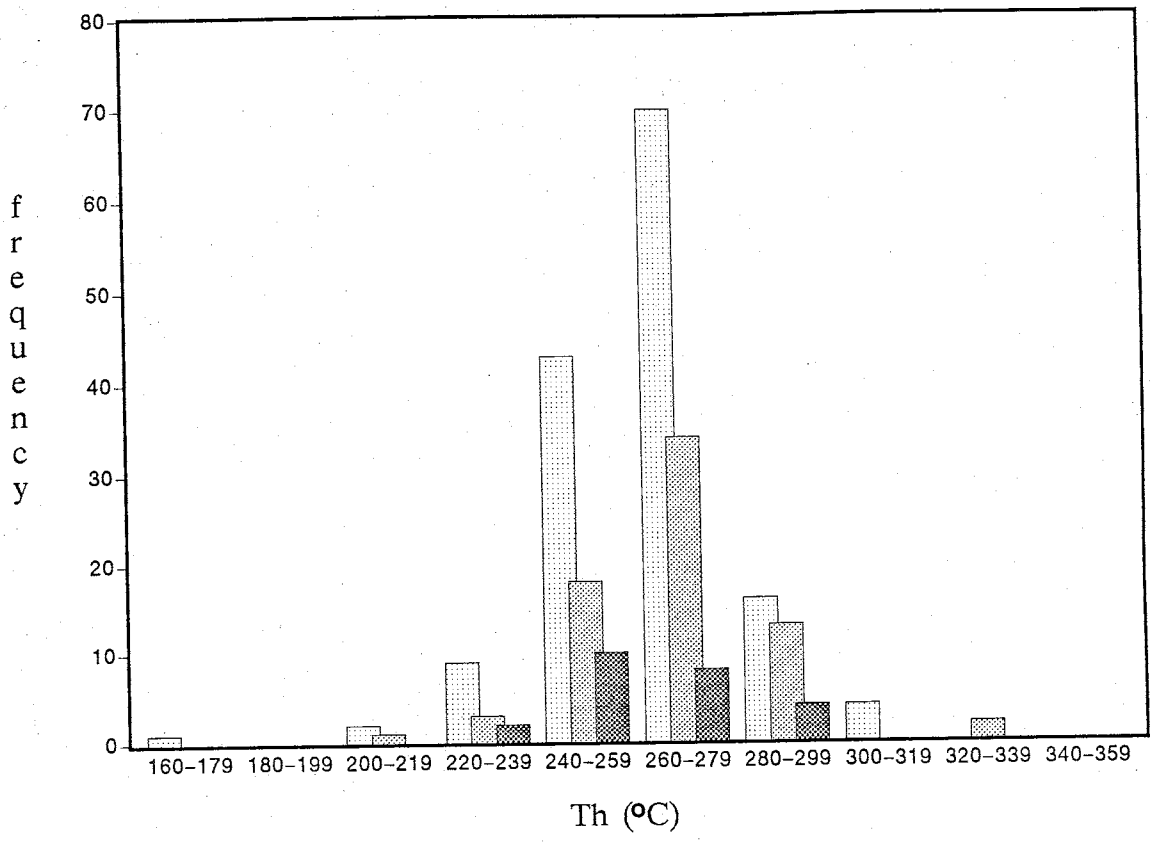
frequency
80
70
60
50
40
30
20
10
0
160–179
180–199
200–219
220–239
240–259
260–279
280–299
300–319
320–339
340–359
Th (°C)

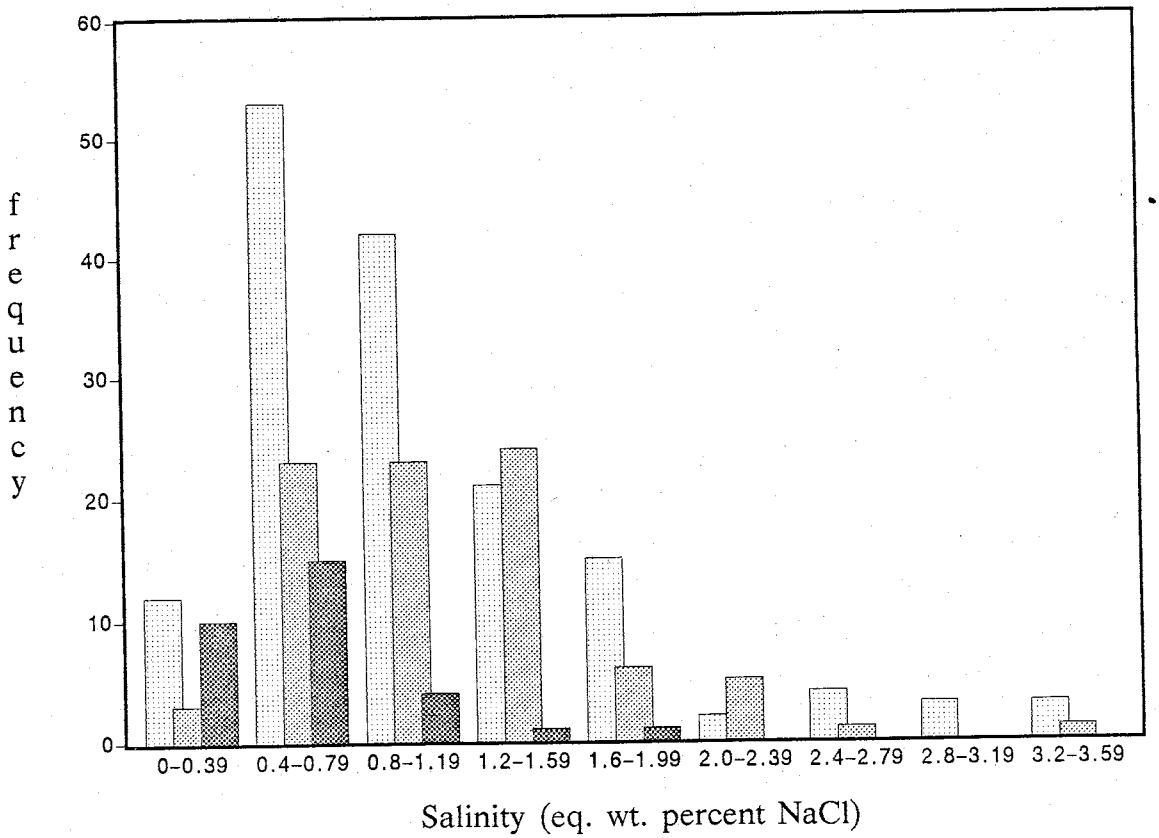
frequency
60
50
40
30
20
10
0
0–0.39
0.4–0.79
0.8–1.19
1.2–1.59
1.6–1.99
2.0–2.39
2.4–2.79
2.8–3.19
3.2–3.59
Salinity (eq. wt. percent NaCl)

U.S. Treasury

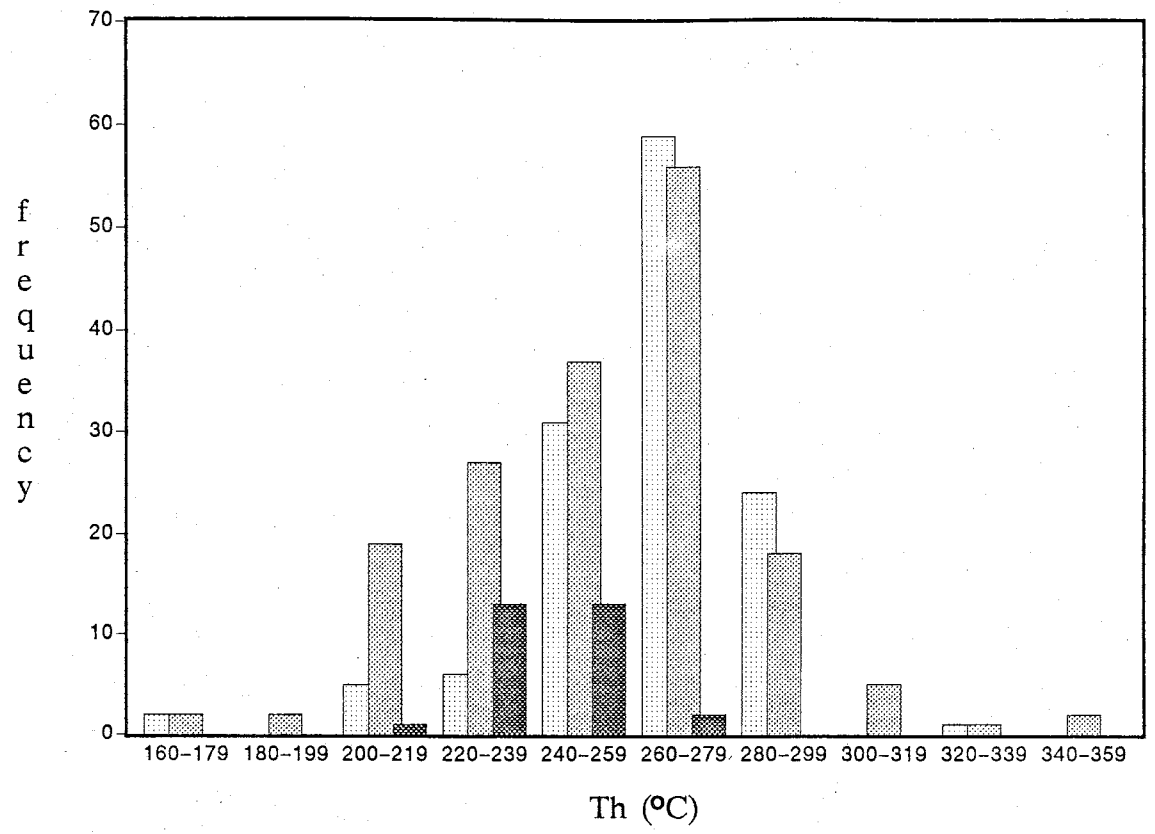
frequency
70
60
50
40
30
20
10
0
160–179
180–199
200–219
220–239
240–259
260–279
280–299
300–319
320–339
340–359
Th (°C)

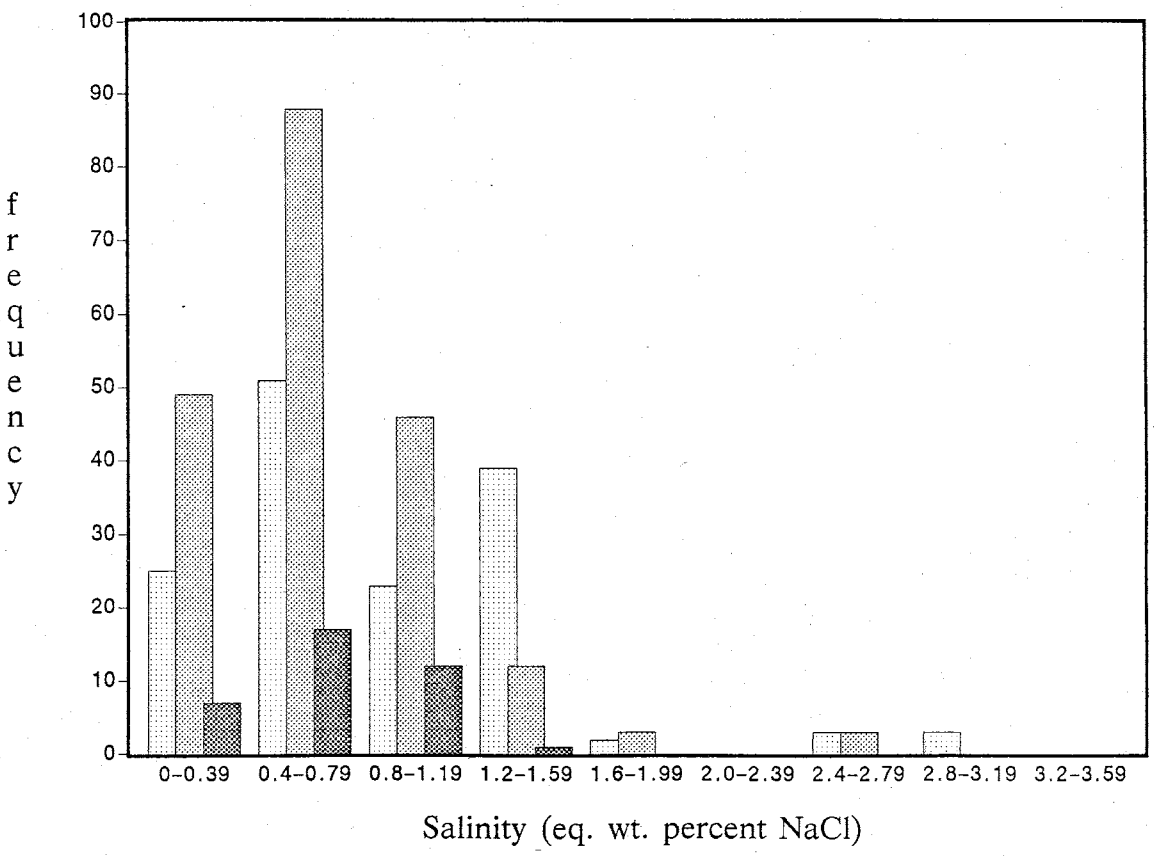
frequency
100
90
80
70
60
50
40
30
20
10
0
0–0.39
0.4–0.79
0.8–1.19
1.2–1.59
1.6–1.99
2.0–2.39
2.4–2.79
2.8–3.19
3.2–3.59
Salinity (eq. wt. percent NaCl)

Figure 8. Plots of Salinity versus Th from the St. Cloud and U.S. Treasury Mines for each Stage of Mineralization from Both Mines.

St. Cloud – Stage 1

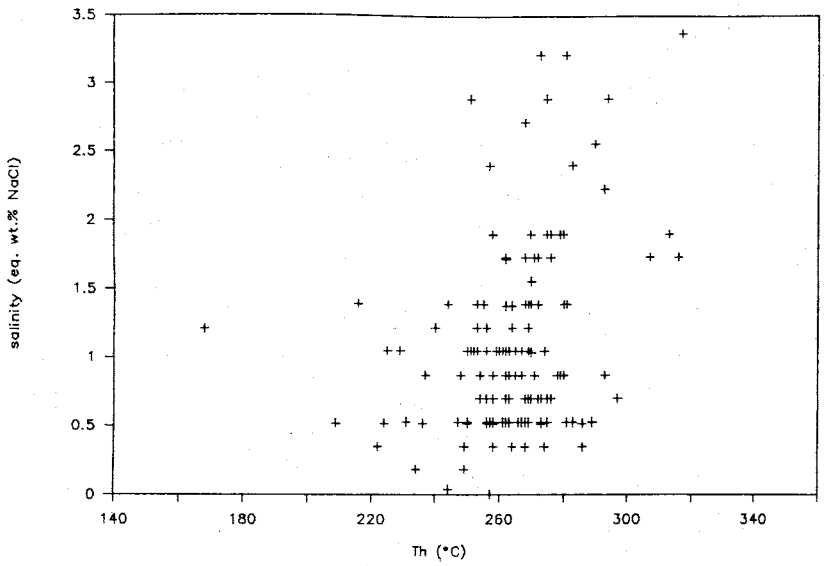

St. Cloud – Stage 2

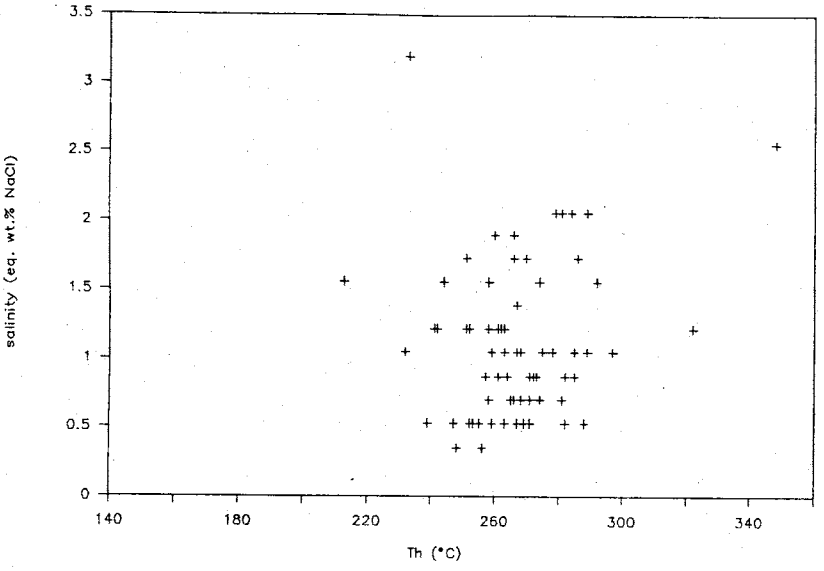

St. Cloud – Non-Ore-Grade

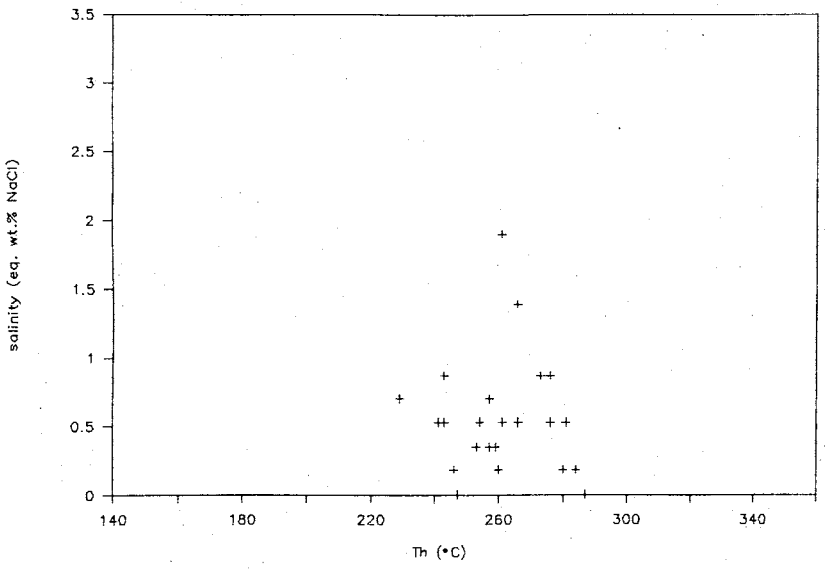

U.S. Treasury – Stage 1

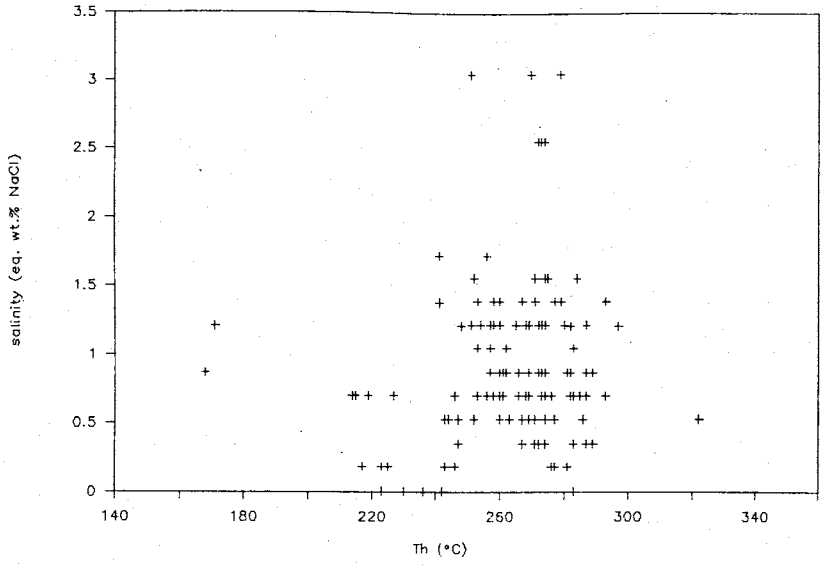

U.S. Treasury – Stage 2

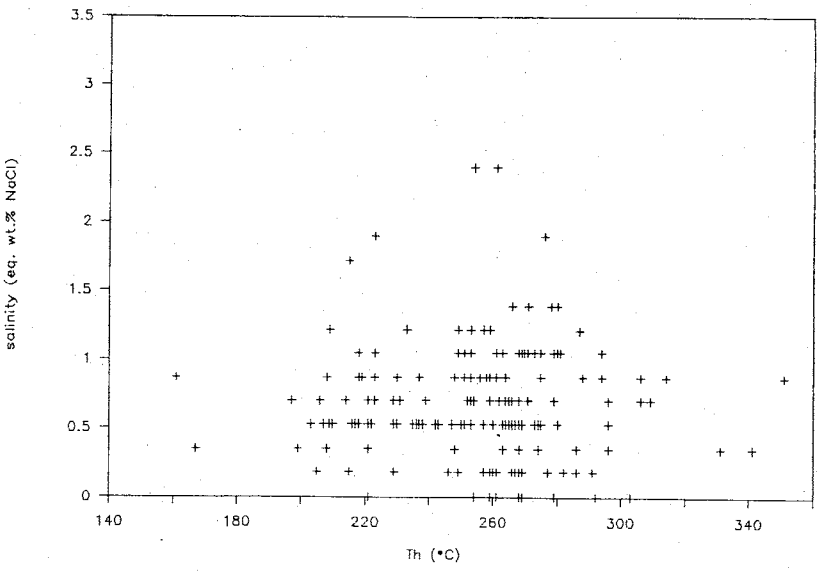

U.S. Treasury – Non-Ore-Grade

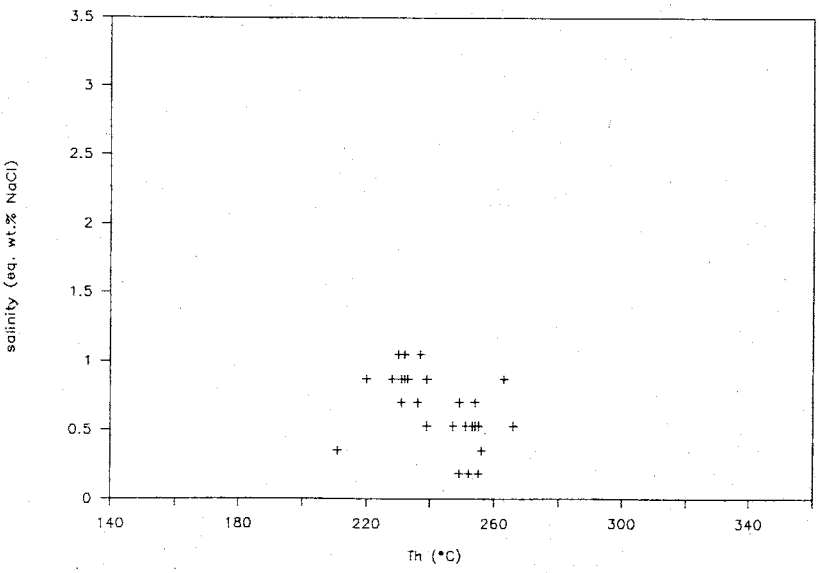

Figure 9. Th and Salinity Histograms for Different Mine Elevations in each Mineralization Stage of Both Mines.

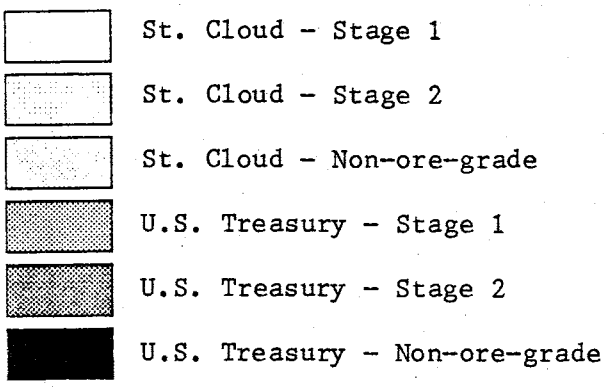

St. Cloud

7000 feet
(2134 meters)

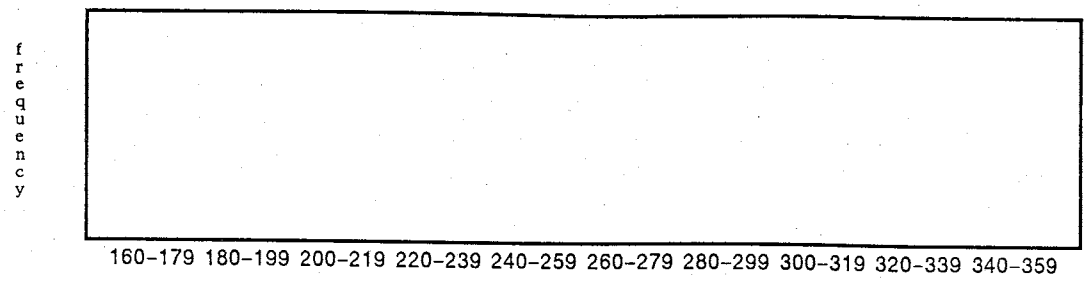

6800 feet
(2073 meters)

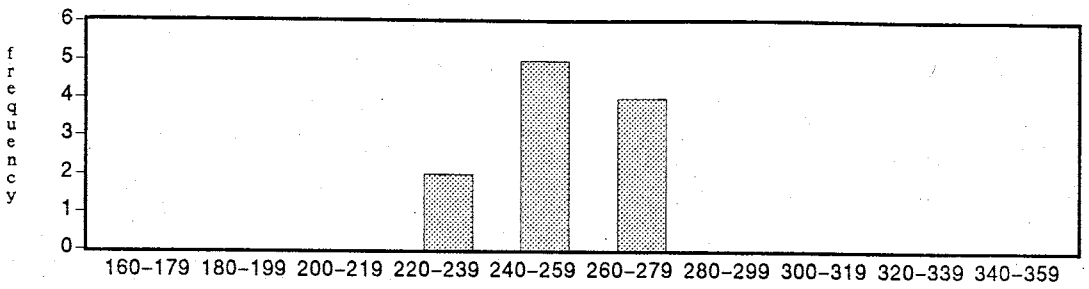

6600 feet
(2012 meters)

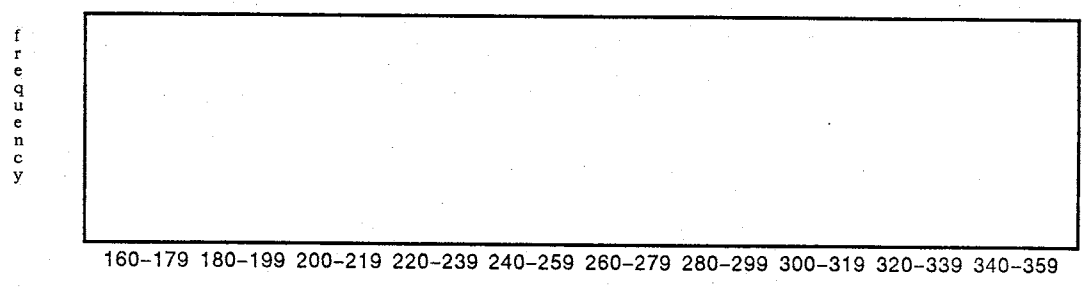

6400 feet
(1951 meters)

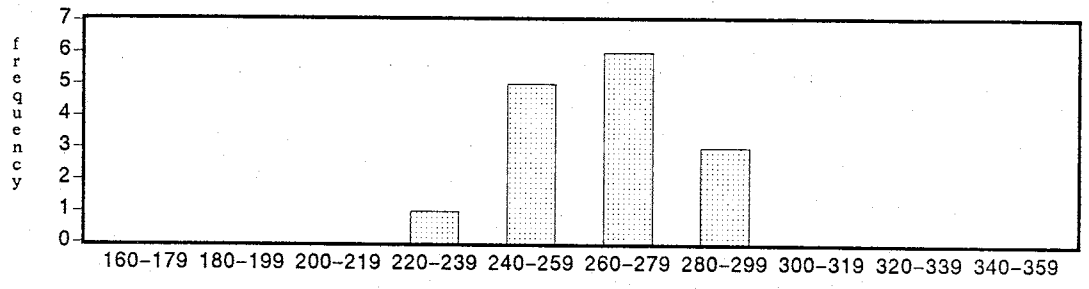

6200 feet
(1890 meters)

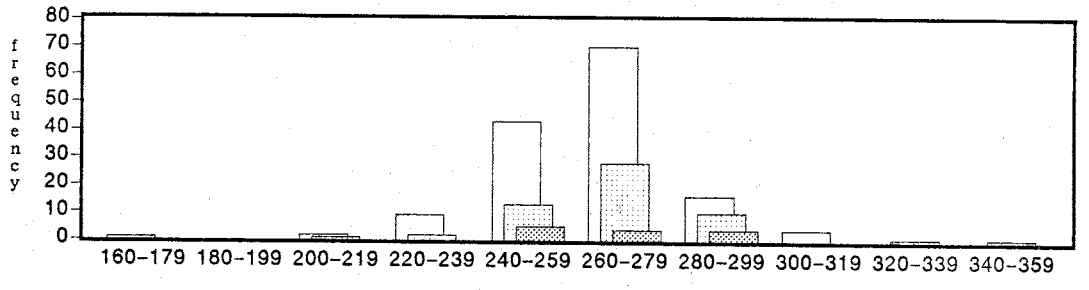

6000 feet
(1829 meters)

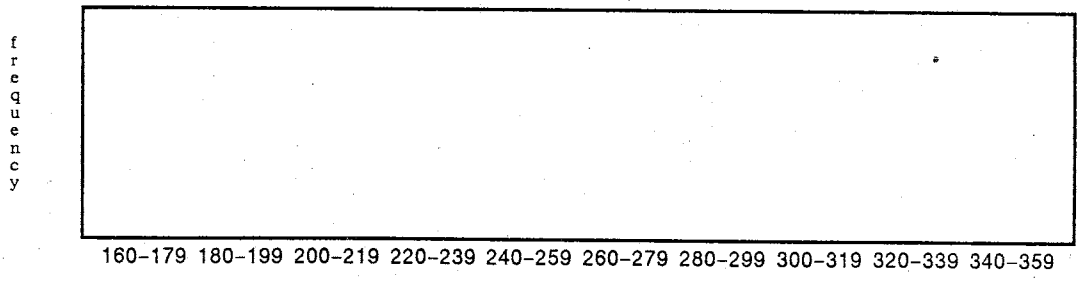

Th (℃)

St. Cloud

7000 feet
(2134 meters)

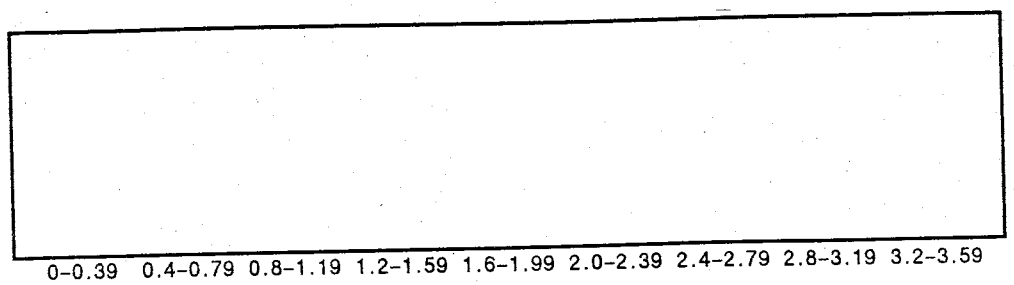

6800 feet
(2073 meters)

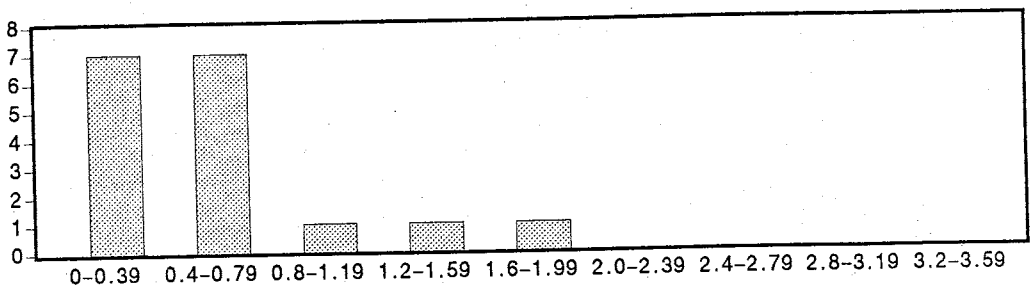

6600 feet
(2012 meters)

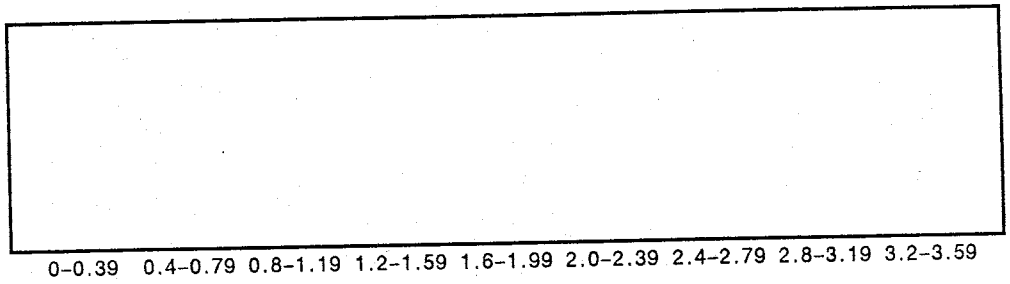

6400 feet
(1951 meters)

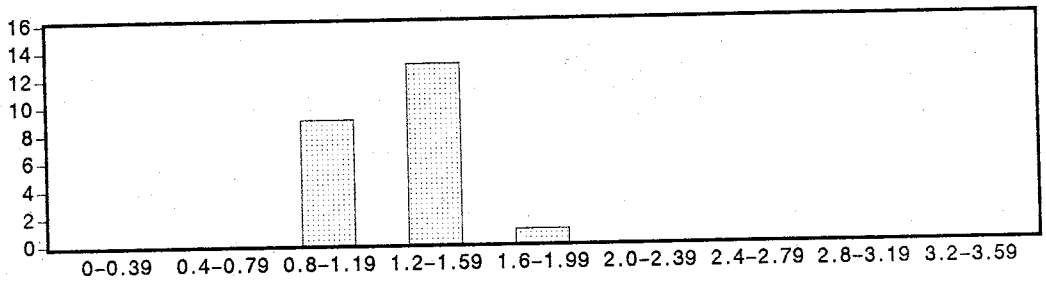

6200 feet
(1890 meters)

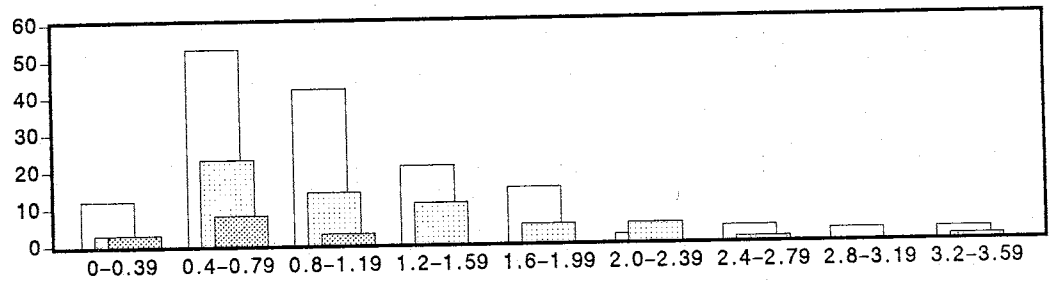

6000 feet
(1829 meters)

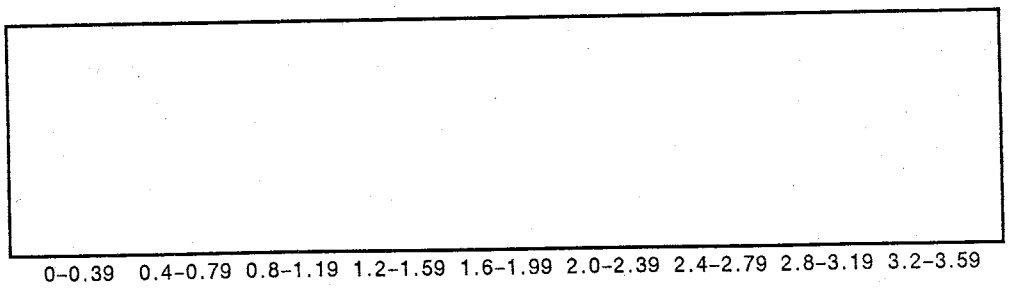

Salinity (eq. wt. percent NaCl)

U.S. Treasury

7000 feet
(2134 meters)

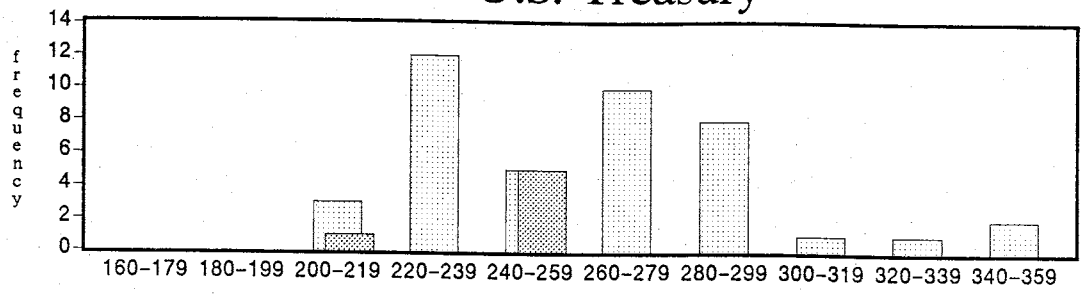

6800 feet
(2073 meters)

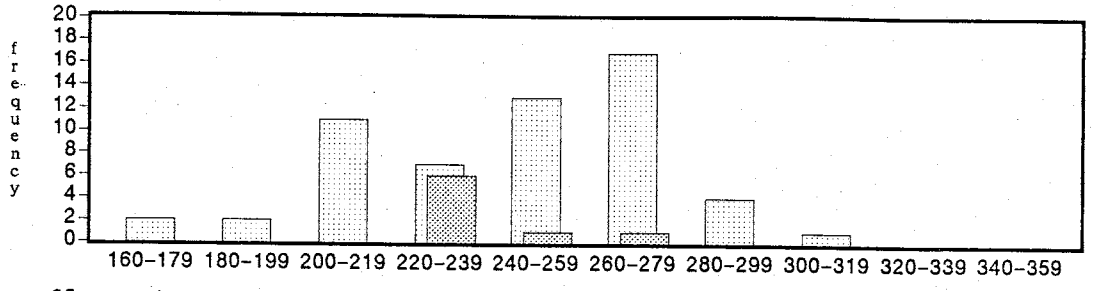

6600 feet
(2012 meters)

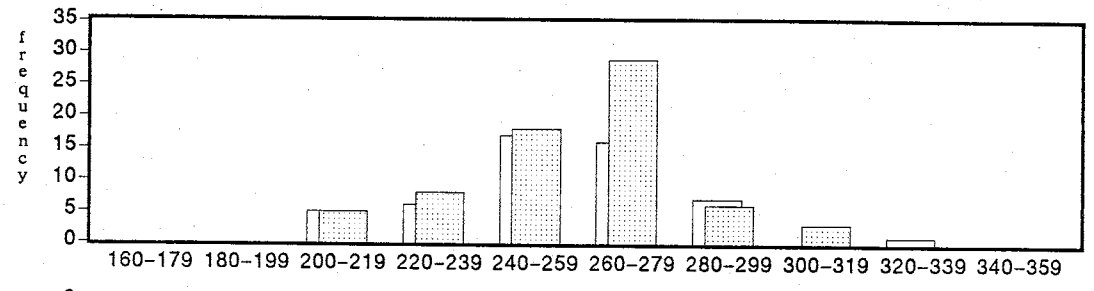

6400 feet
(1951 meters)

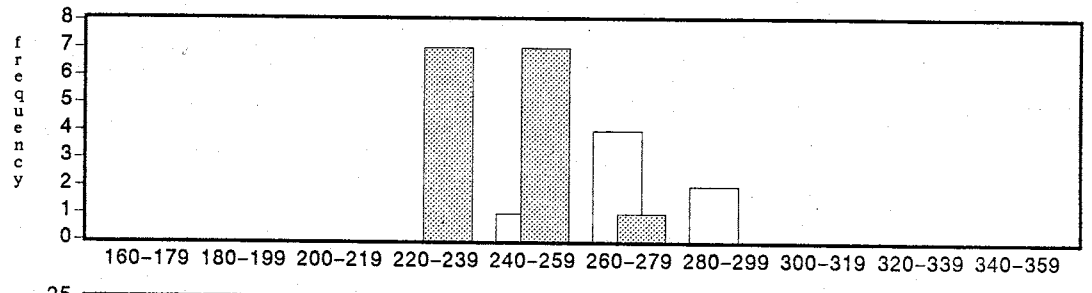

6200 feet
(1890 meters)

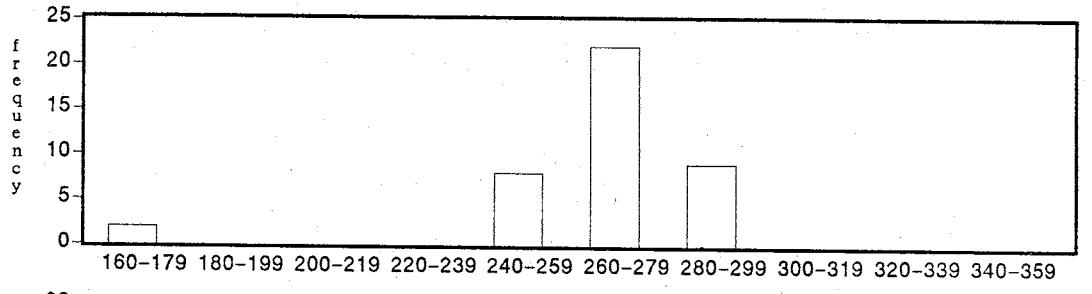

6000 feet
(1829 meters)

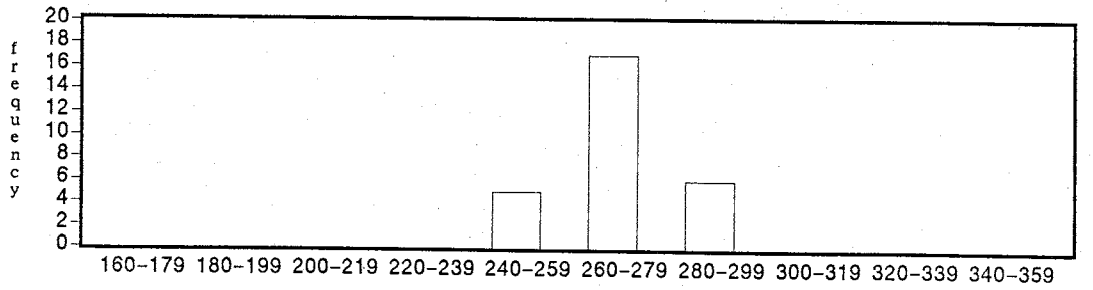

Th (°C)

U.S. Treasury

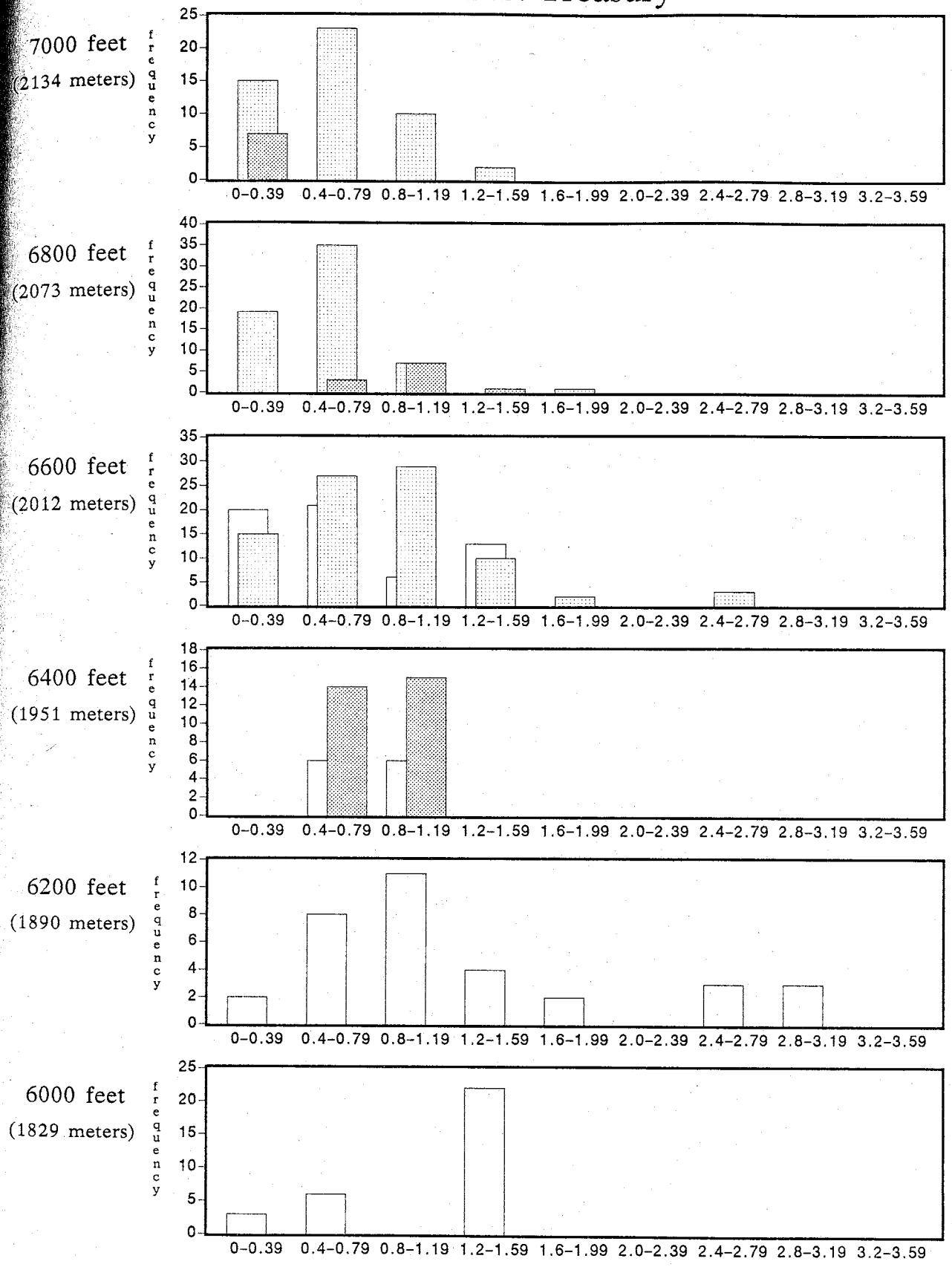
7000 feet
(2134 meters)
6800 feet
(2073 meters)
6600 feet
(2012 meters)
6400 feet
(1951 meters)
6200 feet
(1890 meters)
6000 feet
(1829 meters)
frequency
0–0.39
0.4–0.79
0.8–1.19
1.2–1.59
1.6–1.99
2.0–2.39
2.4–2.79
2.8–3.19
3.2–3.59
Salinity (eq. wt. percent NaCl)

Table 2. Temperature and Salinity Averages for Mineralization Stages of the St. Cloud-U.S. Treasury Deposit.

	T°C (average)	standard deviation	number of samples	salinity (wt.% NaCl eq.)	standard deviation	number of samples
St. Cloud stage 1	263	19	145	1.05	0.66	155
St. Cloud stage 2	267	19	71	1.12	0.54	86
St. Cloud non-ore-grade	260	16	24	0.55	0.38	31
U.S. Treasury stage 1	263	22	128	0.89	0.57	146
U.S. Treasury stage 2	255	29	169	0.66	0.42	199
U.S. Treasury non-ore-grade	243	13	29	0.65	0.26	37

The data in Table 2 and Figure 7 indicate that the St. Cloud mine had equal or slightly higher temperatures and salinities compared to those of the U.S. Treasury mine. Average temperature of stage 1 samples from both mines were 263°C. Average temperatures from stage 2 were higher in the St. Cloud mine at 267°C as compared to 255°C in the U.S. Treasury mine. Temperatures for mineralized stages from U.S. Treasury samples also have a greater range than those from St. Cloud samples. St. Cloud salinities are higher and have a greater range than those of the U.S. Treasury mine. The temperatures and salinities from non-ore-grade samples are the lowest in the system for each mine.

The plots in Figure 8 indicate general trends of ore fluids cooling with decreasing salinities. The mineralization stages in the St. Cloud mine best show this relationship. The U.S. Treasury samples

show a wide range in temperatures which obscures the relationship between temperature and salinity.

The histograms in Figure 9 show general trends of decreasing temperature and salinity in ore fluids with increasing elevation in both mines. This suggests that cooling and dilution of ore fluids occurred as the solutions rose in the St. Cloud-U.S. Treasury vein system.

Gas Analyses

The volatile species measured in inclusion fluids were carbon dioxide, nitrogen, organic compounds, hydrogen sulfide, methane, hydrogen, carbon monoxide, helium, and argon in decreasing order of concentration. Total gasses measured averaged 0.5 mole percent. The precision of the volatile analyses are estimated to be $\pm$10 percent (Norman and Sawkins, 1987).

The amounts of the major volatiles vary with elevation in both mines (Figure 10). In general, the concentrations of gaseous species increase with increasing elevation. A notable exception to this is hydrogen sulfide concentrations which decrease with increasing elevation.

Relatively high gas concentrations were measured in surface samples and in a few samples collected within ore zones. The greatest measured concentrations of gasses were from surface samples which were collected along the strike length of the vein. These samples are not indicative of processes which occurred within the studied ore zones;

Figure 10. Plots of Elevation versus Amounts of Volatiles from Fluid Inclusion Analyses for each Mineralization Stage of Both Mines.

1 = Stage 1

2 = Stage 2

3 = Non-Ore-Grade

4 = Surface

CARBON DIOXIDE

ST. CLOUD

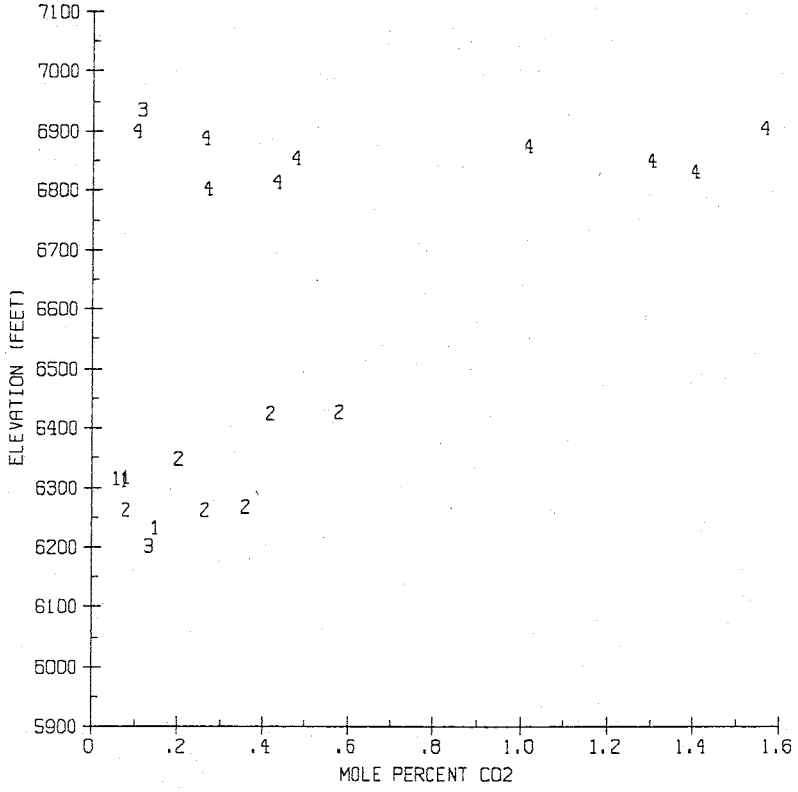

U.S. TREASURY

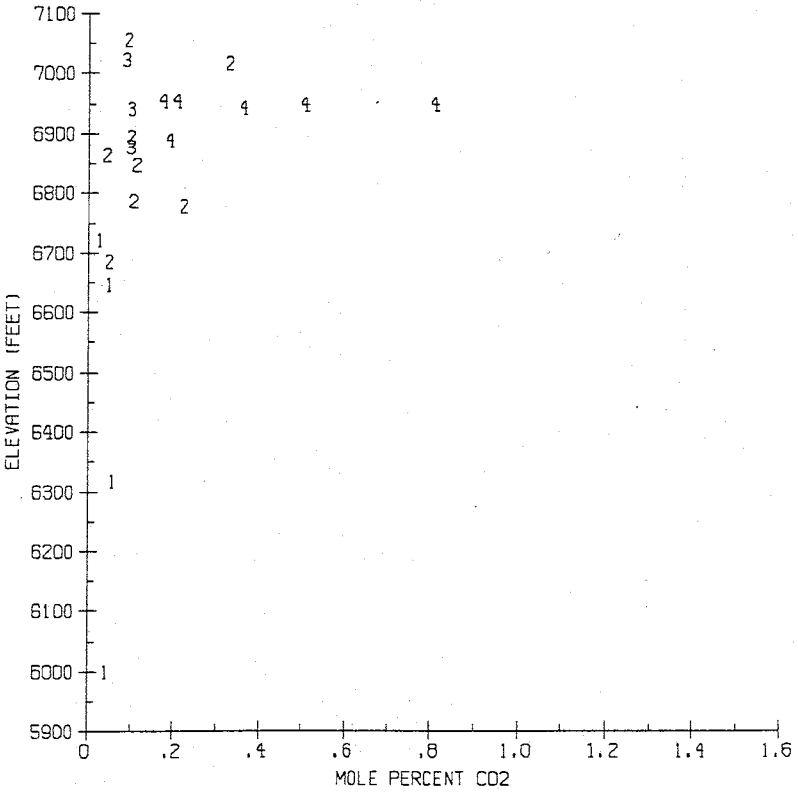

NITROGEN

ST. CLOUD

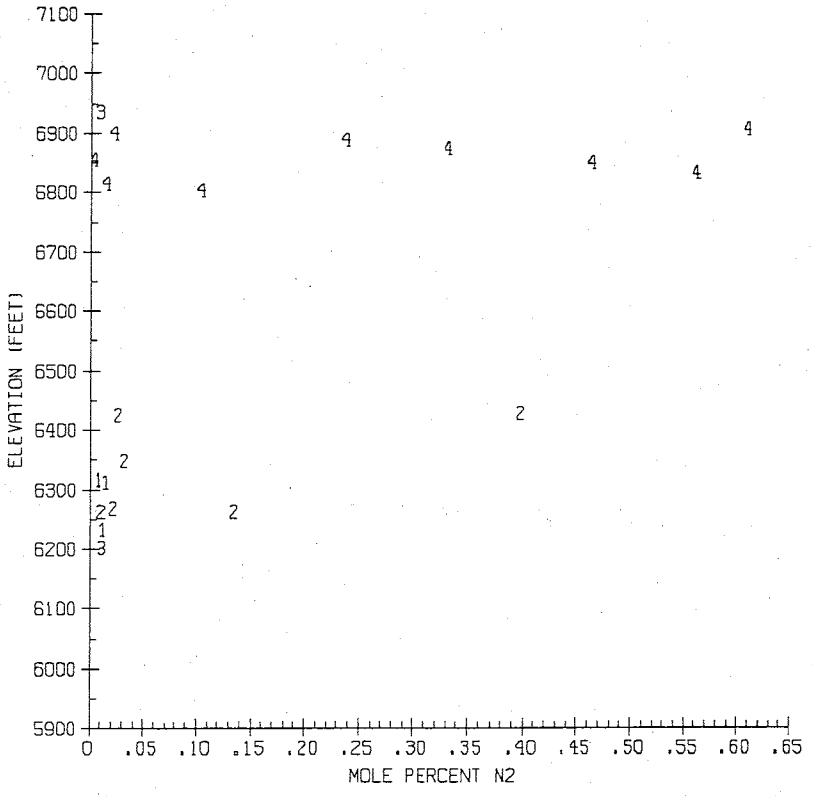

U.S. TREASURY

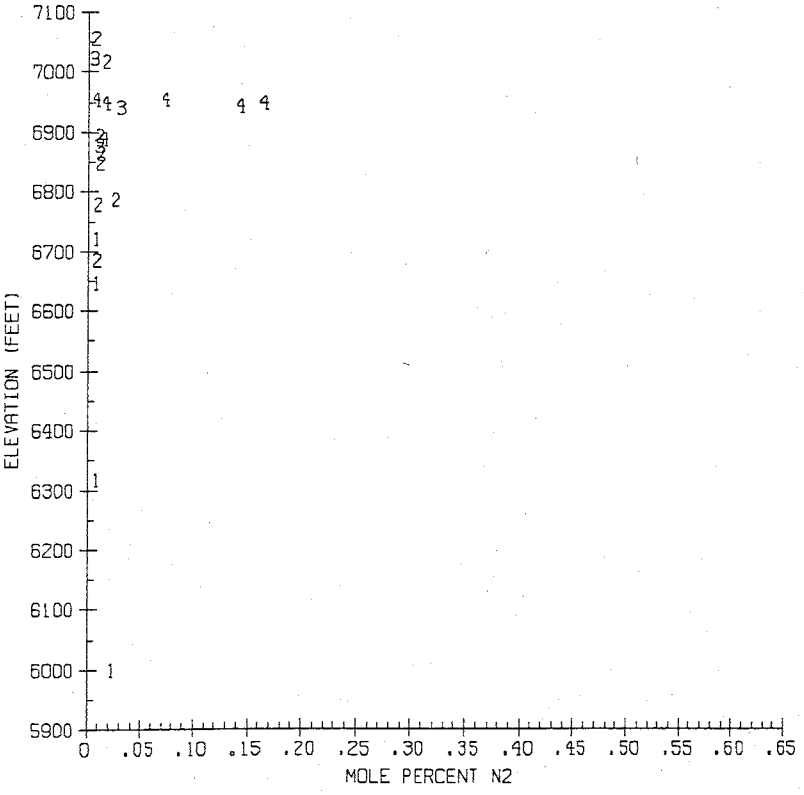

ORGANIC SPECIES

ST. CLOUD

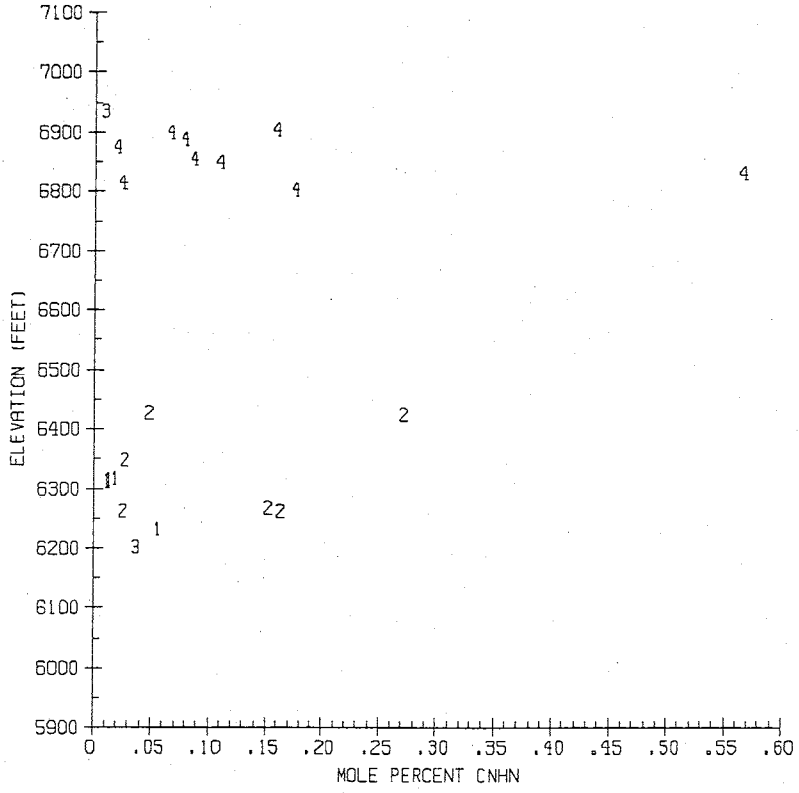

U.S. TREASURY

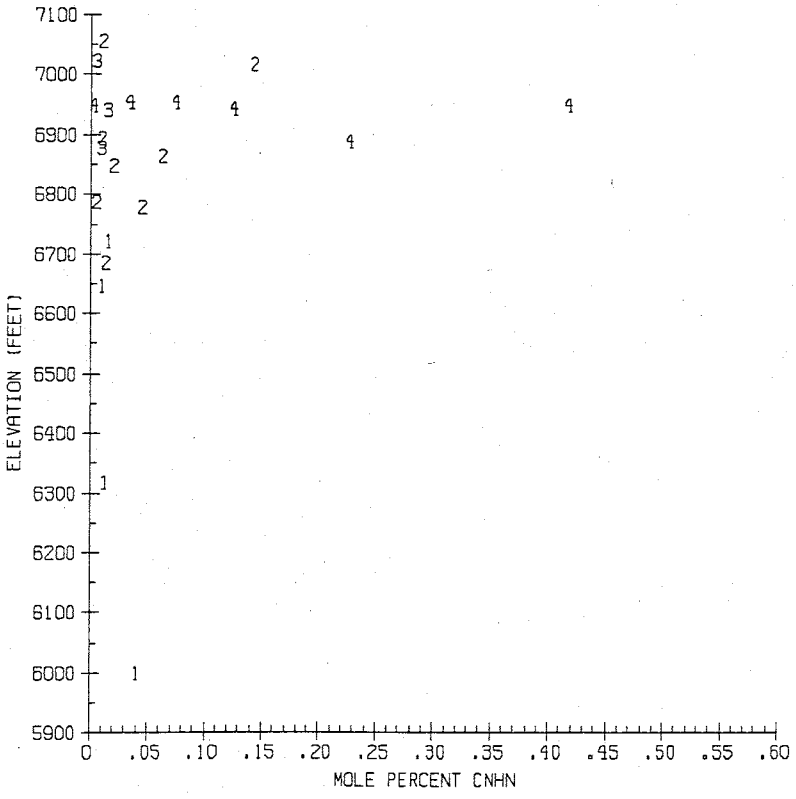

HYDROGEN SULFIDE

ST. CLOUD

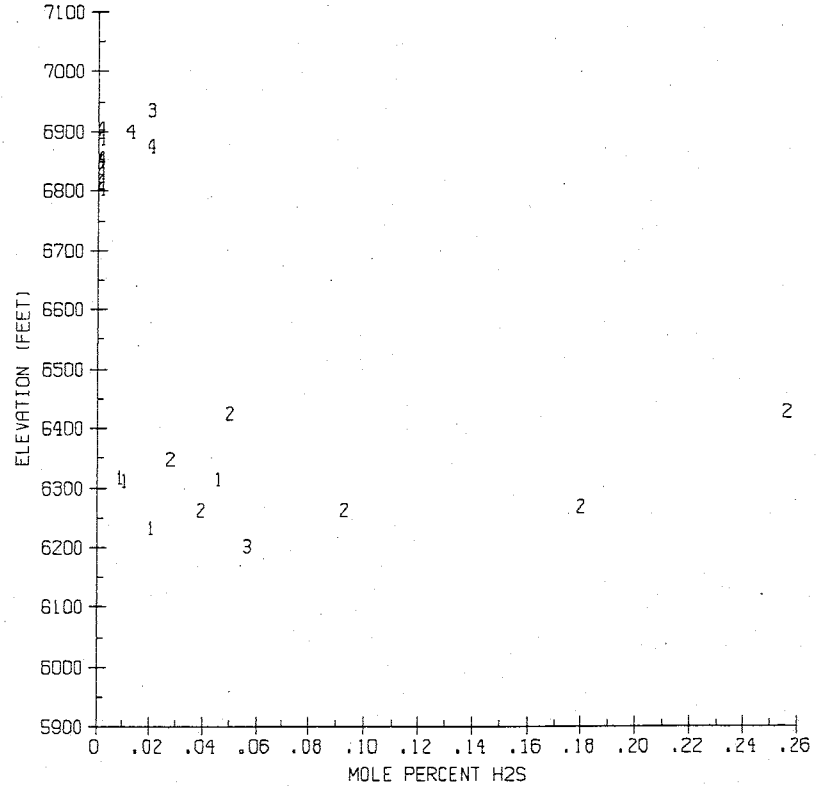

U.S. TREASURY

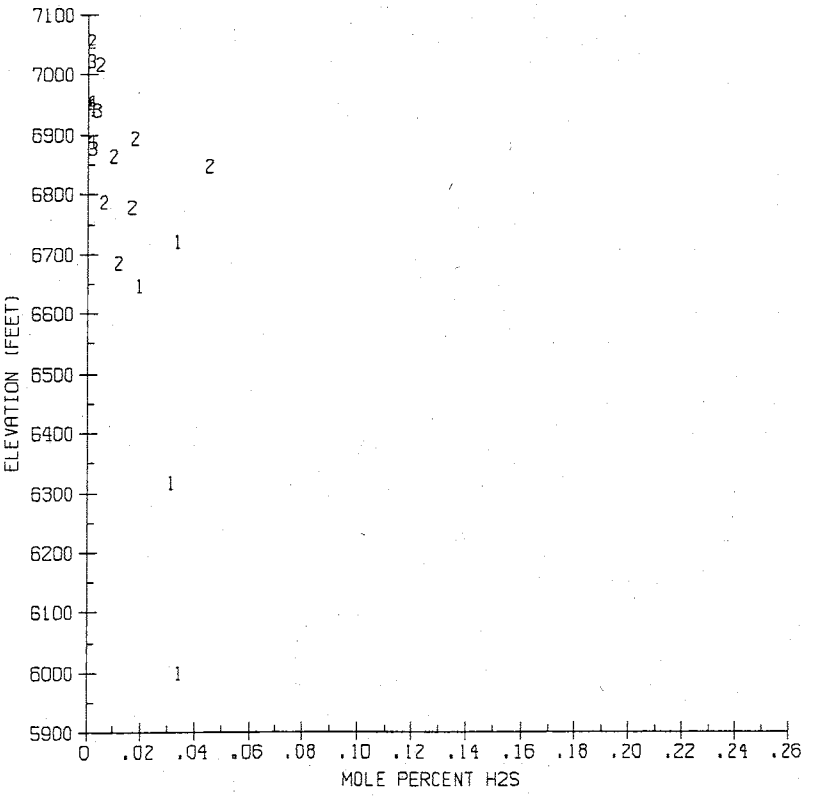

METHANE

ST. CLOUD

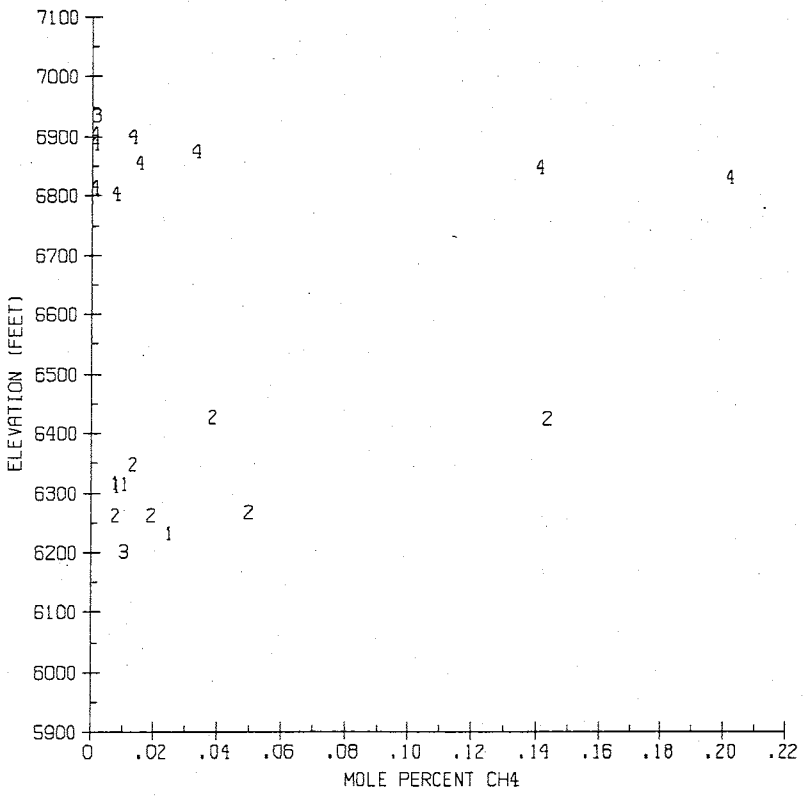

U.S. TREASURY

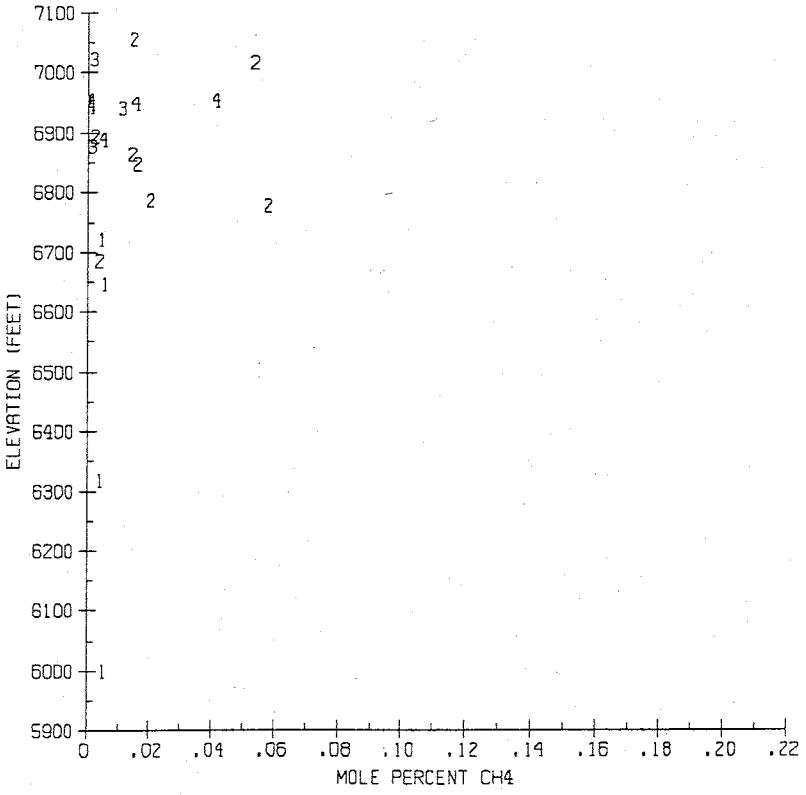

HYDROGEN

ST. CLOUD

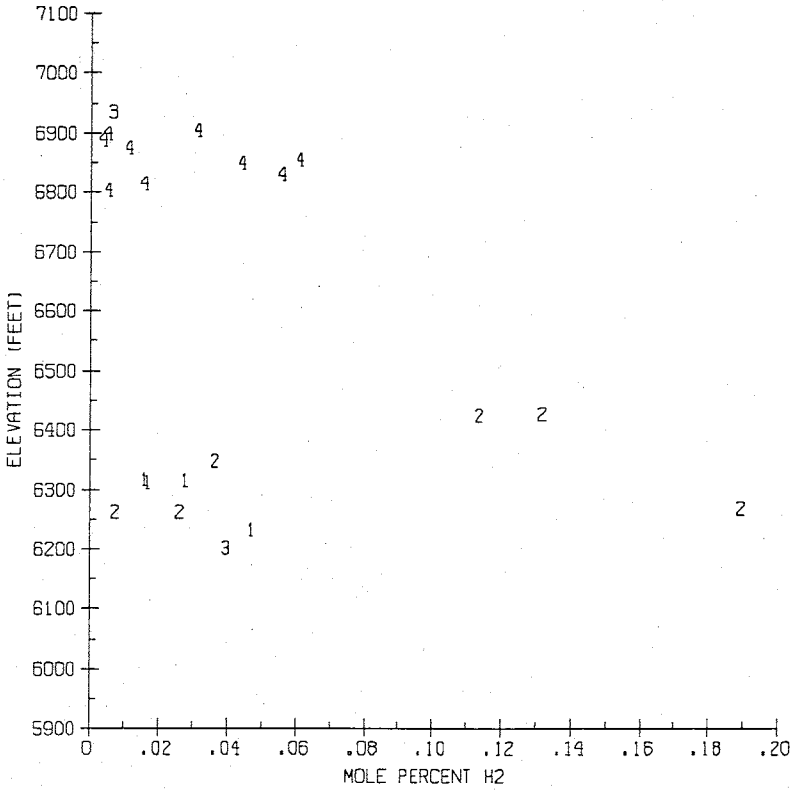

U.S. TREASURY

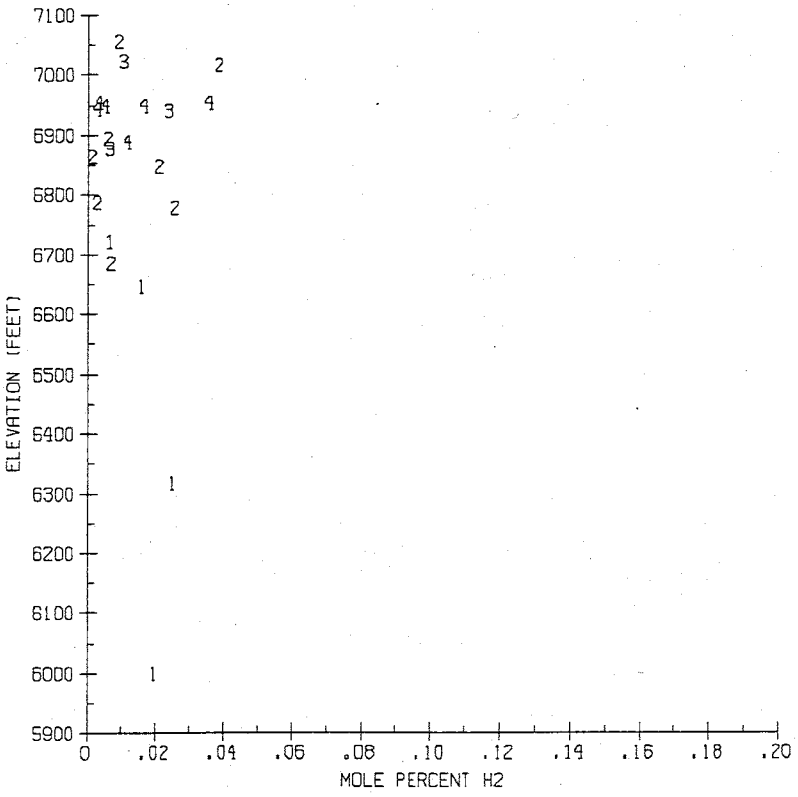

CARBON MONOXIDE

ST. CLOUD

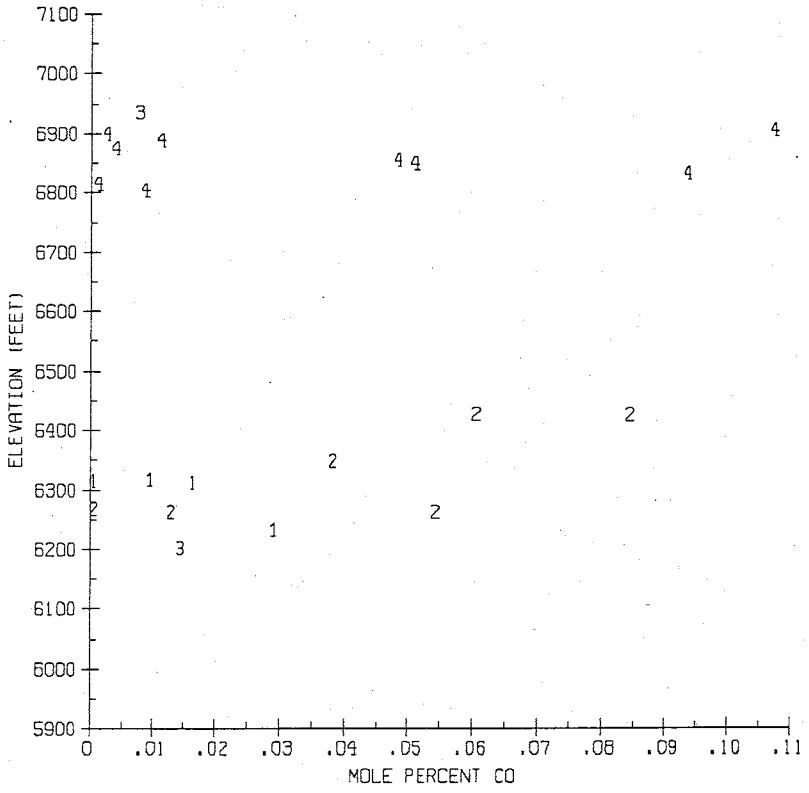

U.S. TREASURY

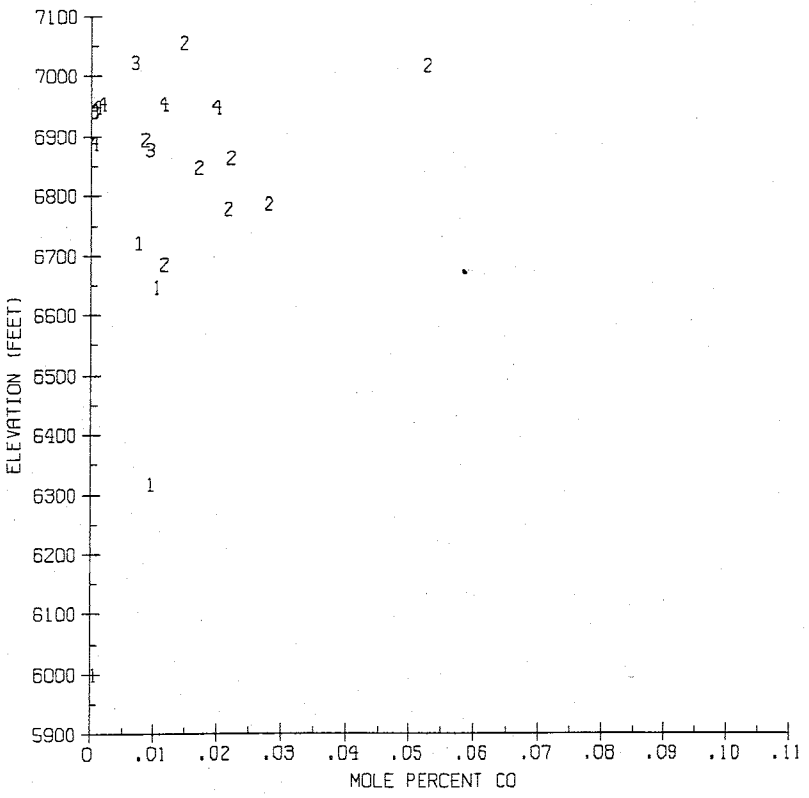

HELIUM

ST. CLOUD

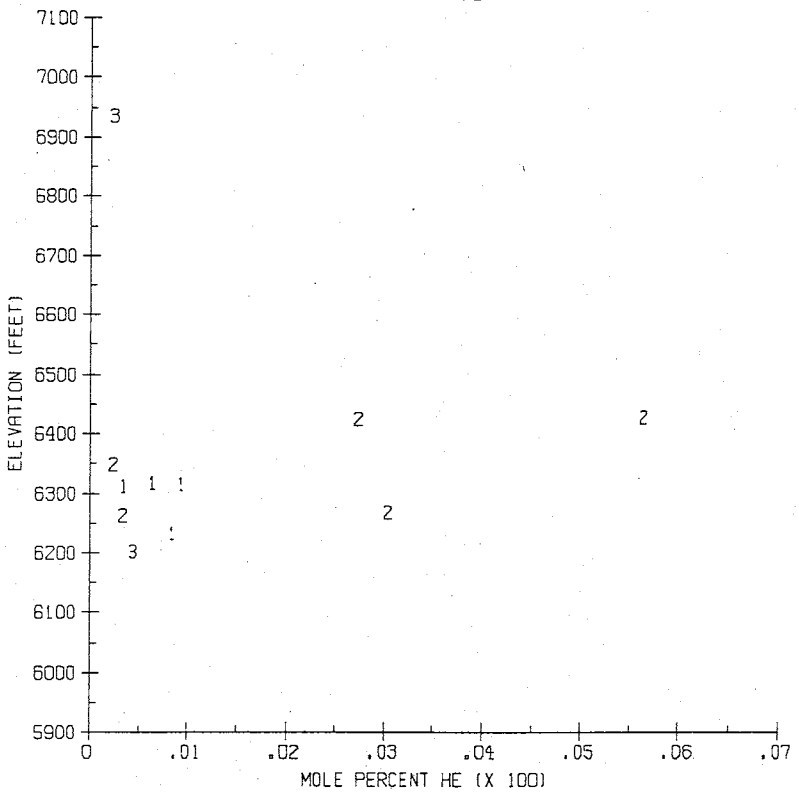

U.S. TREASURY

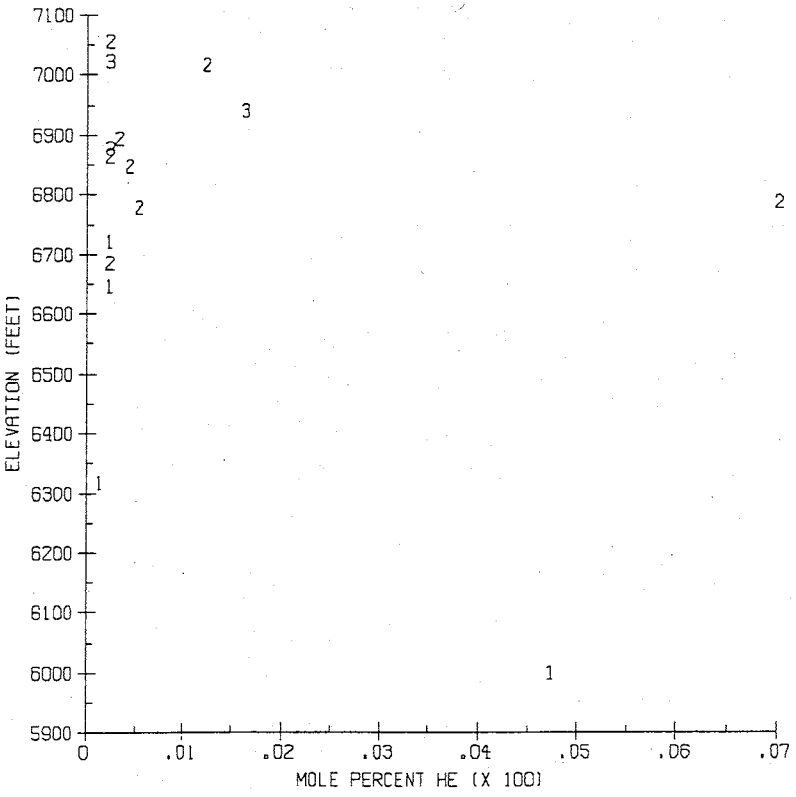

however, they illustrate that fluid inclusions formed over ore mineralization trap exsolved volatiles bouyantly segregated from a mineralizing fluid. Relatively high gas contents were measured in six samples from stage 2 and surface samples from the St. Cloud mine (SC70B, SC70C, U14B, SC09, SC010, SC015). These high concentrations suggest that volatiles which exsolved from mineralizing solutions during boiling were preferentially trapped in fluid inclusions; as ore fluids boil, vapor bubbles nucleate on fluid-solid interfaces and can be trapped in an inclusion resulting in high gas-content measurements in the inclusions (Norman and Sawkins, 1987).

The data of Figure 10 and Appendix C show relatively high concentrations of hydrogen and carbon dioxide in sample analyses. Considering that the gas analyses were conducted on samples obtained through thermal decrepitation, it is suspected that the gasses have reequilibrated at a temperature higher (500°C) than the homogenization temperature of the inclusions. This reequilibration would produce increased amounts of hydrogen and carbon dioxide according to the reaction:

$$2\ H_2O + CH_4 \rightarrow CO_2 + 4\ H_2.$$

Using this equation, calculations were made to determine gas concentrations more representative of the phases present at the temperature of inclusion formation. A computer program, GASFIX, (Norman, unpublished) was used to make these calculations. A listing of this program and the recalculated gas data are in Appendix D. The GASFIX program also calculates oxygen and sulfur fugacities (Table 3) from the measured gas concentrations based on the reactions:

$$H_2O \leftrightarrow H_2 + 1/2\ O_2 \quad \text{and} \quad 2\ H_2S + O_2 \leftrightarrow S_2 + 2\ H_2O.$$

Table 3. Results of log $f(O_2)$ Calculations.

	Sample	log $f(O_2)$	log $f(S_2)$
St. Cloud stage 1	SC4E	-37.1	-12.5
	SC4F	-38.0	-11.2
	SC4H	-37.5	-12.4
	U19A	-38.2	-12.0
St. Cloud stage 2	SC4C	-37.5	-11.5
	SC70C	-37.9	-11.4
	U14B	-36.0	-9.9
	U15B	-38.0	-10.3
	U15C	-36.4	-11.1
St. Cloud non-ore-grade	S10	-37.6	-11.1
	U16E	-37.4	-10.9
U.S. Treasury stage 1	SC53C	-37.0	-11.3
	SC58C	-37.2	-11.3
	SC59A	-39.8	-12.0
	RH3	-37.1	-11.3
U.S. Treasury stage 2	SC60B	-37.6	-11.7
	SC61	-36.0	-13.3
	SC62A	-39.4	-12.4
	SC62B	-37.1	-12.9
	S6	-39.8	-16.9
	RH1	-42.1	-11.8
	RH2	-38.0	-11.1
	RH4	-37.0	-12.1
U.S. Treasury non-ore-grade	SC63	-39.7	-14.0
	S5	-37.8	-23.9

Volatile organic species were observed from mass spectrometric analyses. The different high-mass-number species could not be discerned, so species were approximated and their mole percent concentration totals from data reduction procedures were reported as C_nH_n, or organic species (Appendix C). Differentiating these hydrocarbon species was achieved by gas chromatography-mass spectrometry (GC/MS). Samples for GC/MS analyses were limited and in some cases, samples were lost during the analytical procedures, or

concentrations of carbon dioxide, water, or air dominated the spectra. However, enough analyses were made to identify species in the different zones of the deposit. The hydrocarbons observed are C_3 to C_5 alkenes: propylene, butene, and pentene. Quantitatively, the amount of pentene is approximately half the amounts of propylene and butene. These three species were observed to exist in both mineralizing stages and in non-ore-grade zones with the exception of pentene which was not observed in the samples from non-ore-grade zones.

Solute Analyses

Concentrations of sodium, potassium, calcium, and magnesium were measured by inductively-coupled plasma atomic-emission spectroscopy (ICP), and concentrations of chloride and sulfate were measured by high-performance liquid chromatography (HPLC); nitrate and other metals were below the detections limits of the analyses. The results of these analyses and the percent error of the ion balance calculations are in Appendix E. The ICP analyses are precise to approximately 100 ppm, except for potassium analyses which are precise to approximately 500 ppm. The HPLC analyses are precise to approximately 100 ppm. The dilution techniques used for these measurements was prone to experimental error due to the small volumes of inclusion fluids and the large dilutions necessary to obtain sufficient sample for analysis.

The results from these analyses indicate that sodium, calcium, and chloride were the principle solute components in inclusion fluids. To evaluate these measurements, thermometrically-measured salinities were compared to solute concentrations determined from HPLC-ICP analyses

(Table 4). These salinity values were converted to equivalent weight percent NaCl and corrected for volatile concentrations; the average gas-content of 0.5 mole percent in this system can add up to 0.5 equivalent weight percent NaCl to salinity calculations measured thermometrically (Hedenquist and Henley, 1985).

In addition, the Na-K-Ca chemical geothermometer proposed by Fournier and Truesdell (1973) was used to estimate temperatures based on the solute analyses. This empirical geothermometer calculates an equilibrium temperature based on the equation:

$$T(K) = \frac{1647}{\log (Na/K) + 1/3 \ (\log (\sqrt{Ca}/Na) + 2.06) + 2.47}$$

The calculated temperatures are compared to thermometrically determined temperatures also in Table 4.

The evaluation of solute concentrations by salinity comparisons shows that the HPLC-ICP-measured and thermometrically-measured salinity values differ by a range of +2.2 to -1.3 equivalent weight percent NaCl. Sample contamination may have resulted in increased HPLC-ICP salinity results; low HPLC-ICP salinities may have resulted from insufficient leaching of the grain surfaces or solutes may have been lost during inclusion decrepitation. The chemical geothermometry calculations show a poorer correlation with thermometric values. Temperature values between the measured and calculated values varies from differences of +87 to -157, but average only $-4^{\circ}C$. The sources of error mentioned above would also account for these deviating values. Both techniques yield values comparable in range to values obtained thermometrically, but geothermometry should not be used as an alternative method to thermometric analyses.

Table 4. Comparison of ICP-HPLC Solute Concentrations to Thermometric Results through Salinity and Chemical Geothermometry Calculations (salinity as equivalent weight percent NaCl; D = difference).

	salinity			T (°C)			
Sample	HPLC-ICP	thermometric	D	thermometric	Na-K-Ca	D	pH
St. Cloud stage 1							
SC4E	0.2	1.0	-0.8	269	273	-4	5.5
SC4F	1.3	0.6	+0.7	260	249	+11	5.8
SC4H	0.3	1.3	-1.0	264	289	-25	5.4
U19A	2.9	0.7	+2.2	257	194	+63	5.8
stage 2							
SC4C	0.7	0.7	0.0	264	227	+37	5.8
SC70C	0.6	1.2	-0.6	263	242	+21	5.5
U14B	0.3	1.2	-0.9	286	278	+8	5.4
U15B	0.3	1.0	-0.7	256	260	-4	5.6
U15C	0.4	1.6	-1.2	278	262	+16	5.3
non-ore-grade							
S10	0.2	0.5	-0.3	253	247	+6	5.9
U16E	1.5	0.6	-0.9	265	178	+87	5.8
U.S. Treasury stage 1							
SC53C	0.2	1.5	-1.3	269	287	-18	5.4
SC58C	0.3	1.4	-1.1	268	222	+46	5.4
SC59A	0.2	0.6	-0.4	237	290	-53	6.0
RH3	0.2	0.7	-0.5	269	426	-157	5.7
stage 2							
SC62B	0.1	0.1	0.0	268	270	-2	6.6
S6	0.1	0.6	-0.5	238	268	-30	5.9
RH1	0.1	0.5	-0.4	217	222	-5	6.1
RH2	0.3	0.4	-0.1	258	259	-1	6.0
RH4	0.1	1.1	-1.0	268	286	-18	5.5
non-ore-grade							
SC63	0.1	0.9	-0.8	237	304	-67	5.7
S5	0.2	0.3	-0.1	254	250	+4	6.2

The Na-K-Ca geothermometer was also used to calculate the pH of the ore fluids since it could not be measured experimentally. The results of the calculations are also shown in Table 4. The calculated pH-values have a limited range from 5.3 to 6.6. This pH range is approximately neutral; neutral pH at 250°C is 5.6. The pH-values were

used to calculate bicarbonate concentrations in the ore fluids using the reaction:

$$H_2CO_3 \rightarrow H^+ + HCO_3^-.$$

Thermodynamic data for this reaction was taken from Helgeson (1969). The results of this calculation are in Appendix E. Bicarbonate concentrations were also included in the ion balance calculations in Appendix E.

Isotope Analyses

The d ^{18}O and d D of the mineralizing fluids was determined from six samples of quartz and the waters extracted from their fluid inclusions. The d ^{18}O composition of the inclusion fluids was calculated from the d ^{18}O composition measured in the quartz using average Th values and the fractionation equation of Clayton et al. (1972):

$$10^3 \ln a = ((3.38 \times 10^6) \times T^2) - 3.40$$

The data and calculations are shown in Table 5 and Figure 11.

Table 5. Oxygen and Hydrogen Stable Isotope Data (expressed as parts per thousand).

	sample	elevation (feet)	d ^{18}O quartz	d ^{18}O water	d D water
Stage 1	U19A	6232	5.84	-2.79	-42
	SC59A	6009	5.02	-4.75	-44
Stage 2	SC61	7017	6.84	-0.65	-52
	SC60B	6864	7.65	-1.21	-69
	SC62A	6779	6.71	-2.53	-79
	SC70C	6425	6.78	-1.58	-85

Figure 11. Plot of Ore-fluid Hydrogen and Oxygen Stable Isotopic Compositions.

+ = Stage 1

* = Stage 2

■ = Composition of Tertiary Meteoric Water (Taylor, 1974)

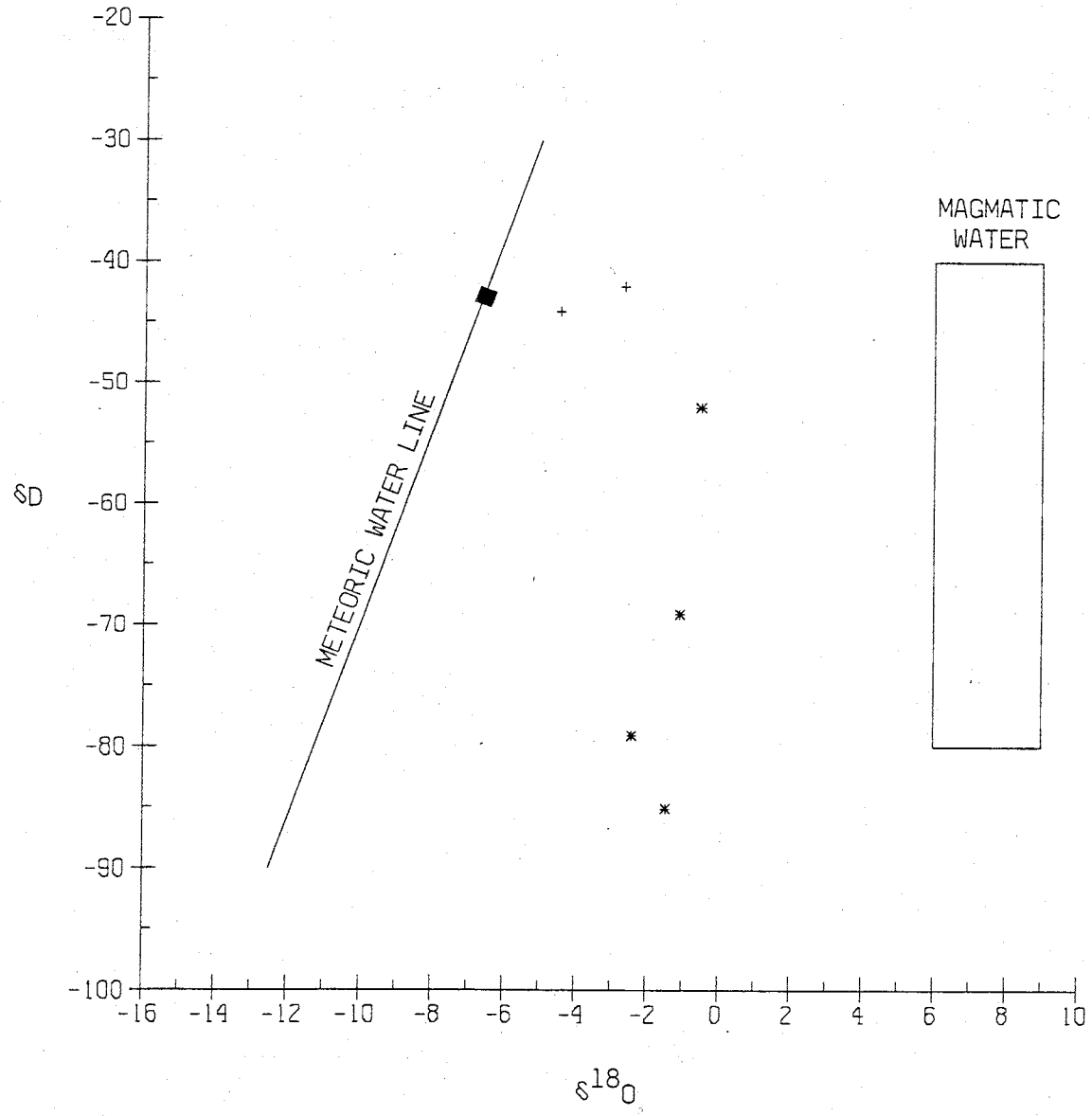
-20
-30
-40
-50
-60
-70
-80
-90
-100
δD
-16
-14
-12
-10
-8
-6
-4
-2
0
2
4
6
8
10
δ18O
METEORIC WATER LINE
MAGMATIC
WATER

The analyses for stage 1 have heavier d D and lighter d ^{18}O values with respect to stage 2 values. The d ^{18}O composition has a limited range of -0.65 to -4.57 °/oo. The d D compositions have a large range from -42 to -85 °/oo and stage two values show a trend of increasing d D with increasing elevation. In epithermal systems, a single meteoric water will have a fairly constant d D value, and a range in d ^{18}O as a result of interactions with silicate rocks of varying isotopic compositions, or variable amounts of fluid interactions with silicate rocks. The differences in d D between the two fluid-stages suggests two unique fluids were responsible for mineralization.

Helium isotopic compositions were measured to aid in determining fluid origins. Helium isotope data is denoted as ratios (R) of the ^{3}He to ^{4}He compositions and is expressed in a ratio with the R-value of air (R(air): 1.4×10^{-6}). The R/R(air) ratios of the two stages of mineralization at the St. Cloud-U.S. Treasury deposit, as well as the ratios of components which may have affected their helium isotopic signatures are shown in Table 6.

Table 6. Helium Isotope Data.

	R/R(air)
SC-UST stage 1	0.17
SC-UST stage 2	0.50
Mantle	8.57
Atmosphere	1.00
Crust	0.01
U-Th-minerals	0.0007

To distinguish between contributions of mantle or ground-water helium in mineralizing fluids, the R-values of possible fluid sources

are compared to those measured from gasses dissolved in inclusion fluids. Primordial helium, retained in the earth's mantle, is believed to be enriched in the ^{3}He isotope so that any mantle-derived fluids would have high $^{3}He/^{4}He$ ratios (R(mantle)=1.2 x 10^{-5}) (Lupton, 1983; Ozima and Podosek, 1983; Mamyrin and Tolstikhin, 1984). A fluid derived from the mantle is distinguished by its low $^{3}He/^{4}He$ ratio. The helium signature of fluids that have contacted uranium-bearing terrestrial rocks is distinctive in its high R-value. The in-situ radioactive decay of uranium and thorium produces helium with a $^{3}He/^{4}He$ ratio of 1.0 x 10^{-9}. The average crust has an R-value of 2.0 x 10^{-8} (Mamyrin and Tolstikhin, 1984). Contamination of small amounts of atmospheric helium within fluid inclusions causes R/R(atm) ratios to approach 1. A ratio greater than 1 is indicative of a mantle component of helium.

The values obtained for the helium in fluid inclusions from the St. Cloud-U.S. Treasury mines are inconclusive. Only values greater than 1, or much less than 1, are indicative of fluid origins. The measured compositions have probably been altered by many possible sources, including interactions with the uranium-bearing Abo Formation. Evidence does not exist to distinguish mantle or meteoric water sources of the helium compositions.

Conodont Analyses

Conodonts are microscopic fossils of a Paleozoic marine organism in the phyllum Conodonta; this organism has been described by Briggs et al. (1983) and Aldridge (1987). Conodonts have found application to

geothermometry (Epstein et al. 1977; Cook, 1986) in that their color alters progressively and irreversibly as a function of temperature and time, but independent of pressure (Epstein et al. 1977). Conodonts are initially pale-yellow, turning black, to gray, to opaque-white with increasing temperature. This color change occurs as organic matter within the fossil undergoes carbon-fixing then carbon-loss with increasing temperature. The range of the color-alteration-index (CAI) values is one to eight corresponding to temperatures of 50°C to greater than 450°C. The data from four samples is in Table 7.

Time is a significant parameter in the color alteration of conodonts hence an Ahrrenius plot (Epstein et al., 1977) is used to account for time-factors and to better establish temperatures consistent with CAI measurements (Figure 12). A temperature interval of 230 to 340°C is consistent with thermometrically-measured temperatures and results from a duration of 10^6 years on the Ahrrenius plot. This time interval produces a temperature of approximately 230°C for samples 1 and 2, and a temperature of greater than 340°C is estimated for sample 4. The average duration of a geothermal system ranges between 10^4 and 10^5 m.y., but some systems are known to be longer; Steamboat Springs, NV has a suggested age of 10^6 years (Ellis, 1979). The 10^6 year persistence of hydrothermal fluids in the St. Cloud-U.S. Treasury system is compatible with durations of geothermal systems. It is unlikely that the temperature of the hydrothermal fluids was fixed for the full duration of the active-cycle of the system; however, these data indicate regional heating and higher temperatures near the mineralized vein.

Figure 12. Ahrrenius Plot for Conodont Alteration Index Measurements (after Epstein et al., 1977).

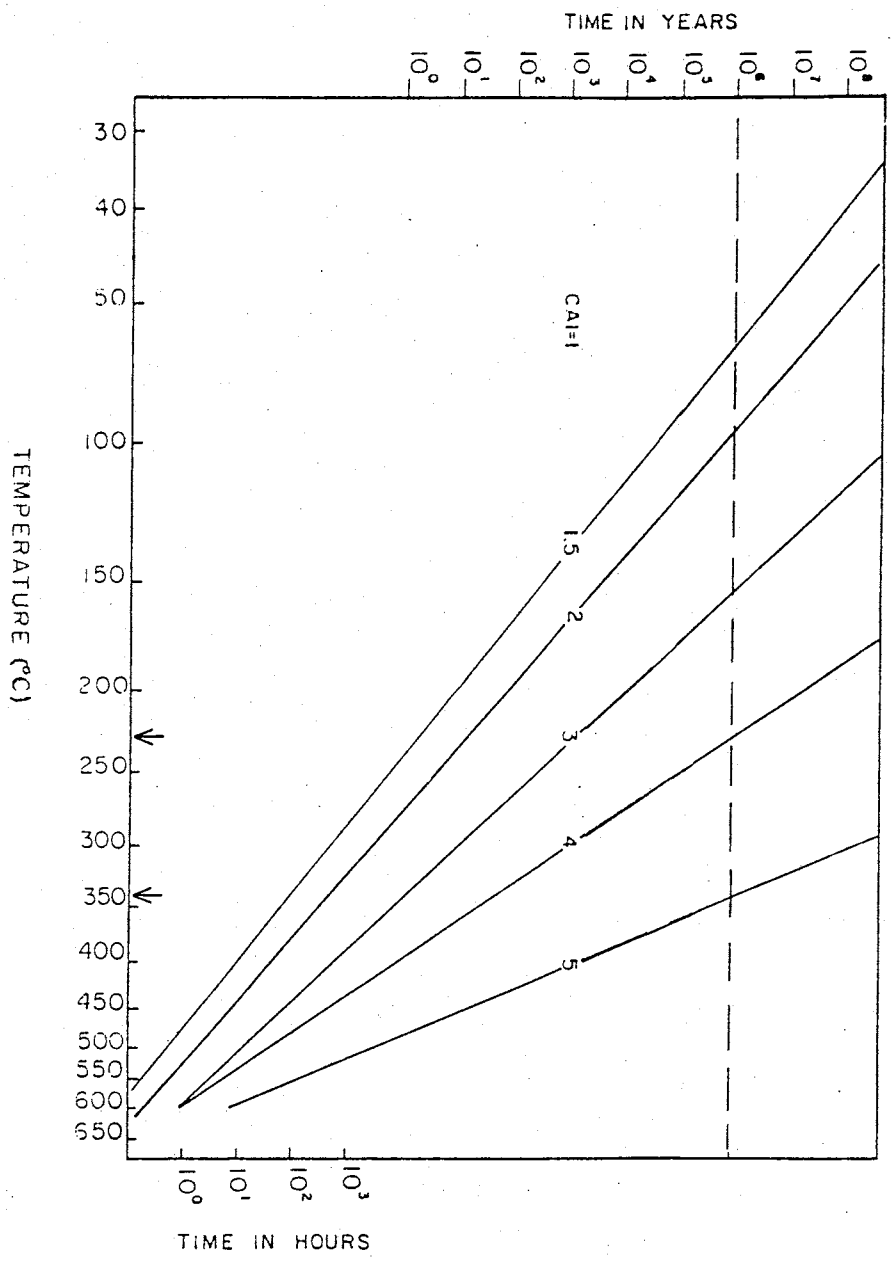
TIME IN YEARS
10^0 10^1 10^2 10^3 10^4 10^5 10^6 10^7 10^8
TEMPERATURE (°C)
30
40
50
100
150
200
250
300
350
400
450
500
550
600
650
CAI=1
1.5
2
3
4
5
10^0 10^1 10^2 10^3
TIME IN HOURS

Table 7. Results of Conodont Analyses.

sample	location	no. of conodonts	CAI	T (^{o}C)	species
1	300m from vein, within a large limestone block	6	4.0	190-300	Idiognathodus delicatus Neognathodus cf. N. bassleri
2	same as above	5	4.0	190-300	both species above, and Idiognathodus cf. I. delicatus
3	on vein contact, near a limestone-andesite contact	0	...	...	...
4	6m from vein and near a limestone-andesite contact	7	>5	300-400	Idiognathodus delicatus Neognathodus cf. N. medexultimus

DISCUSSION

Sulfide Deposition from the St. Cloud-U.S. Treasury Ore Fluids

Based on the results of the analyses and calculations, the hydrothermal fluids which mineralized the St. Cloud-U.S. Treasury system were neutral, slightly reduced, dilute, sodium and calcium chloride solutions with volatile contents averaging 0.2 mole percent. Stable isotope results suggest there were two ore-fluids in the system, one responsible for each sulfide mineralization stage. The means by which these fluids deposited the metals of each stage in both mines can be evaluated based on field observations, analytical results, and computer modeling.

To evaluate the oxidation conditions and pH of the ore fluids, the calculated ranges in oxygen fugacity and corresponding pH are plotted in Figure 13. This diagram depicts sulfide mineral stability fields calculated at 250°C with a log total sulfur of -2. To further investigate the stability fields, oxygen and sulfur fugacities are plotted in Figure 14. This diagram is also calculated at 250°C. The ranges in the parameters for each mineralization stage are shaded in both diagrams and listed in Table 8.

The limited range in pH calculated in all stages is approximately neutral at 250°C. This may have resulted from ore-fluid interactions with the Madera Limestone which could have acted to buffer the pH values. This pH range is consistent with alteration mineral assemblages which are dominantly potassium-feldspar and potassium-mica.

Figure 13. Log $f(O_2)$-pH Diagram Depicting Sulfide Mineral Assemblages at 250°C and log Total Sulfur = -2 (after Hayba et al., 1985).

Stage 1

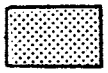

Stage 2

Non-Ore-Grade

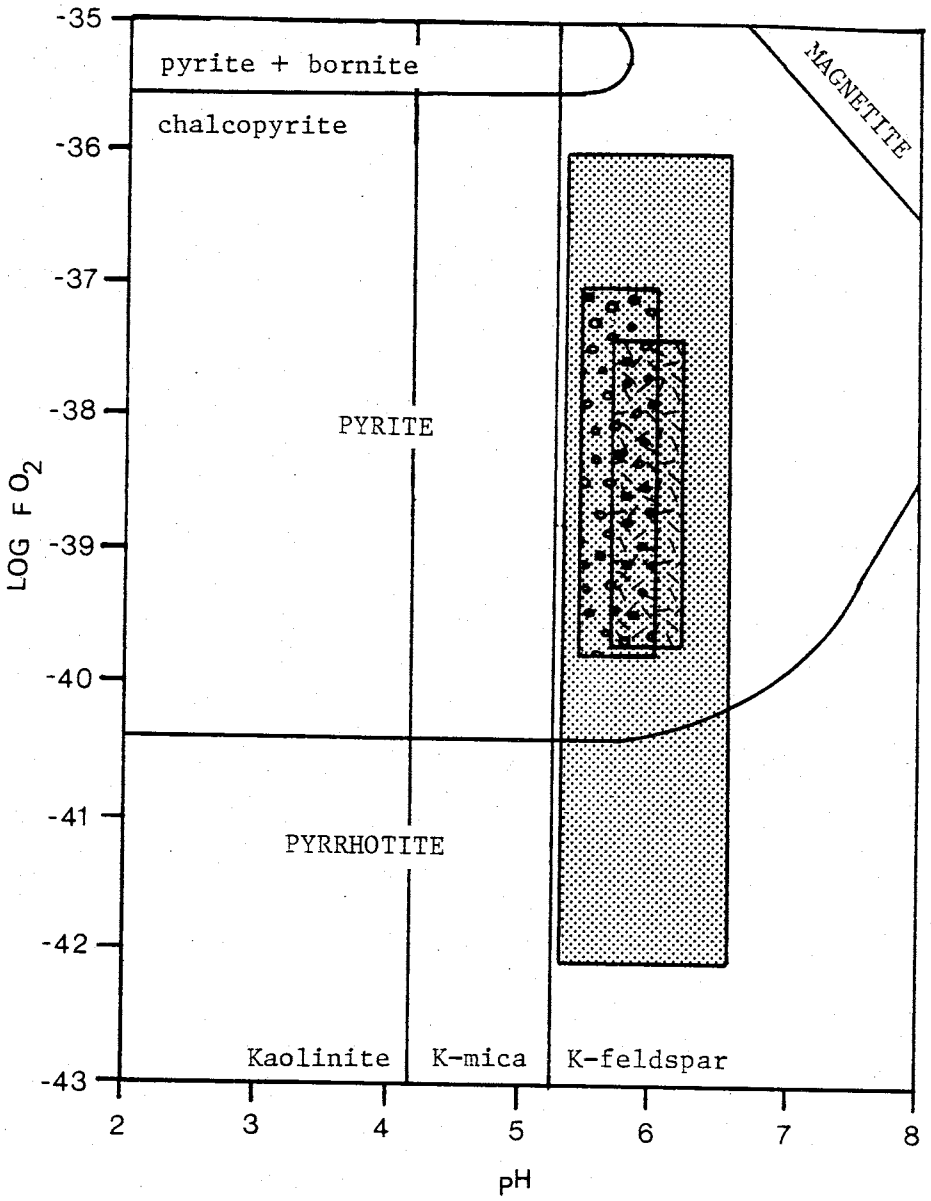
-35
-36
-37
-38
-39
-40
-41
-42
-43
LOG F O_2
pyrite + bornite
chalcopyrite
MAGNETITE
PYRITE
PYRRHOTITE
Kaolinite
K-mica
K-feldspar
2
3
4
5
6
7
8
pH

Figure 14. Log $f(S_2)$-$f(O_2)$ Diagram Depicting Sulfide Mineral Assemblages at 250°C (after Hayba et al., 1985).

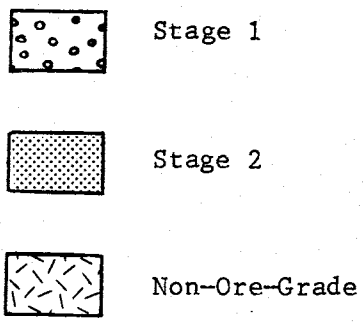

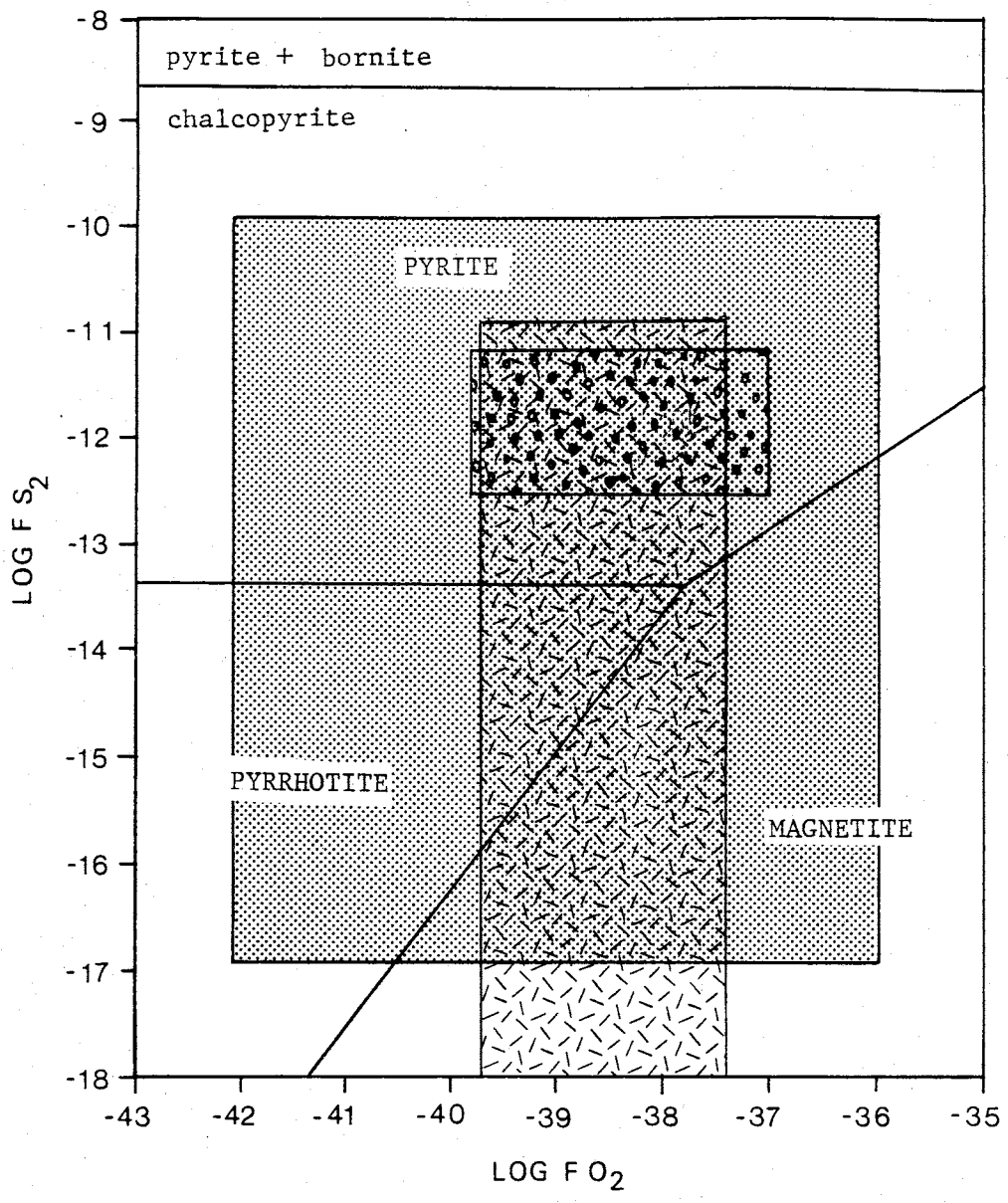
pyrite + bornite
chalcopyrite
PYRITE
PYRRHOTITE
MAGNETITE
-8
-9
-10
-11
-12
-13
-14
-15
-16
-17
-18
LOG F S_2
-43
-42
-41
-40
-39
-38
-37
-36
-35
LOG F O_2

Table 8. Averages and Ranges in Oxygen and Sulfur Fugacities and pH Values for each Mineralization Stage.

		Average	Minimum	Maximum
Stage 1	pH	5.6	5.4	6.0
	fO_2	-37.8	-39.8	-37.0
	fS_2	-11.8	-12.5	-11.2
Stage 2	pH	5.8	5.3	6.6
	fO_2	-37.9	-42.1	-36.0
	fS_2	-12.0	-16.9	-9.9
Non-Ore-Grade	pH	5.9	5.7	6.2
	fO_2	-38.2	-39.7	-37.4
	fS_2	-11.8	-23.9	-10.9

The log oxygen fugacity values cover a wide range in the diagrams with stage 2 values from -42.1 to -36.0 and stage 1 and non-ore-grade values ranging from -39.8 to -37.0. The higher values are consistent with the sulfide mineral assemblage observed in the system, but the lower values are not. The reducing conditions they represent may be explained by excess gasses trapped in fluid inclusions during gas exsolution from boiling ore fluids. Excess hydrogen would cause oxygen fugacity values to be anomalously low. If the original ore fluids were reduced, oxidation would be necessary to produce the sulfide mineral assemblage observed. The effect of ore-fluid oxidation would be deposition of bisulfide-complexed metals from ore fluids.

Evidence for oxidation of ore fluids is shown in the plot of elevation versus mole percent hydrogen sulfide (Figure 10). High concentrations of hydrogen sulfide are measured within some samples in mineralized zones, but all samples over ore zones show low concentrations suggesting that oxidation occurred in the solutions to deplete hydrogen sulfide over mineralized zones. Also, the organic

species measured in the gas analyses are alkenes; these species are stable at relatively high oxygen fugacity values.

The log sulfur fugacity values also cover a wide range in the diagrams from -23.9 to -9.9. The higher values are consistent with the sulfide mineral assemblage observed in the system, but the lower values are not. These low values probably represent a fluid depleted in hydrogen sulfide upon oxidation by surface-derived waters. Thus, the calculated sulfur fugacity values are not representative of the sulfide assemblage which deposited from the fluid.

The largest stability field included in the data range in Figures 13 and 14 is pyrite, however, pyrite occurs in very minor amounts throughout the system; chalcopyrite is deposited in favor of pyrite. The reaction:

$$CuFeS_2 + FeCl^+ + S_2 + 1/2\ H_2O \leftrightarrow CuCl + 2\ FeS_2 + H^+ + 1/4\ O_2$$

strongly favors the products at 250°C. Therefore, deposition of chalcopyrite over pyrite requires special chemical conditions in the ore fluid. If the ore fluid is acidic or has high oxygen and/or low sulfur fugacities, chalcopyrite deposition would result. In addition if concentrations of copper-chloride complexes were greater than those of iron chloride, chalcopyrite deposition would be favored.

Evidence from ore-mineral assemblages reveals differences in ore-fluid chemistry between the two mineralization stages. Stage 1 mineralization is dominated by galena, sphalerite, and chalcopyrite while stage 2 consists mainly of bornite, chalcocite, and covellite. These differences indicate higher oxygen and/or sulfur fugacities in the fluids of stage 2 ore mineralization. This suggests that the

calculated oxygen and sulfur fugacity values are slightly lower than would be expected based on ore mineral assemblages.

Areas of non-ore-grade mineralization exist within sulfide mineralization zones. The geochemical data indicate that fluids responsible for quartz deposition in these areas had salinities and temperatures notably less than those of the mineralizing fluids. These fluids may have resulted from cooling and dilution of ore fluids after sulfide-mineralization. These spent fluids could have continued to deposit quartz with decreasing temperature. It is also possible that this mineralization resulted from heated, surface-derived meteoric waters which had no interaction with metal-bearing fluids.

The evidence provided by the analytical data points to two depositional processes for the St. Cloud-U.S. Treasury vein system: mixing and boiling. Surface-derived meteoric waters mixed with the ore fluids would result in cooling, dilution, and oxidation. Histograms from thermometric analyses show that ore fluids were cooled and diluted with increasing elevation (Figure 9); gas analyses indicate decreasing hydrogen sulfide concentrations with elevation which possibly reflects oxidation of ore fluids with elevation (Figure 10). Isotope data from stage 2 samples show increasing d D with increasing elevation indicating an increased meteoric water component in ore fluids with elevation. Fluid inclusion observations and gas analyses suggest boiling as a depositional mechanism. High vapor to liquid ratios are seen in some fluid inclusions and high concentrations of volatiles are observed in some gas analyses indicating that gaseous species exsolved from the ore fluids.

To evaluate the possibility of ore-fluid boiling, a boiling point-depth curve was calculated (Figure 15). This curve represents the maximum temperature a solution with 1 equivalent weight percent NaCl and 0.2 mole percent carbon dioxide could reach, at a given depth, before boiling occurs (Henley et al., 1984). The data points were plotted based on the thermometrically-determined temperature and the hydrostatic depth. The hydrostatic depth was calculated from the total gas pressure of each sample as determined by gas analyses (corrected by the GASFIX program). Figure 15 shows that most of the data points plot along the trend of the curve which indicates ore fluids were at, or near, the boiling point.

Three points from stage 2 of the St. Cloud mine are well below the trend of the curve. These anomalous depths may result from ore-fluid boiling or system over-pressuring. Fluid inclusions which trap excess gasses from boiling ore fluids contain anomalously high gas pressures. Over-pressuring results when silica deposition seals a system and gas concentrations become supersaturated; fluid inclusions formed under these conditions also contain excess gasses. Trapped excess gasses in inclusions result in calculated hydrostatic depths that plot significantly below the boiling point-depth curve.

Typically in a boiling system, host rocks are altered by acid fluids formed over boiling zones (Buchanan, 1981), but no acidic alteration is observed to be associated with ore zones in the St. Cloud-U.S. Treasury vein system. Since the time of mineralization of this system, the Tertiary section has been partially eroded. The lower Rubio Peak Formation is exposed in the area of the vein, therefore any

Figure 15. Boiling Point-Depth Curve Calculated for a Solution with 1 Equivalent Weight Percent NaCl and 0.2 Mole Percent CO_2; Circled Data Points Represent Samples which Exhibited Evidence of Boiling Through Fluid Inclusion Microanalyses.

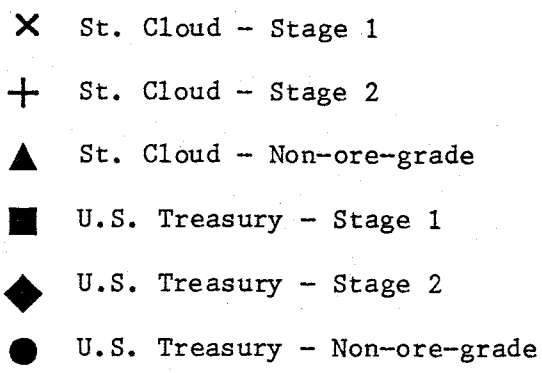

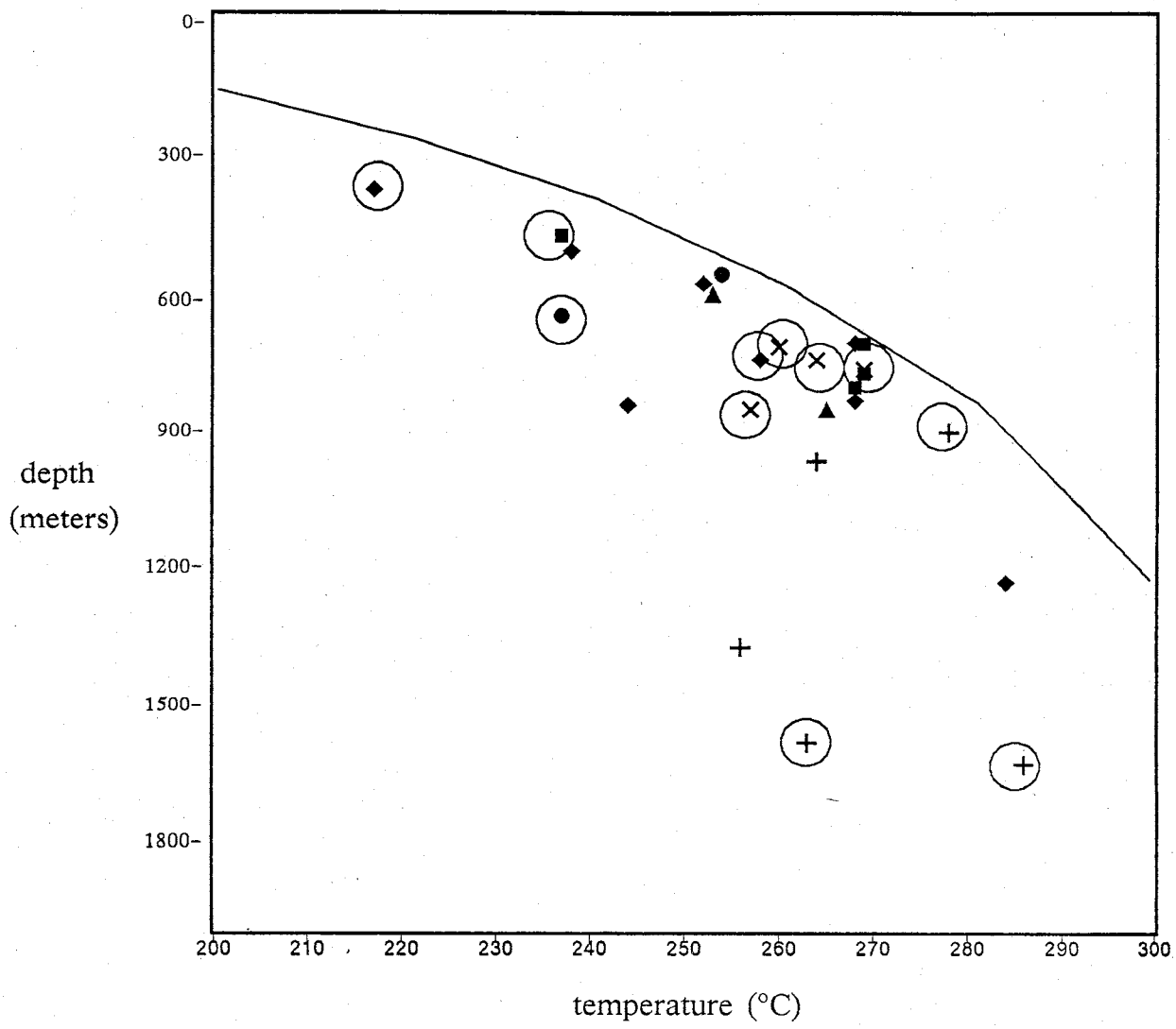
0-
300-
600-
900-
1200-
1500-
1800-
depth
(meters)
200
210
220
230
240
250
260
270
280
290
300
temperature (°C)

acidic alteration formed over mineralized zones has likely been removed by erosion.

The graph of Figure 15 also reveals information about the depth at the time of sulfide mineralization. Most of the data points occur between 500 and 900 meters depth. The thickness of the Tertiary section in the Chloride District ranges from 1100 to 1900 meters (Harrison, 1984) and the mineralization of the St. Cloud-U.S. Treasury vein covers approximately 400 meters in the lower Tertiary section. This suggests that in the area of the vein, the thickness of the Tertiary section was at a minimum during mineralization.

GEOMOD Model Calculations

GEOMOD (Norman, in prep.) is a computer model used to calculate concentrations of ore metals in solution. The program contains two calculation options, one for ore-metal solubility at specified fluid conditions, the second for ore-metal solubility resulting from ore-fluid boiling. The boiling option can be executed under three types of conditions: a closed system with a single-step gas separation from the fluid; an open system with multistep gas separations; or an open system with continuous gas separations. Both calculation options of the model include selections for pH and oxygen-fugacity calculations. The ore-fluid pH may be input or calculated by the model using the Na-K-Ca chemical geothermometer (Truesdell, 1973). The ore-fluid oxygen fugacity may be input, calculated by the reaction:

$$CH_4 + O_2 \rightarrow CO_2 + 2\ H_2,$$

or calculated by the water reaction. Other input parameters of both model options include temperature, salinity, and gas concentrations of carbon dioxide, hydrogen sulfide, hydrogen, nitrogen, methane, and water.

Output for the solubility option is total fluid concentrations of zinc, lead, silver, copper, gold, and iron. These concentrations include all the possible chloride and bisulfide complexes for each metal. Output for the boiling option includes the same ore-metal concentrations, but they are calculated for each specified temperature increment during the boiling processes. In addition, pH and gas concentrations at each temperature increment are calculated.

The results of the solubility calculations are in Appendix F. Figure 16 illustrates the relationship of ore-metal concentrations with elevation in stage 1, stage 2, and non-ore-grade mineralization. Results suggest that the ore fluids had a high capacity to transport zinc which occurs in the highest concentration in all mineralization stages. The fluids of stage 2 mineralization show the highest concentrations of total metals.

The solubility option of GEOMOD was also used to evaluate the changes in ore-metal solubility during mixing of a metal-bearing ore fluid with meteoric water. The mixing calculation uses 6 different proportions of each fluid. The first mixture is 100 percent meteoric water. Each mixture is a 20 percent change in the proportions of the ore fluid resulting in the sixth mixture as 100 percent ore fluid. The characteristics of the two fluids used in the calculation and the results are in Table 9.

Figure 16. Ore-metal Concentrations versus Elevation for each Mineralization Stage.

Stage 1

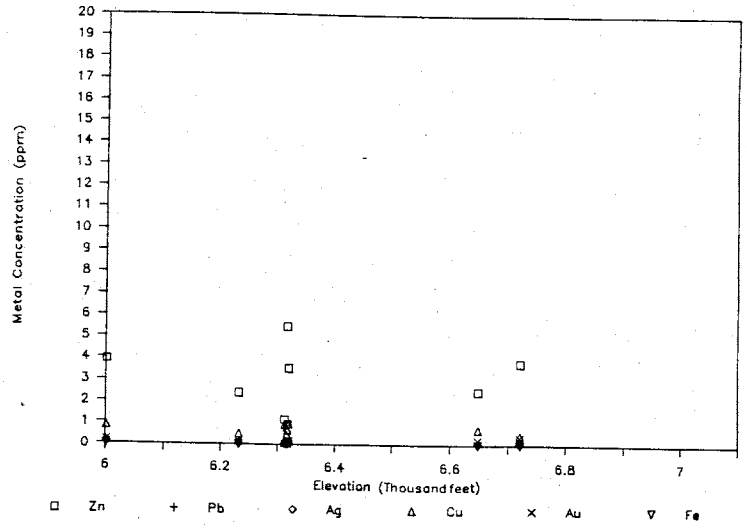

Stage 2

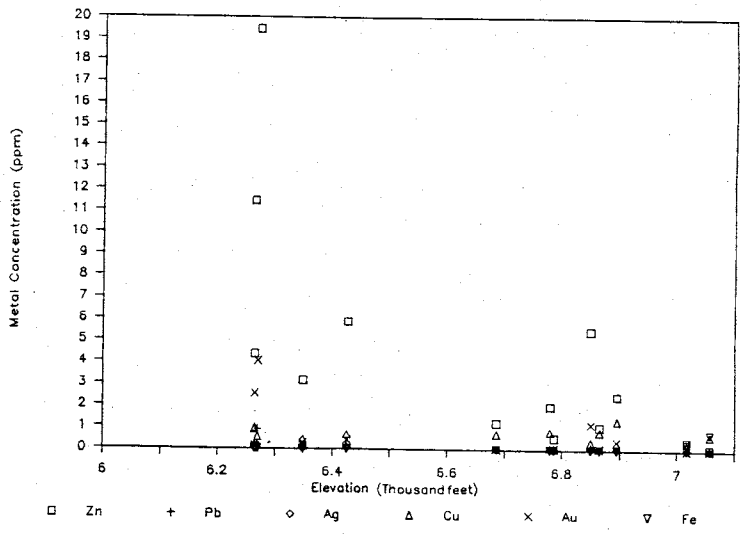

Non-Ore-Grade

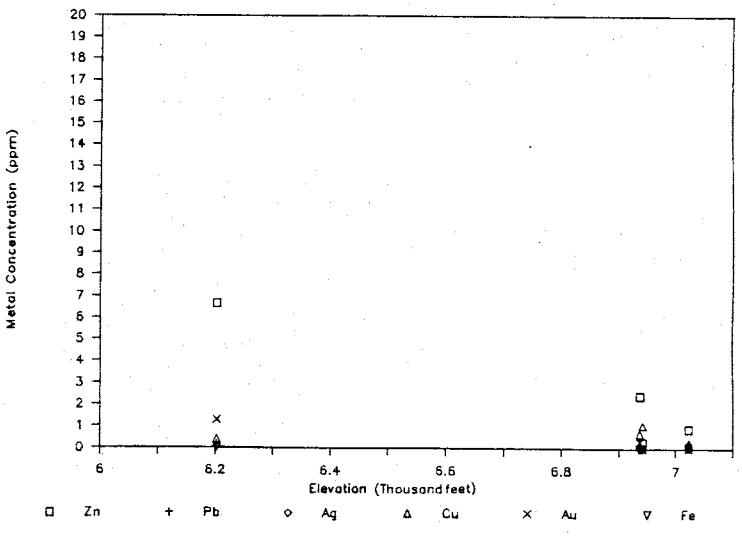

Table 9. Input Parameters and Results of the Mixing Calculations.

INPUT:

Mix	Temperature (°C)	Salinity (wt.%)	CO_2 (mol%)	H_2S (mol%)	H_2 (mol%)	N_2 (mol%)	CH_4 (mol%)	H_2O (mol%)
1	200	0.00	0.01	0.00	0.000	0.00	0.00	99.98
2	221	0.70	0.04	0.04	0.0004	0.03	0.08	99.76
3	242	0.14	0.07	0.07	0.001	0.05	0.17	99.55
4	263	0.21	0.09	0.11	0.001	0.08	0.25	99.33
5	282	0.28	0.12	0.14	0.002	0.10	0.34	99.12
6	300	0.35	0.15	0.18	0.002	0.13	0.42	98.90

OUTPUT:

Mix	pH	Log $f(O_2)$	Zn (ppm)	Pb (ppm)	Ag (ppm)	Cu (ppm)	Au (ppm)	Fe (ppm)
1	6.37	-44.0	0.0000	0.0000	0.0000	0.0000	0.0000	0.0000
2	5.95	-42.0	5.9906	0.0507	0.0785	0.8549	0.7419	0.0000
3	5.53	-40.2	9.3765	0.1431	0.0581	0.9498	0.7248	0.0000
4	5.25	-37.7	13.3155	0.3516	0.0762	1.3493	1.2748	0.0007
5	5.03	-36.3	15.8034	0.6737	0.2507	1.7204	1.1262	0.0176
6	4.82	-34.4	20.5535	1.3533	1.2326	6.0685	1.4514	0.1565

Calculations show increasing pH and decreasing oxidation with increasing amounts of meteoric water. This trend in oxidation is inconsistent with the fact that meteoric water is oxidizing; it would be more likely to increase oxidation with increasing amounts of meteoric water. Figure 17 illustrates the trends of ore-metal concentrations in the mixing calculations. Again, zinc complexes are most soluble in the ore fluid. All metal concentrations decrease with increasing amounts of meteoric water. This is consistent with mixing as a possible depositional mechanism for metals in the St. Cloud-U.S. Treasury vein system.

The boiling option of the GEOMOD program was used to calculate the changing concentrations of ore-metals upon boiling of St. Cloud-U.S. Treasury ore-fluids. Calculations were made for an open system with multistep gas separations which is considered to best represent the

Figure 17. Ore-metal Concentrations from the Mixing Calculations.

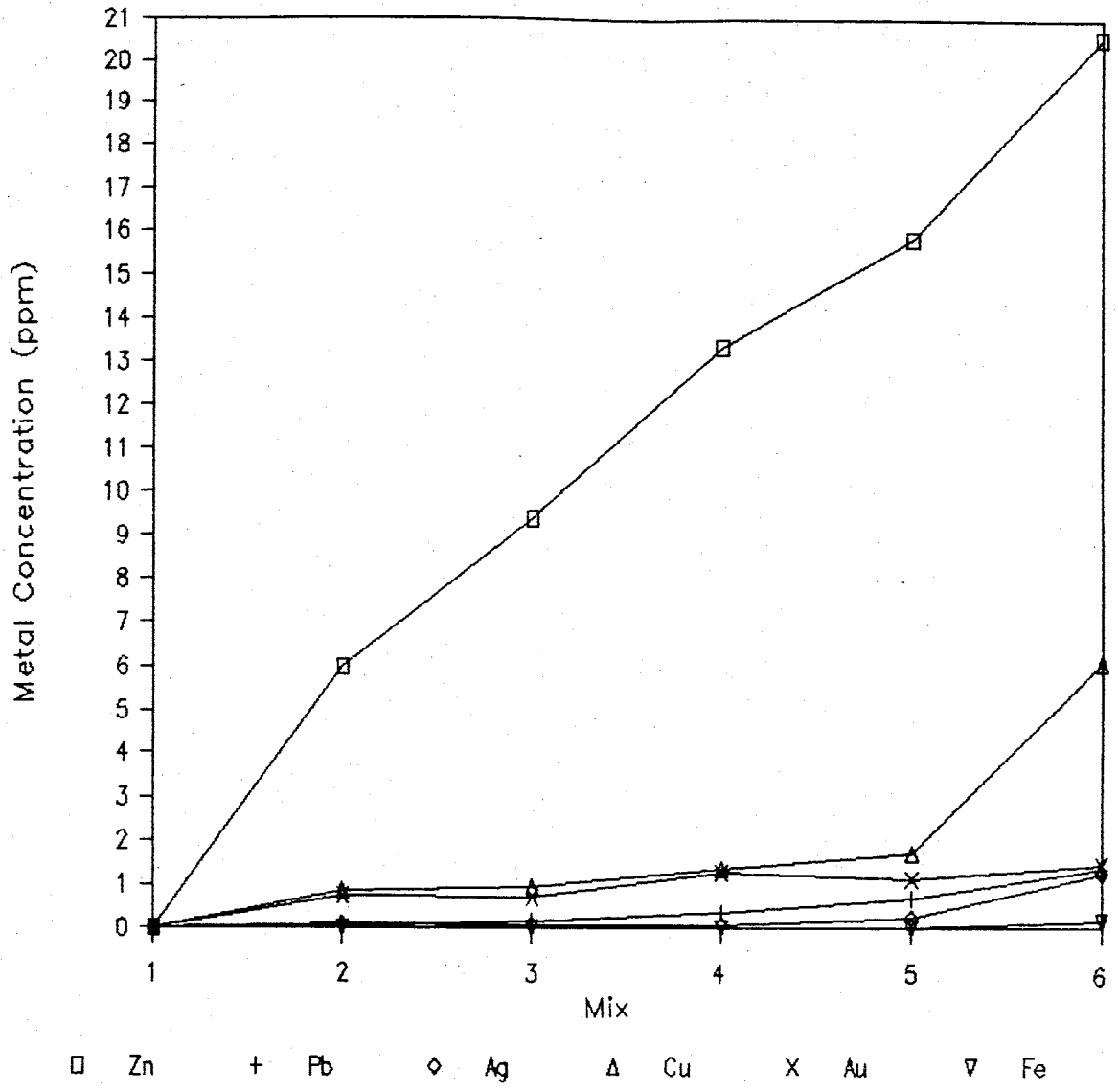
Metal Concentration (ppm)
21
20
19
18
17
16
15
14
13
12
11
10
9
8
7
6
5
4
3
2
1
0
1
2
3
4
5
6
Mix
□ Zn
+ Pb
◇ Ag
Δ Cu
X Au
▽ Fe

conditions of the system during mineralization. The boiling calculations were executed from 300 to 200°C with a salinity of 0.81 weight percent NaCl equivalent (estimates for ore-fluids in the system). Initial gas concentrations (in mole percent) are averages for the system: carbon dioxide as 0.05555, hydrogen sulfide as 0.03018, hydrogen as 0.00078, nitrogen as 0.01549, and methane as 0.04802. The results are in Table 10 and Figure 18. They show increasing pH with decreasing temperature. As with the other GEOMOD calculations, zinc-complex solubility is greatest in the ore fluids. Calculations show decreasing metal concentrations with ore-fluid boiling with the exception of copper which shows slight retrograde solubility. Copper complexes would not be expected to be more soluble with boiling, but rather deposit with decreasing temperature. The trends of decreasing metal concentrations upon ore-fluid boiling also makes boiling a possible depositional mechanism for metals in the St. Cloud-U.S. Treasury vein system.

Table 10. Results of the Boiling Calculations.

Temperature (°C)	pH	Zn (ppm)	Pb (ppm)	Ag (ppm)	Cu (ppm)	Au (ppm)	Fe (ppm)
300	5.45	3.125	0.204	0.066	0.588	0.283	0.028
280	5.72	1.448	0.060	0.020	0.379	0.074	0.005
260	5.85	0.760	0.019	0.007	0.370	0.018	0.001
240	5.93	0.430	0.006	0.003	0.430	0.004	0.000
220	5.96	0.257	0.002	0.001	0.571	0.001	0.000
200	5.97	0.159	0.001	0.001	0.838	0.000	0.000

Figure 18. Ore-metal Concentrations from the Boiling Calculations.

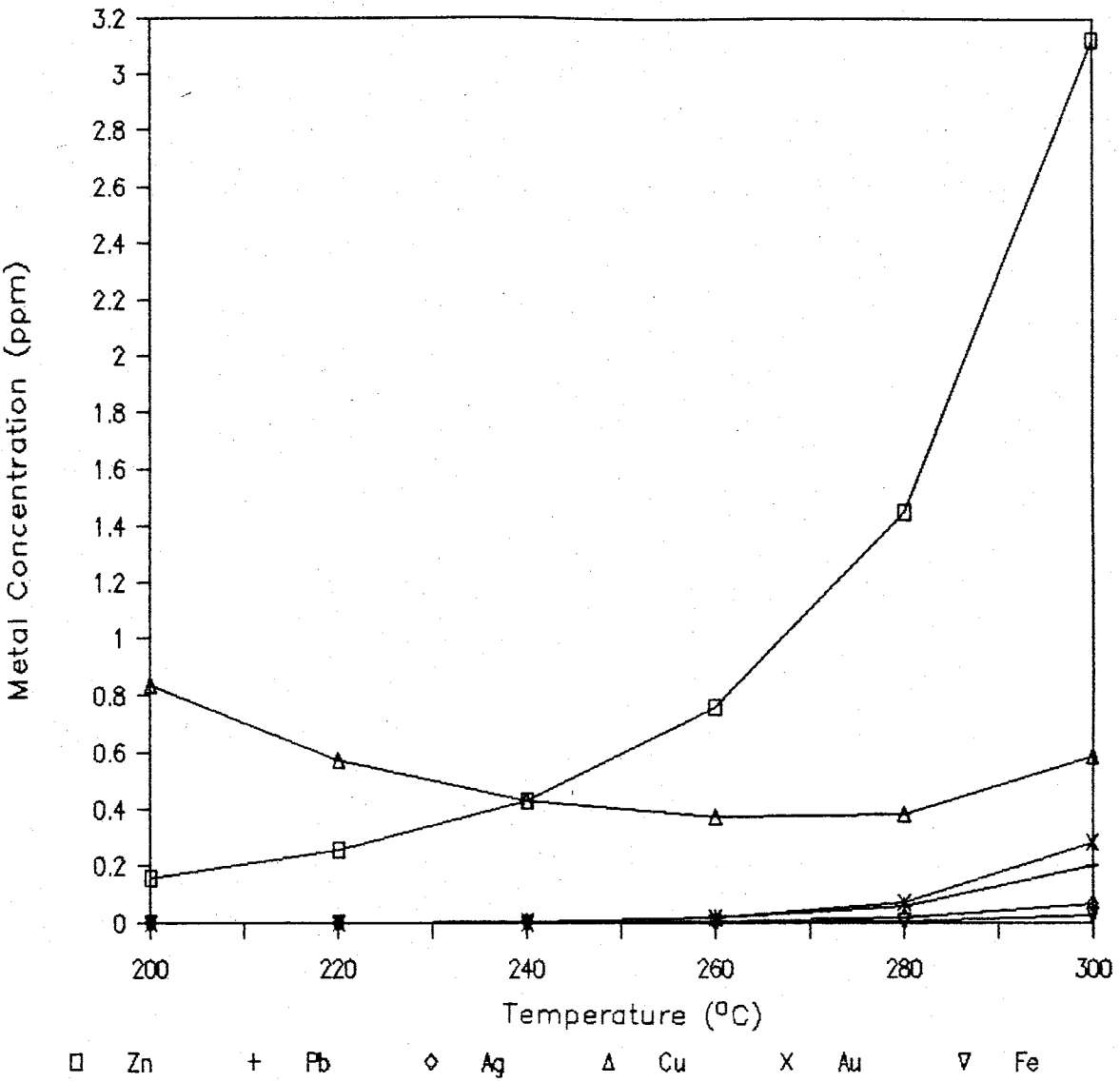
Metal Concentration (ppm)
3.2
3
2.8
2.6
2.4
2.2
2
1.8
1.6
1.4
1.2
1
0.8
0.6
0.4
0.2
0
200
220
240
260
280
300
Temperature (°C)
Zn
Pb
Ag
Cu
Au
Fe

Classification and Depositional Model

The idea that epithermal systems are paleo-geothermal systems has been noted in many studies (White, 1955, 1981; Ewers and Keays, 1977; Henley and Ellis, 1983; Berger, 1985; Sillitoe and Bonham 1984; Hedenquist and Henley, 1985; Henley, 1985). The physical and chemical processes observed in active geothermal systems can be used to interpret features seen in epithermal systems. These features include regional structure, fluid chemistry, and alteration and sulfide mineral assemblages.

Regional structure is important in controlling the formation of geothermal and epithermal systems (Ellis and Mahon, 1977; Ellis, 1979; Henley and Ellis, 1983; Sillitoe and Bonham, 1984). These systems are typically fault-hosted in extensional tectonic and recent volcanic terranes. Especially favorable structures for localizing mineralization are normal faults that intersect major structures such as rifts, grabens, or calderas. Recent volcanism associated with these systems is commonly felsic or andesitic in composition and provides a heat source to drive convective fluids. The fault system in the Chloride district is consistent with structural features necessary for the genesis of a geothermal system. The St. Cloud-U.S. Treasury deposit is hosted by a normal fault that lies in a complexly faulted area near a series of cauldron complexes and the Rio Grande rift.

Comparisons of fluid chemistries between epithermal and geothermal systems show similar constituents (both metal and non-metal) in comparable amounts (Ellis and Mahon, 1977; Ewers and Keays, 1977; Ellis, 1979; Weissberg et al., 1979; Henley and Ellis, 1981; White,

1981). The fluids in these systems are dominantly meteoric waters with minor, variable amounts of magmatic waters. Hydrothermal fluids have been classified into two types of waters: neutral-chloride waters and acid-sulfate waters (Henley, 1984). Heald et al. (1987) define two types of epithermal deposits based on this fluid classification: the adularia-sericite type and the acid-sulfate type. An acid-sulfate type fluid forms in the roots of a volcanic dome with mineral deposition localized vertically (<500 meters) and occurring within the proximity of the host volcanic system. High concentrations of magmatic volatiles exist in the fluid phase which create low pH waters with high temperatures, salinities, and oxygen fugacities. Precious metal contents vary in acid-sulfate fluids, but high base metal concentrations (especially copper) are common. Alteration of host rocks by these waters is advanced argillic including the minerals alunite and kaolinite and a distinguishing high-sulfur sulfide-mineral assemblage of enargite and pyrite with lesser covellite. Examples of acid-sulfate deposits include Goldfield, NV; Julcani, Peru; Lake City II, CO; Red Mountain, CO; and Summitville, CO.

The fluids of the adularia-sericite type are derived by meteoric waters mixing with heated, saline waters generated from a deep heat-source. Mineral deposition occurs over a large vertical range (up to 1000 meters). It is more distant from and above the heat source than acid-sulfate-type deposits. The fluids are neutral to weakly acidic, have low volatile contents, and have varying salinities with lower temperatures and oxygen fugacities than those of the acid-sulfate type. Base-metal contents in this fluid-type vary, but are usually low in copper. Host rock alteration by these waters is propylitic,

including the minerals adularia, sericite, and chlorite. Adularia-sericite deposition from neutral-chloride fluids lacks the sulfide mineral assemblages which characterize acid-sulfate deposition. Examples of this deposit-type include Comstock, NV; Creede, CO; Eureka, CO; Oatman, AZ; Panchua, Mexico; Round Mountain, NV; and Tonapah, NV.

The physical and chemical environment of the St. Cloud-U.S. Treasury system can be defined as an adularia-sericite deposit formed by neutral-chloride waters. The heat source for the deposit and others in the Chloride District is not definitely known; there is no spatial association of the fluids to a unique heat source. Deposition is extensive laterally and vertically, possible geometries for either deposit-type. The alteration associated with mineralization is propylitic and the fluids are relatively cool and dilute, have a neutral pH, slightly reducing conditions, low volatile contents, and a low-sulfur mineralogy. A characteristic inconsistent with an adularia-sericite deposit is the relatively high amounts of copper in the system. The high copper concentrations may be the result of copper-leaching of the red bed Abo formation (Hatchell et al., 1982) during fluid circulation lower in the system.

Figure 19 depicts all of the features previously discussed which characterize the adularia-sericite type deposit and indicate its applicability to the St. Cloud-U.S. Treasury system. In this model, intrusive volcanic rocks (possibly the Moccassin-John rhyolite flow-dome complex) provide the heat to drive the system, a source for dissolved solids, and volatiles in the ore fluids. Evolving meteoric waters circulating in the system would be heated and acquire minor concentrations of precious and base-metals from the igneous and

Figure 19. Schematic Cross-section of an Adularia-sericite Type Depositional System: A model for the St. Cloud-U.S. Treasury Deposit (adapted from Henley and Ellis, 1983).

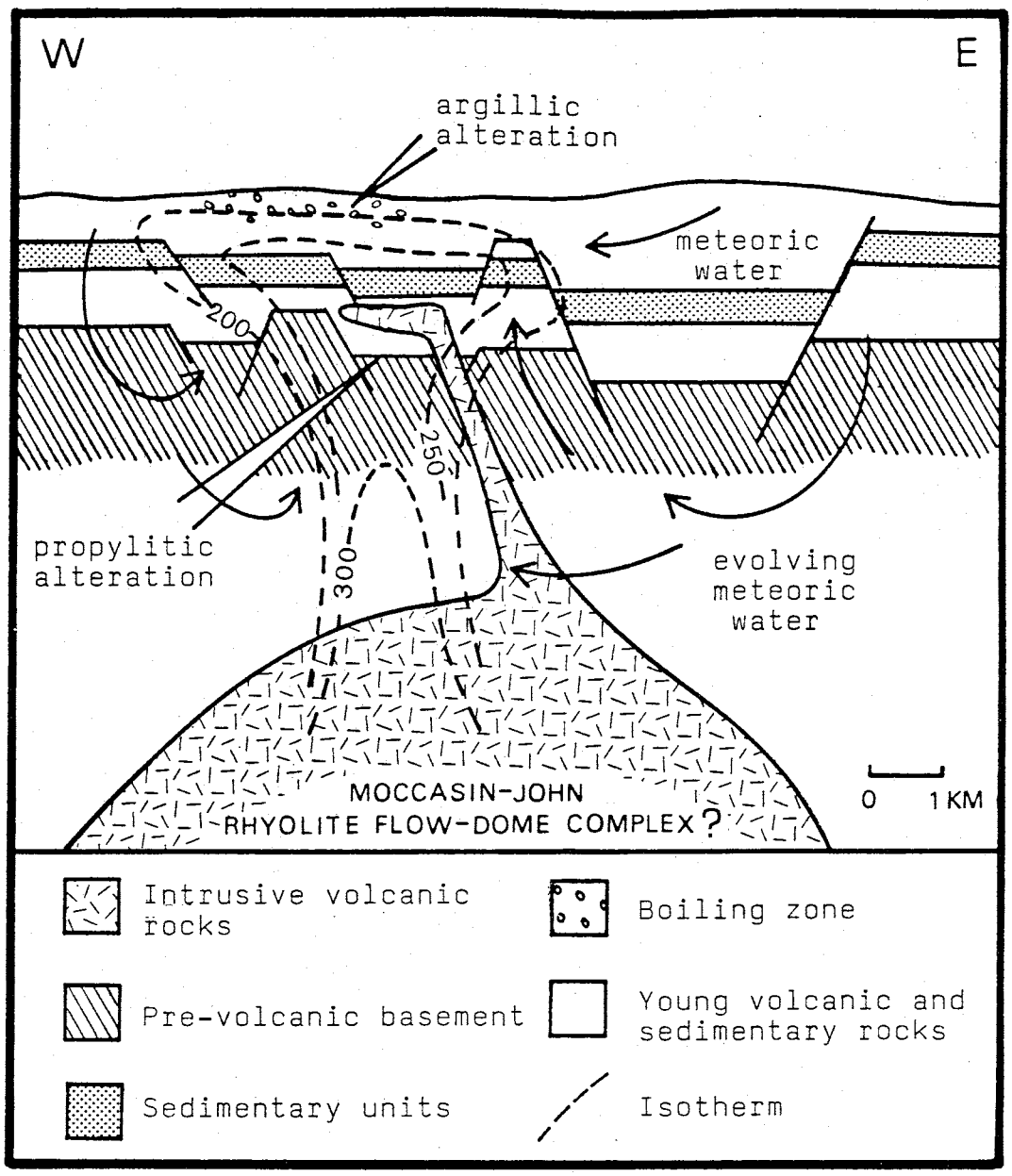
W
E
argillic
alteration
meteoric
water
200
250
300
propylitic
alteration
evolving
meteoric
water
MOCCASIN-JOHN
RHYOLITE FLOW-DOME COMPLEX?
0
1 KM
Intrusive volcanic rocks
Boiling zone
Pre-volcanic basement
Young volcanic and sedimentary rocks
Sedimentary units
Isotherm

sedimentary host rocks. As these fluids reached higher elevations, they would encounter the fault-structures within the Pennsylvanian limestones, Permian sandstones, and Tertiary volcanic rocks. The St. Cloud-U.S. Treasury mineralization was deposited in a high-angle normal fault within the area of propylitic alteration near the 250°C isotherm. There the fluids interacted with cool, dilute, oxidized, surface-derived meteoric water. Mixing of the two solutions resulted in cooling, dilution and oxygenation of the ore fluids. Boiling of ore fluids also occurred, aiding in localizing sulfide mineralization.

CONCLUSIONS

The St. Cloud-U.S. Treasury epithermal ore deposit is an eroded paleo-geothermal system that exposes the mineralization of the lower portions of the geothermal system from which it formed. Results of analyses and calculations indicate that there were two fluids responsible for the two stages of sulfide mineralization. Stage one fluids had slightly higher salinities and produced a more base-metal-rich ore. Stage two fluids had slightly higher sulfur fugacities, or lower oxygen fugacities, and produced a more precious-metal-rich ore. Fluids from areas of non-ore-grade deposition had notably lower temperatures and salinities and were probably relict hydrothermal ore fluids or meteoric waters that had limited, or no interaction with metal-bearing hydrothermal fluids.

Analyses of fluid inclusion chemistry indicates that the fluids had temperatures ranging from 220 to 300°C; salinities from 0 to 3.5 equivalent weight percent NaCl; pH values from 5.3 to 6.6; log $f(O_2)$ values from -35.1 to -45.5; and log $f(S_2)$ values from -23.9 to -9.9. The processes of cooling, dilution, and oxidation were operative in the system with the ranges in parameters resulting from boiling hydrothermal ore-fluids and mixing of these fluids with surface-derived meteoric water. These processes acted to deposit metal sulfides in the system.

The hydrothermal fluids were derived from deeper portions of the system, near the heat source which drove the circulating fluids. These fluids remobilized metals from sedimentary and igneous host-rocks

during circulation and deposited them at higher elevations upon boiling and interaction with meteoric waters within fault structures.

The chemical and physical mechanisms which controlled deposition, the sulfide-mineral assemblage, propylitic alteration, and the extensional tectonic environment and associated volcanism in the St. Cloud-U.S. Treasury deposit are all features satisfying requirements for the adularia-sericite type classification of epithermal systems.

APPENDIX A

Results of Fluid Inclusion Thermometric Analyses (elevation in feet; Th in degrees C; salinity in equivalent weight percent NaCl, calculated from Ts where salinity = $(1.76958 \times Ts) - ((4.2384 \times 10^{-2}) \times Ts^2) + ((5.2778 \times 10^{-4}) \times Ts^3)$, (Roedder, 1984)).

	Sample	Elevation	Th	Salinity
St. Cloud	stage 1			
	U15A	6284	273	0.53
			274	0.35
				0.87
			269	0.53
			272	0.70
			281	0.53
	U19A	6232	266	
			258	
			249	0.18
			249	0.18
			257	0.00
			256	0.52
			209	0.52
			278	0.87
			258	0.52
			258	0.70
			224	0.52
			250	0.52
			262	1.72
			236	0.52
			273	3.21
			281	3.21
			234	0.18
			264	1.38
			168	1.21
			262	1.38
			270	1.04
			286	0.52
			273	0.52
	SC4D	6321	264	1.22
			267	0.53
				0.53
			275	0.70
			262	0.87
			271	1.73
			268	1.39
			317	3.37
			294	2.89
			276	1.90

Sample	Elevation	Th	Salinity
SC4E	6317	283	0.53
		286	0.35
		289	0.53
		257	0.53
		266	0.53
		256	0.70
			0.07
		293	2.23
			2.06
		256	1.22
		263	1.05
		269	1.39
			1.39
		253	1.39
		259	
SC4F	6316	244	0.35
		222	0.35
		249	0.35
		268	0.35
		264	0.35
		231	0.53
		262	0.53
		250	0.53
		250	1.05
		256	1.05
			0.70
		275	0.53
			0.70
		256	0.53
		258	0.53
		258	0.53
		254	0.70
		262	0.87
		273	0.70
		275	0.70
		276	0.70
		268	0.53
		263	0.53
		261	0.53
		247	0.53
		256	0.53
		257	2.40
		263	0.70
		276	0.70
		279	0.87
		268	0.70
		297	0.70

Sample	Elevation	Th	Salinity
		237	0.87
		270	0.70
SC4G	6315	258	0.35
		271	0.87
			0.70
		293	0.87
		248	0.87
		270	1.39
		280	1.39
		262	1.05
			1.05
		274	1.05
		229	1.05
		266	0.53
		273	0.53
		272	1.39
		244	1.39
SC4H	6312	251	2.89
		275	2.89
		268	2.72
		290	2.56
		283	2.40
		225	1.05
		280	1.90
		240	1.22
		258	1.90
		260	1.05
		265	1.05
			1.05
		313	1.90
		270	1.90
		307	1.73
		316	1.73
		269	0.70
		263	0.70
		265	0.87
		280	0.87
		237	0.87
		279	1.90
		275	1.90
		254	0.87
		258	0.87
		252	1.05
		261	1.05
		262	0.70
			0.87

	Sample	Elevation	Th	Salinity
			258	0.70
			271	0.87
			262	1.73
			276	1.73
			272	1.73
				0.87
			248	0.87
			252	1.05
			251	1.05
			253	1.05
			255	1.39
			253	1.05
			216	1.39
			270	1.56
			253	1.22
			259	1.05
			268	1.73
			281	1.39
			269	1.22
				1.22
			272	0.70
			267	1.05
			269	1.05
			267	1.05
			267	0.87
			263	0.87
St. Cloud	stage 2			
	U14A	6293	267	0.53
			271	0.53
			271	0.70
			273	0.87
			271	0.87
			281	0.70
	U14B	6292	275	1.05
			297	1.05
			285	0.87
			322	1.22
				0.70
			233	3.20
			348	2.56
			259	1.05
			268	1.05

Sample	Elevation	Th	Salinity
U15B	6264	241	1.22
		252	1.22
		258	1.22
		261	1.22
		260	1.90
		247	0.53
		239	0.53
		271	0.70
		248	0.35
		282	0.53
		256	0.35
		259	0.53
		251	1.73
		274	1.56
		266	1.73
U15C	6263	213	1.56
		274	1.56
		292	1.56
			1.39
			1.56
		279	2.06
		286	1.73
		281	2.06
		266	1.90
		284	2.06
			2.23
		289	2.06
		263	1.05
			1.05
			1.05
		267	1.05
SC4C	6348	265	0.70
		261	0.87
		252	0.53
		263	0.53
		267	0.53
		271	0.53
		255	0.53
		253	0.53
		288	0.53
		269	0.53
			0.18
		274	0.70
		272	0.87
		258	0.70

	Sample	Elevation	Th	Salinity
			264	0.87
			266	0.70
			268	0.70
	SC70C	6425	262	1.22
				1.22
				1.22
			270	1.73
			258	1.56
			232	1.05
			289	1.05
				1.56
				1.39
			242	1.22
			267	1.39
			244	1.56
			285	1.05
				0.87
				0.87
				1.22
			263	1.22
			278	1.05
			262	1.22
				0.87
			282	0.87
			257	0.87
			251	1.22
St. Cloud	non-ore-grade			
	S10	6936	276	0.53
				0.53
			259	0.35
			266	1.39
			261	1.90
			257	0.35
				0.35
				0.53
			253	0.35
			243	0.87
				0.70
			229	0.70
				0.70
			229	0.70
				0.00
			246	0.18
			260	0.18

	Sample	Elevation	Th	Salinity
	U16E	6202	243	0.53
			241	0.53
			261	0.53
				0.53
			273	0.87
			257	0.70
			287	0.00
				0.87
			280	0.18
			266	0.53
			247	0.00
			284	0.18
			276	0.87
			254	0.53
			281	0.53
U.S. Treasury	stage 1			
	SC53A	6461	263	0.53
				0.53
			287	0.70
				0.70
				0.70
				0.70
				1.05
			274	0.87
			269	0.87
			272	0.87
			289	0.87
			257	0.87
	SC53B	6328	274	0.53
			277	0.53
				0.35
			274	0.53
			271	0.53
			258	0.70
			266	0.70
			269	0.70
			274	0.70
			260	0.53
				0.35
			267	0.53
			274	0.87
			287	0.87
			260	0.87

Sample	Elevation	Th	Salinity
		256	0.70
		273	0.70
		281	0.87
		276	0.70
SC53C	6319	266	0.87
		285	0.70
		168	0.87
		171	1.21
		297	1.21
		282	1.21
		270	3.05
		279	3.05
		248	1.21
		251	3.05
		272	2.56
		273	2.56
		274	2.56
		256	1.72
		241	1.72
		261	0.87
		282	0.87
		282	0.70
		283	0.70
		282	0.87
		273	0.87
		262	0.87
		246	0.70
		253	0.70
SC58A	6009	287	0.70
			0.70
			0.70
		243	0.53
SC58B	6005	276	0.18
		281	0.18
		283	0.00
		286	0.53
		268	0.70
SC58C	6001	287	1.22
		274	1.22
		265	1.22
		271	1.56
		275	1.56
		267	1.39
		258	1.22

Sample	Elevation	Th	Salinity
		269	1.22
		258	1.39
		260	1.39
		252	1.56
		271	1.39
		279	1.39
		268	1.22
		257	1.22
		260	1.22
		265	1.22
		272	1.22
		274	1.22
		274	1.56
			1.56
		284	1.56
SC59A	6648	241	1.38
		214	0.70
		215	0.70
		254	1.22
		253	1.39
		254	1.22
		257	1.05
		260	0.70
		223	0.18
		252	0.53
		322	0.53
		243	0.18
		246	0.18
		236	0.00
		223	0.00
		242	0.00
		217	0.18
		225	0.18
		219	0.70
		219	0.70
		227	0.70
		263	0.53
		230	0.00
SC59B	6608	243	0.53
		289	0.35
		287	0.35
		283	0.35
		247	0.35
		277	1.39
		293	1.39
		251	1.22

	Sample	Elevation	Th	Salinity
			253	1.05
				0.53
			269	0.53
			261	0.70
			293	0.70
	RH3	6721	258	0.70
			268	0.70
			277	0.18
			272	0.35
				0.18
				0.35
			272	1.22
				1.22
			262	1.05
			247	0.53
			283	1.05
				1.05
			273	1.22
			280	1.22
				1.22
				1.22
			274	0.53
			256	0.70
				0.53
			244	0.53
			267	0.35
			271	0.35
			274	0.35
			273	0.87
U.S. Treasury	stage 2			
	UST8	6758	288	0.87
			209	1.22
			218	1.05
			218	0.53
				0.53
			231	0.70
			251	0.53
				0.53
				0.53
			254	2.40
				2.40
			261	2.40
			253	0.70
			259	0.70

Sample	Elevation	Th	Salinity
		262	0.70
		296	0.70
		223	0.70
		306	0.70
		309	0.70
		247	0.53
		243	0.53
			0.70
		239	0.70
			0.70
		269	1.05
		271	1.05
		275	1.05
SC60B	6864	161	0.87
		223	1.05
			1.05
		294	0.87
		215	1.72
		251	1.05
		267	0.53
		264	0.70
		206	0.70
		263	0.35
		273	0.53
		167	0.35
		277	0.18
		291	0.18
		197	0.70
		314	0.87
		261	0.87
		271	0.70
		286	0.18
		268	0.00
		199	0.35
		254	0.00
SC61	7017	294	0.87
		249	1.05
		351	0.87
		279	0.70
		287	1.21
		286	0.18
		268	0.35
		331	0.35
		341	0.35
		296	0.35

Sample	Elevation	Th	Salinity
		259	0.18
		286	0.35
			0.53
			0.35
		274	0.53
		274	0.35
		263	0.53
		268	0.70
		281	1.05
		257	1.22
		303	0.00
			0.18
		296	0.53
SC62A	6779		1.39
		249	1.22
		269	0.53
			0.53
			0.53
			0.53
		276	1.90
		223	1.90
		259	1.22
		253	1.22
		233	1.22
		223	0.87
			0.87
			0.87
		251	0.87
		256	0.87
		230	0.87
		218	0.87
		208	0.87
			0.87
		253	0.87
		265	0.70
SC62B	6786	221	0.00
			0.00
		279	0.00
		292	0.00
		261	0.00
		261	0.18
		259	0.00
		260	0.18
		266	0.18
		260	0.18

Sample	Elevation	Th	Salinity
		269	0.00
		268	0.00
		267	0.18
		266	0.18
		282	0.18
		306	0.87
SC62C	6772	263	1.05
		270	1.05
		273	1.05
		254	0.70
		266	0.70
		259	0.70
		253	0.70
		280	1.05
		253	1.05
		279	1.05
		275	0.87
		258	0.87
			0.87
		259	0.87
			0.87
		264	0.87
		271	1.39
		266	1.39
		280	1.39
		278	1.39
RH1	6894	203	0.53
		209	0.53
		207	0.53
		210	0.53
		221	0.70
		218	0.53
			0.53
		252	0.70
		231	0.70
		229	0.70
		252	0.70
		237	0.53
		216	0.53
		208	0.35
		205	0.18
		229	0.18
		221	0.35
		215	0.18

Sample	Elevation	Th	Salinity
RH2	6849	266	0.53
		280	0.53
		251	0.53
			0.53
		265	0.53
		264	0.53
		268	0.53
		260	0.53
		264	0.53
		257	0.53
		247	0.53
		246	0.18
		249	0.18
		257	0.18
		268	0.18
		248	0.35
		266	0.18
		253	0.53
		265	0.53
			0.53
			0.53
		250	0.53
RH4	6686	268	1.05
S6	7057	219	0.87
			0.87
		238	0.53
		235	0.53
		242	0.53
		229	0.53
		235	0.53
		266	0.18
		269	0.18
			0.18
			0.18
		238	0.53
		236	0.53
		275	0.53
		214	0.70
			0.70
		248	0.87
		237	0.87
		261	1.05
		294	1.05
		230	0.53
		235	0.53

	Sample	Elevation	Th	Salinity
			229	0.53
			217	0.53
			221	0.53
			222	0.53
				0.53
U.S. Treasury	non-ore-grade			
	SC30	6532	236	0.70
			239	0.53
			231	0.70
				0.53
			233	0.87
			239	0.87
			231	0.87
				0.87
			249	0.70
			228	0.87
			255	0.53
			253	0.53
			247	0.53
			254	0.53
			251	0.53
			266	0.53
			251	0.53
				0.53
				0.53
	SC63	6941	220	0.87
			263	0.87
				0.70
				0.70
			254	0.70
			228	0.87
			230	1.05
			232	1.05
				1.22
			237	1.05
			232	0.87
	S5	7023	256	0.35
			252	0.18
				0.18
			249	0.18
			256	0.35
			255	0.18
			211	0.35

APPENDIX B

Averages from Fluid Inclusion Data for each Sample: Th = average homogenization temperature in degrees C; sd = standard deviation; m(CI) = mean of the 95% confidence interval; n(T) = number of temperature measurements; S(wt%) = salinity as equivalent weight percent NaCl; and n(S) = number of salinity measurements.

Sample	Elevation (feet)	Th	sd	m(CI)	n(T)	S(wt%)	sd	m(CI)	n(S)
St. Cloud									
U-14-A	6293	272	5	272	6	0.70	0.15	0.70	6
U-14-B	6292	285	36	286	8	1.42	0.86	1.19	9
U-15-A	6284	274	4	274	5	0.59	0.18	0.59	6
U-15-B	6264	258	12	256	15	1.02	0.55	1.02	15
U-15-C	6263	272	22	278	11	1.62	0.42	1.62	16
U-16-E	6202	265	16	265	13	0.53	0.26	0.57	14
U-19-A	6232	253	26	257	23	0.92	0.88	0.68	21
SC-4-C	6348	265	9	264	16	0.62	0.17	0.65	17
SC-4-D	6321	277	18	272	9	1.51	0.98	1.51	10
SC-4-E	6317	269	14	269	12	1.04	0.60	1.04	14
SC-4-F	6316	260	15	260	32	0.67	0.35	0.62	34
SC-4-G	6315	265	17	268	13	0.97	0.34	0.97	15
SC-4-H	6312	265	18	264	51	1.52	1.43	1.34	55
SC-70-C	6425	263	16	263	15	1.20	0.25	1.17	23
S10	6936	253	15	253	11	0.61	0.46	0.53	17
U.S. Treasury									
UST-8	6758	256	28	256	21	0.91	0.56	0.73	28
SC-30	6532	244	11	244	15	0.65	0.15	0.65	19
SC-53-A	6461	273	12	273	7	0.77	0.15	0.77	12
SC-53-B	6328	270	8	270	17	0.65	0.16	0.65	19
SC-53-C	6319	261	32	269	24	1.45	0.86	1.45	24
SC-58-A	6009	265	31	265	2	0.66	0.09	0.66	4
SC-58-B	6005	279	7	279	5	0.32	0.29	0.32	5
SC-58-C	6001	269	9	268	21	1.35	0.15	1.35	22
SC-59-A	6648	241	24	237	23	0.56	0.46	0.56	23
SC-59-B	6608	271	19	271	12	0.73	0.40	0.73	13
SC-60-B	6864	248	42	252	21	0.63	0.42	0.56	22
SC-61	7017	287	27	284	20	0.56	0.35	0.56	23
SC-62-A	6779	244	20	244	15	0.98	0.38	0.89	22
SC-62-B	6786	269	19	268	15	0.13	0.22	0.08	16
SC-62-C	6772	267	9	267	18	0.99	0.24	0.99	20
SC-63	6941	237	14	237	8	0.91	0.17	0.91	11
RH1	6894	221	15	217	17	0.50	0.18	0.50	18
RH2	6849	259	9	258	19	0.44	0.15	0.44	22
RH3	6721	268	11	269	17	0.74	0.38	0.74	24
RH4	6686	268	0	268	1	1.05	0.00	1.05	1
S5	7023	247	18	254	6	0.25	0.09	0.25	7
S6	7057	240	21	238	22	0.58	0.24	0.58	27

APPENDIX C

Volatile Contents as Mole Percent Including Water as a Gaseous Species (the surface samples are taken from Norman (unpublished) and include analyses along the entire strike length of the vein).

sample	He	H_2	N_2	Ar	CO	CH_4	H_2S	CO_2	C_nH_n	H_2O
St. Cloud stage 1										
SC4E	0.00006	0.01453	0.00461	0.00011	0.00896	0.00663	0.00744	0.07117	0.01556	99.87094
SC4F	0.00009	0.02677	0.00474	0.00019	0.00000	0.00974	0.04454	0.04930	0.00968	99.85495
SC4H	0.00003	0.01547	0.01140	0.00032	0.01581	0.00722	0.00897	0.06500	0.00895	99.85683
U19A	0.00008	0.04573	0.00847	0.00007	0.02860	0.02377	0.01908	0.13785	0.05219	99.68419
St. Cloud stage 2										
SC4C	0.00002	0.03531	0.02849	0.00095	0.03775	0.01205	0.02637	0.19278	0.02331	99.64290
SC70B	0.00056	0.13072	0.39384	0.00610	0.06001	0.03737	0.25463	0.56988	0.04443	98.50245
SC70C	0.00027	0.11254	0.02268	0.00008	0.08391	0.14212	0.04881	0.40885	0.26793	98.91281
U14B	0.00030	0.18826	0.01827	0.00002	0.00000	0.04870	0.17839	0.35067	0.14864	99.06674
U15B	0.00003	0.00613	0.13070	0.00267	0.05368	0.01800	0.09171	0.25530	0.15968	99.58694
U15C	0.00003	0.02493	0.00647	0.00017	0.01236	0.00659	0.03821	0.07050	0.02200	99.81872
St. Cloud non-ore-grade										
S10	0.00002	0.00533	0.00555	0.00014	0.00719	0.00040	0.01910	0.10512	0.00560	98.85063
U16E	0.00004	0.03845	0.00760	0.00007	0.01384	0.00934	0.05540	0.12302	0.03308	99.71916
St. Cloud surface										
SC7	0.00000	0.00394	0.01899	0.00009	0.00198	0.01190	0.01121	0.09454	0.06352	99.79383
SC8	0.00000	0.01011	0.32859	0.00000	0.00343	0.03204	0.01918	1.00565	0.01629	98.58470
SC9	0.00000	0.04308	0.46037	0.00049	0.05044	0.13995	0.00000	1.29247	0.10669	97.90652
SC10	0.00000	0.05472	0.55778	0.00050	0.09310	0.20070	0.00000	1.39498	0.56335	97.13487
SC11	0.00000	0.01446	0.01160	0.00002	0.00065	0.00000	0.00000	0.42333	0.02101	99.52893
SC12	0.00000	0.00408	0.10058	0.00040	0.00814	0.00674	0.00000	0.26132	0.17320	99.44555
SC13	0.00000	0.05986	0.00000	0.00033	0.04778	0.01413	0.00000	0.46726	0.08361	99.32702
SC14	0.00000	0.00266	0.23451	0.00284	0.01074	0.00000	0.00000	0.25431	0.07560	99.41935
SC15	0.00000	0.03031	0.60663	0.00000	0.10697	0.00000	0.00000	1.55782	0.15607	97.54219

sample	He	H_2	N_2	Ar	CO	CH_4	H_2S	CO_2	C_nH_n	H_2O
U.S. Treasury stage 1										
SC53C	0.00001	0.02373	0.00505	0.00024	0.00893	0.00293	0.02960	0.04767	0.00914	99.87270
SC58C	0.00047	0.01833	0.01981	0.00000	0.00000	0.00415	0.03295	0.03337	0.03763	99.85330
SC59A	0.00002	0.01462	0.00415	0.00018	0.00986	0.00456	0.01790	0.04135	0.00698	99.90038
RH3	0.00002	0.00531	0.00488	0.00010	0.00695	0.00371	0.03209	0.01757	0.01200	99.91735
U.S. Treasury stage 2										
SC60B	0.00002	0.00018	0.00918	0.00000	0.02159	0.01330	0.00828	0.03583	0.05953	99.85210
SC61	0.00012	0.03749	0.01320	0.00025	0.05208	0.05261	0.00323	0.32197	0.13989	99.37915
SC62A	0.00005	0.02457	0.00617	0.00008	0.02111	0.05689	0.01510	0.21551	0.04181	99.61871
SC62B	0.00007	0.00160	0.02223	0.00001	0.02748	0.01917	0.00470	0.09663	0.00227	99.82584
S6	0.00002	0.00793	0.00365	0.00006	0.01407	0.01359	0.00007	0.08523	0.00793	99.86745
RH1	0.00003	0.00480	0.00730	0.00034	0.00797	0.00129	0.01621	0.09255	0.00690	99.86281
RH2	0.00004	0.01985	0.00829	0.00004	0.01655	0.01482	0.04416	0.10536	0.01740	99.77300
RH4	0.00002	0.00568	0.00511	0.00018	0.01101	0.00288	0.01006	0.03992	0.01011	99.91503
U.S. Treasury non-ore-grade										
SC63	0.00016	0.02263	0.02728	0.00009	0.00000	0.01016	0.00204	0.09159	0.01170	99.83435
S4	0.00002	0.00524	0.00659	0.00013	0.00863	0.00034	0.00029	0.08919	0.00628	99.88329
S5	0.00002	0.00935	0.00244	0.00005	0.00628	0.00092	0.00000	0.07965	0.00249	99.89879
U.S. Treasury surface										
SC3A	0.00000	0.00169	0.13970	0.00086	0.00000	0.00000	0.00000	0.35516	0.12228	99.38030
SC3.5A	0.00000	0.00409	0.16173	0.00000	0.01930	0.01438	0.00000	0.80243	0.41437	98.58370
SC4A	0.00000	0.00225	0.00466	0.00003	0.00126	0.00000	0.00000	0.16760	0.07160	99.75261
SC5A	0.00000	0.03465	0.06989	0.00013	0.01090	0.04023	0.00000	0.20035	0.03088	99.61296
SC5.5A	0.00000	0.01541	0.01402	0.00004	0.00046	0.00000	0.00000	0.49912	0.00000	99.47094
SC6A	0.00000	0.01065	0.01152	0.00009	0.00000	0.00414	0.00000	0.18302	0.22363	99.56695

APPENDIX D

Listing of GASFIX Program (Norman, unpublished)

```
10 'program to back calculate gas analyses considering that volatiles
20 'equilibrated above Th
30 CLS
40 PRINT:INPUT"Do you want only f(O2) calculation (yes=1)";Q1$
50 N=0
60 G=1/LOG(10)
70 CLS
75 INPUT"SAMPLE";SAMP$
80 PRINT"INPUT GAS DATA IN MOL. %"
90 INPUT"CH4";C4
100 INPUT"CO2";C2
110 INPUT"CO";CO
120 INPUT"H2";H2
130 INPUT"H2S";H2S
140 VO(1)=C2:V$(1)="CO2"
150 VO(2)=C4 : V$(2)="CH4"
160 VO(3)=H2 : V$(3)= "H2"
170 VO(4)=CO : V$(4)= "CO"
180 VO(5)=H2S : V$(5)= "H2S"
190 H2=H2/100
200 CO=CO/100
210 C2=C2/100
220 C4=C4/100
230 H2S=H2S/1.8
240 PRINT:INPUT"ENTER TEMPERATURE FOR GAS EQUILIBRIA";T
250 IF Q1$="1" THEN GOTO 410
260 Q=G*LOG(C2) +4*G*LOG(H2) -G*LOG(C4)
270 A=.01959
280 B=-5.922-Q
290 C=-13178
300 TC=(-B+SQR(B^2-4*A*C ))/(2*A )
310 TC=TC-273
320 N=N+1
330 PRINT"T=";TC
340 IF N>1 THEN GOTO 360
350 TB=TC
360 IF T>TC THEN GOTO 410
370 H2=H2*.9
380 C2=C2*.975
390 C4=C4/.975
400 GOTO 260
410 PRINT
420 PRINT"T=";TC
430 PRINT
440 H2=H2*100 : VN(3)=H2
450 CO=CO*100 : VN(4)=CO
460 C4=C4*100 : VN(2)=C4
470 C2=C2*100 : VN(1)=C2
480 VN(5)=VO(5)
490 TK=T+273
500 K1=7.6-14564.13/(T+273)  :REM H2
```

```
510 K2=.168 + 20543.6/TK :REM CO2
520 K3=-5.1 +4253.4/TK    : REM CH4
530 KH=7.3334-.005625*TK
540 KC4=7.1287 -.005425*TK
550 KC2=5.0149-.002515*TK
560 KS2=-9.99 +21287.7/TK
570 KC4OCO2=-9.932+45418.46/TK
580 FH= 10^ KH*H2/100
590 FC2=C2*10^KC2/100
600 FC4=C4*10^KC4/100
610 FO2H=2*(K1-G*LOG(FH) )
620 FOCO2=G*LOG(FC2)-K2
630 FOC4C2=.5*(-KC4OCO2-G*LOG(FC4)+G*LOG(FC2))
640 FOALL=K3-K2+G*LOG(FC2)+2*G*LOG(FH)-G*LOG(FC4)
650 FS1= KS2+2*G*LOG(H2S)+FO2H
660 FS2= KS2+2*G*LOG(H2S)+FOCO2
670 FS3= KS2+2*G*LOG(H2S)+FOALL
680 FS4= KS2+2*G*LOG(H2S)+FOC4C2
690 CLS
695 PRINT SAMP$ 700 PRINT"SPECIE       OLD VALUES          NEW VALUES"
710 PRINT USING"              T=###                  T=###";TB,TC
720 PRINT
730 FOR I=1 TO 5
740 PRINT USING" /   /         #.#####          #.########";  V$(I),
    VO(I),VN(I)
750 NEXT I
760 PRINT
770 PRINT
780 PRINT"FOR T=";T  :PRINT
790 PRINT USING "LOG(FO2)-(H2-H2O)     = ####.#      LOG(FS2)=
    ###.#";FO2H,FS1
800 PRINT USING"LOG(FO2)-(H2-CH4-CO2) = ####.#      LOG(FS2)=
    ####.#";FOALL,FS3
810 PRINT USING"LOG(FO2)-(C-CO2)      = ####.#      LOG(FS2)=
    ####.#";FOCO2,FS2
820 PRINT USING"LOG(FO2)-(CH4-CO2-H2O)= ####.#      LOG(FS2)=
    ####.#";FOC4C2,FS4
830 PRINT:PRINT
840 PRINT:PRINT:INPUT"another ? (yes=1/no=2)";Q$
850 IF Q$="1" THEN GOTO 50
860 STOP
```

Results of GASFIX Program; gas concentrations expressed in mole percent.

Sample	CO_2	H_2	CH_4
St. Cloud stage 1			
SC4E	0.03685	0.00094	0.01281
SC4F	0.02138	0.00083	0.02246
SC4H	0.03199	0.00081	0.01467
U19A	0.05136	0.00075	0.06380
St. Cloud stage 2			
SC4C	0.07749	0.00080	0.02998
SC70C	0.13765	0.00121	0.42214
U14B	0.12109	0.00225	0.14104
U15B	0.13905	0.00049	0.03305
U15C	0.03470	0.00130	0.01339
St. Cloud non-ore-grade			
S10	0.04918	0.00023	0.00085
U16E	0.04945	0.00087	0.02324
U.S. Treasury stage 1			
SC53C	0.02175	0.00091	0.00642
SC58C	0.01642	0.00096	0.00843
SC59A	0.01620	0.00030	0.01164
RH3	0.01172	0.00098	0.00556
U.S. Treasury stage 2			
SC60B	0.03583	0.00018	0.01330
SC61	0.15451	0.00177	0.10963
SC62A	0.08446	0.00050	0.14517
SC62B	0.08301	0.00085	0.02231
S6	0.03988	0.00034	0.02905
RH1	0.03448	0.00008	0.00346
RH2	0.04686	0.00068	0.03332
RH4	0.02468	0.00077	0.00466
U.S. Treasury non-ore-grade			
SC63	0.03327	0.00033	0.02797
S5	0.03543	0.00032	0.00207

APPENDIX E

Results of ICP-HPLC Analyses.

Sample	Na ppm	K ppm	Ca ppm	Mg ppm	Cl ppm	SO_4 ppm	HCO_3 ppm	Percent error ion balance *
St. Cloud stage 1								
SC4E	510	0	620	210	1130	0	150	+2
SC4F	3150	730	1450	480	7140	120	510	-14
SC4H	580	0	860	290	1010	0	160	+19
U19A	8960	670	2130	2200	14630	180	610	-5
St. Cloud stage 2								
SC4C	1760	0	1610	440	2490	440	410	+7
SC70B	2210	0	2210	630	0	320	-	-
SC70C	2110	0	1890	420	1050	210	220	+50
U14B	890	0	1250	360	890	0	48	+45
U15B	1010	0	870	140	870	0	410	+23
U15C	1200	0	1030	170	1370	0	58	+25
St. Cloud non-ore-grade								
S10	610	200	540	140	410	200	960	-3
U16E	4090	270	1330	0	9420	90	390	-27
U.S. Treasury stage 1								
SC53C	510	0	760	130	250	130	120	+47
SC58C	680	170	1190	340	680	0	130	+49
SC59A	640	0	960	160	320	0	1990	-13
RH3	220	660	550	110	110	0	240	+63
U.S. Treasury stage 2								
SC62B	440	0	530	90	90	0	2050	-34
S6	370	0	440	70	150	220	540	-37
RH1	350	89	350	90	180	0	4150	-66
RH2	800	320	1120	160	160	0	910	+38
RH4	410	0	510	0	300	0	160	-33
U.S. Treasury non-ore-grade								
SC63	310	0	520	100	210	0	1000	-13
S4	400	0	500	0	400	0	-	-
S5	540	0	540	80	150	230	1810	-31

* percent error of the ion balance = $\frac{(\text{cations} - \text{anions})}{(\text{cations} + \text{anions})} \times 100$

APPENDIX F

Results of the GEOMOD Model Calculations (concentrations in ppm).

Sample	Zinc	Lead	Silver	Copper	Gold	Iron
St. Cloud stage 1						
SC4E	0.9116	0.0362	0.0267	0.6349	0.0123	0.0366
SC4F	5.4622	0.1330	0.0454	0.4260	0.7720	0.0001
SC4H	1.1314	0.0399	0.0335	0.9013	0.0148	0.0263
U19A	2.3760	0.0539	0.0140	0.4827	0.1350	0.0003
St. Cloud stage 2						
SC4C	3.1739	0.0856	0.0202	0.4362	0.2654	0.0004
SC70C	5.9042	0.1558	0.0340	0.6491	0.4096	0.0008
U14B	19.4314	0.8823	0.1334	0.5347	4.0517	0.0015
U15B	11.4558	0.2520	0.0883	0.9588	2.5589	0.0000
U15C	4.3870	0.1783	0.0805	0.8968	0.1797	0.0194
St. Cloud non-ore-grade						
S10	2.4223	0.0494	0.0174	0.6948	0.3097	0.0000
U16E	6.6351	0.1829	0.0615	0.3839	1.2841	0.0001
U.S. Treasury stage 1						
SC53C	3.5121	0.1124	0.0398	0.9219	0.1422	0.0060
SC58C	3.9132	0.1198	0.0337	0.8321	0.1839	0.0037
SC59A	2.4613	0.0328	0.0203	0.6979	0.2174	0.0000
RH3	3.7769	0.1154	0.0236	0.4425	0.3156	0.0007
U.S. Treasury stage 2						
SC60B	1.0571	0.0212	0.0058	0.8264	0.0622	0.0001
SC61	0.3830	0.0270	0.0213	0.2404	0.0032	0.3072
SC62A	2.0038	0.0325	0.0102	0.8222	0.0764	0.0002
SC62B	0.5549	0.0165	0.0100	0.0516	0.0670	0.0000
S6	0.0526	0.0081	0.0049	0.6670	0.0000	0.7573
RH1	2.4822	0.0187	0.0314	1.3338	0.3823	0.0000
RH2	5.4665	0.1265	0.0642	0.3495	1.1751	0.0000
RH4	1.2147	0.0419	0.0230	0.7101	0.0246	0.0151
U.S. Treasury non-ore-grade						
SC63	0.2861	0.0047	0.0034	1.0684	0.0017	0.0029
S5	0.8883	0.2216	0.0137	0.2732	0.0000	0.0000

REFERENCES

Aldridge, R.J., 1987. Conodont palaeobiology: A historical review. In: Palaeobiology of Conodonts, R.J. Aldridge (ed.), Ellis Harwood Limited, West Sussex, England. 11-34.

Anderson, E.C., 1957. The metal resources of New Mexico and their economic features through 1954. New Mex. Bur. Mines and Min. Res. Bull. 39, 121-2.

Arnorsson, S., Sigurdson, S., and Svarvarsson, H., 1982. The chemistry of geothermal waters in Iceland. I. Calculation of aqueous speciation from 0 to 370°C. Geochim. Cosmochim. Acta, 46, 1513-32.

Barnes, H.L., 1979. Solubilities of ore minerals. In: Geochemistry of Hydrothermal Ore Deposits, Barnes, H.L., (ed.), John Wiley and Sons, New York, 404-54.

Barton, P.B. Jr., and Toulmin, P., 1961. Some mechanisms for cooling hydrothermal fluids. Geol. Survey Research, D-348-D-352.

Berger, B.R., 1983. Conceptual models of epithermal precious metal deposits. In: Cameron Vol. on Unconventional Mineral Deposits, W.C. Shanks III (ed). A.I.M.E., New York, 191-205.

-------, 1985. Geologic-Geochemical features of hot-spring precious-metal deposits. U.S.G.S. Bull. 1646, 47-53.

Briggs, D.E.G., Clarkson, E.N.K., and Aldridge, R.J., 1983. The conodont animal. Lethaia 16, 1-14.

Browne, P.R.L., 1969. Sulfide mineralization in a Broadlands geothermal drillhole, Taupo volcanic zone, New Zealand. Econ. Geol. 64, 156-9.

Buchanan, L.J., 1981. Precious metal deposits associated with volcanic environments in the southwest. In: Relations of Tectonics to Ore Deposits in the Southern Cordillera, Dickenson, W.R., and Payne, W.D., (eds.). Arizona Geological Society Digest, 14, 237-62.

Campbell, A., Rye, D., and Peterson, U., 1984. A hydrogen and oxygen isotope study of the San Cristobal mine, Peru: Implications of the role of water to rock ratio for the genesis of wolframite deposits. Econ. Geol. 79, 1818-32.

Clayton, R.N., O'Neil, J.R., and Mayeda, T.K., 1972. Oxygen isotope exchange between quartz and water. Jour. Geophys. Res. 77, 3057-67.

Cook, K., 1986. Conodont color alteration: A possible exploration tool for ore deposits. Masters thesis, New Mexico Institute of Mining and Technology. 125pp.

D'Amore, F., and Panichi, C., 1980. Evaluation of deep temperatures of hydrothermal systems by a new gas geothermometer. Geochim. Cosmochim. Acta, 44, 549-56.

Drummond, S.E. and Ohmoto, H., 1985. Chemical evolution and mineral deposition in boiling hydrothermal systems. Econ. Geol. 80, 126-47.

Ellis, A.J., 1979. Explored geothermal systems. In: Geochemistry of Hydrothermal Ore Deposits, Barnes, H.L., (ed.), John Wiley and Sons, New York, 632-78.

-------, and Mahon, W.A.J., 1977. Chemistry and Geothermal Systems. Academic Press, New York, 392 pp.

Elston, W.E., Rhodes, R.C., and Erb, E.E., 1976. Control of mineralization by Mid-Tertiary volcanic centers, southwestern New Mexico. New Mex. Geol. Soc. Spec. Pub. 5, 125-30.

Epstein, A. G., Epstein, J.B., and Harris, L.D., 1977. Conodont color alteration-an index to organic metamorphism. U.S.G.S. Prof. Paper 995, 27 pp.

Ewers, G.R., and Keays, R.R., 1977. Volatile and precious metal zoning in the Broadlands geothermal field, New Zealand. Econ. Geol. 72, 1337-54.

Fisher, J.R., 1976. The volumetric properties of H_2O-a graphical portrayal. Jour. Research, U.S.G.S. 4, 2, 189-93.

Fournier, R.O., 1983. Self-sealing and brecciation resulting from quartz deposition within hydrothermal systems: Extended abstracts, Fourth International Symposium on Water-rock Interaction, Misasa, Japan. 137-140.

-------, 1985a. Silica deposition as indicators of conditions during gold deposition. U.S.G.S. Bull. 1646, 15-26.

-------, 1985b. The behavior of silica in hydrothermal solutions. In: Geology and Geochemistry of Epithermal Systems. Berger, B.R., and Bethke, P.M., (eds.) Soc. Econ. Geol., Rev. in Econ. Geol., 2, 45-61.

-------, and Truesdell, A.H., 1973. An empirical Na-K-Ca geothermometer for natural waters. Geochim. Cosmochim. Acta 37, 1255-75.

Freeman, P.S., and Harrison, R.W., 1984. Geology and development of the St. Cloud silver deposit, Sierra County, New Mexico. Arizona Geo. Soc. Digest, 15, 231-3.

Giggenbach, W.F., 1980. Geothermal gas equilibria. Geochim. Cosmochim. Acta, 44, 2021-3.

Haas, J.L., Jr., 1971. The effect of salinity on the maximum thermal gradient of a hydrothermal system at hydrostatic pressure. Econ. Geol. 66, 940-6.

Harley, G.T., 1934. The geology and ore deposits of Sierra county, New Mexico. New Mex. Bur. Mines and Min. Res. Bull. 10, 72-90.

Harrison, R.W., 1985. Comparisons of the St. Cloud-U.S. Treasury deposits to other epithermal vein-type systems. Unpublished. 47pp.

------, 1986. General geology of Chloride mining district, Sierra and Catron counties, New Mexico. New Mex. Geol. Soc. Guidebook, 37th Field Conference, 265-72.

------, (in prep.) Mineral paragenesis, structure, and 'ore shoot' geometry at the U.S. Treasury mine, Chloride mining district, New Mexico.

Hatchell, W.O., Blagbrough, J.W., and Hill, J.M., 1982. Stratigraphy and copper deposits of the Abo formation, Abo canyon area, central New Mexico. New Mex. Geol. Soc. Guidebook, 33rd Field Conference. 249-260.

Hayba, D.O., Bethke, P.M., Heald, D., and Foley, N.K., 1985. Geologic, mineralogic, and geochemical characteristics of volcanic-hosted, epithermal precious-metal deposits. In: Geology and Geochemistry of Epithermal Systems, Berger, B.R., and Bethke, P.M. (eds.), Soc. Econ. Geol., Rev. in Econ. Geol., 2, 249-272.

Heald, P., Foley, N.K., and Hayba, D.O., 1987. Comparative anatomy of volcanic-hosted epithermal deposits: Acid-sulfate and adularia-sericite types. Econ. Geol. 82, 1-26.

Heald-Wetlaufer, P., Hayba, D.O., Foley, N.K., and Goss, J.A., 1983. Comparative anatomy of epithermal precious- and base-metal districts hosted by volcanic rocks. U.S.G.S. Open File Report 83-710.

Hedenquist, J.W., and Henley, R.W., 1985. The importance of CO_2 on freezing point measurements of fluid inclusions: Evidence from active geothermal systems and implications for epithermal ore deposition. Econ. Geol. 80. 1379-1406.

Helgeson, H.C., 1964. Complexing and Hydrothermal Ore Deposition. Pergamon Co., New York, NY. 128 pp.

------, 1969. Thermodynamics of hydrothermal systems at elevated temperatures and pressures. Am. Jour. Sci. 267, 729-804.

------, 1970. A chemical and thermodynamic model of ore deposition in hydrothermal systems. Min. Soc. Amer. Spec. Paper 3, 155-86.

Henley, R.W., 1985. The geothermal framework of epithermal deposits. In: Geology and Geochemistry of Epithermal Systems, Berger, B.R., and Bethke, P.M. (eds.), Soc. Econ. Geol., Rev. in Econ. Geol., 2, 1-24.

------ and Brown, K.L., 1985. A practical guide to the chemistry of geothermal and epithermal systems. In: Geology and Geochemistry of Epithermal Systems., Berger, B.R., and Bethke, P.M. (eds.), Soc. Econ. Geol., Rev. in Econ. Geol., 2, 25-45.

------ and Ellis, A.J., 1983. Geothermal systems ancient and modern: A geochemical review. Earth and Science Reviews, 19, 1-50.

------, Truesdell, A.H., and Barton, P.B., Jr., 1984. Fluid-Mineral Equilibria in Hydrothermal Systems: Soc. Econ. Geol., Rev. in Econ. Geol., 1, 267pp.

Kottlowski, F.E., 1963. Paleozoic and Mesozoic strata of southwestern and south-central New Mexico. New Mex. Bur. Mines and Min. Res. Bull. 79, 100pp.

Lindgren, W., Graton, L.C., and Gordon, C. H., 1910. The ore deposits of New Mexico. U.S.G.S. Prof. Paper 68, 260-6.

Loucks, R.R., 1984. Investigations in the Chloride mining district, Sierra County, New Mexico. Parts II, III, IV. Unpublished, 87-153.

Lupton, J.E., 1983. Terrestrial inert gasses: Isotope tracer studies and clues to primordial components in the mantle. Ann. Rev. Earth Planet. Sci. 11, 371-414.

Maxwell, C.H., and Heyl, A.V., 1976. Preliminary geologic map of the Winston quadrangle, Sierra county, New Mexico. U.S.G.S. Open File Report 76-858.

------, and ------, 1980. Mineralization and structure of mineral deposits in the Hermosa, Chloride, and Phillipsburg areas, New Mexico. Global Tectonics and Metallogeny, 1, 129-33.

Mamyrin, B.A., and Tolstikhin, I.N., 1984. Helium Isotopes in Nature. Elsevier, New York, NY, 273pp.

Norman, D.I., 1985. Gasses in hydrous alteration minerals: An exploration tool for ore deposits. Unpublished. 62pp.

------, and Sawkins, F.J., 1987. Analysis of volatiles in fluid inclusions by mass spectrometry. Chem. Geol. 61, 1-10.

Norton, D., and Cathles, L.M., 1979. Thermal aspects of ore deposition. In: Geochemistry of Hydrothermal Ore Deposits, Barnes, H.L., (ed.), John Wiley and Sons, New York, 611-311.

Ohmoto, H., 1986. Stable isotope geochemistry of ore deposits. In: High Temperature Geological Processes, Valley, J.W., Taylor, H.P., and O'Neil, J.R., (eds.) Min. Soc. Amer., Rev. in Min., 16, 491-559.

O'Neil, J.R., and Silberman, M.L., 1974. Stable isotope relations in epithermal Au-Ag deposits. Econ. Geol. 69, 902-9.

Ozima, M., and Podosek, F.A., 1983. Noble Gas Geochemistry. Cambridge University Press, Melbourne, Australia, 367 pp.

Putnam, B., 1980. Fluid inclusion and microchemical analysis of the Hansonburg mississippi valley-type ore deposits in central New Mexico. Masters thesis, New Mexico Institute of Mining and Technology. 126 pp.

Reed, M.H., and Spycher, N.F., 1985. Boiling, cooling and oxidation in epithermal systems: Numerical modeling approach. In: Geology and Geochemistry of Epithermal Systems, Berger, B.R., and Bethke, P.M. (eds.), Soc. Econ. Geol., Rev. in Econ. Geol. 2, 249-272.

Roedder, E., 1979. Fluid inclusions as samples of ore fluids. In: Geochemistry of Hydrothermal Ore Deposits, Barnes, H.L., (ed.), John Wiley and Sons, New York, 684-731.

------, 1984. Fluid Inclusions. Min. Soc. of Amer., Rev. in Min. 12, 644pp.

------, and Bodnar, R.J., 1980. Geologic pressure determinations from fluid inclusion studies. Ann. Rev. Earth Planet. Sci. 8, 263-301.

Seward, T.M., 1973. Thio complexes of gold and the transport of gold in hydrothermal ore solutions. Geochim. Cosmochim. Acta, 37, 379-99.

Sillitoe, R.H., and Bonham, H.F. Jr., 1984. Volcanic landforms and ore deposits. Econ. Geol. 79, 1286-98.

Taylor, H.P., Jr., 1973. Oxygen and hydrogen isotope evidence for large-scale circulation and interaction between ground waters and igneous intrusions, with particular reference to the San Juan volcanic field, Colorado. In: Geochemical Transport and Kinetics, Hofman, A.W., Gileti, B.J., Yoder, H.S., Jr., and Yund, R.A., (eds.), Carnegie Institute, Washington, D.C., 299-324.

------, 1974. The application of oxygen and hydrogen isotope studies to problems of hydrothermal alteration and ore deposition. Econ. Geol. 69, 843-83.

Thompson, M., and Walsh, J.N., 1986. A Handbook of Inductively Coupled Plasma Spectroscopy. Chapman and Hall, New York, 273pp.

Truesdell, A.H., Nathenson, M., and Rye, R.O., 1977. The effects of subsurface boiling and dilution on the isotopic compositions of Yellowstone thermal waters. Jour. Geophy. Res. 82, 26, 3694-704.

Weissberg, B.G., Browne, P.R.L., and Seward, T.M., 1979. Ore metals in active geothermal systems. In: Geochemistry of Hydrothermal Ore Deposits, Barnes, H.L., (ed.), John Wiley and Sons, New York, 684-731.

White, D.E., 1955. Thermal springs and epithermal ore deposits. In: Economic Geology 50th Anniversary Volume I, 99-154.

------, 1974. Diverse origins of hydrothermal ore fluids. Econ. Geol. 69, 954-73.

------, 1981. Active geothermal systems and hydrothermal ore deposits. In: Economic Geology 75th Anniversary Volume, Skinner, B.J., (ed.), 392-423.